JAERI-Conf
99-007

INDC(JPN)-184/U

PROCEEDINGS OF THE SPECIALISTS' MEETING ON DELAYED NEUTRON NUCLEAR DATA

JANUARY 28-29, 1999, JAERI, TOKAI, JAPAN

July 1999

(Ed.) Jun-ichi KATAKURA

日本原子力研究所
Japan Atomic Energy Research Institute

本レポートは、日本原子力研究所が不定期に公刊している研究報告書です。
入手の問合わせは、日本原子力研究所研究情報部研究情報課（〒319-1195　茨城県那珂郡東海村）あて、お申し越し下さい。なお、このほかに財団法人原子力弘済会資料センター（〒319-1195　茨城県那珂郡東海村日本原子力研究所内）で複写による実費領布を行っております。

This report is issued irregularly.
Inquiries about availability of the reports should be addressed to Research Information Division, Department of Intellectual Resources, Japan Atomic Energy Research Institute, Tokai-mura, Naka-gun, Ibaraki-ken 319-1195, Japan.

編集兼発行　日本原子力研究所

JAERI－Conf 99－007 **INDC(JPN)-184/U**

Proceedings of the Specialists' Meeting on Delayed Neutron Nuclear Data January 28-29, 1999, JAERI, Tokai, Japan

(Ed.) Jun-ichi KATAKURA

Japanese Nuclear Data Committee
Tokai Research Establishment
Japan Atomic Energy Research Institute
Tokai-mura, Naka-gun, Ibaraki-ken

(Received June 24, 1999)

This report is the Proceedings of the Specialists' Meeting on Delayed Neutron Nuclear Data. The meeting was held on January 28-29, 1999, at the Tokai Research Establishment of Japan Atomic Energy Research Institute with the participation of thirty specialists, who are evaluators, theorist, experimentalists. Although the fraction of the delayed neutron is no more than 1 % in the total neutrons emitted in the fission process, it plays an important roll in the control of fission reactor. In the meeting, the following topics were reported: the present status of delayed neutron data in the major evaluated data libraries, measurements of effective delayed neutron fraction using FCA (Fast Critical Assembly) and TCA (Tank-type Critical Assembly) and their analyses, sensitivity analysis for fast reactor, measurements of delayed neutron emission from actinides and so on. As another topics, delayed neutron in transmutation system and fission yield data were also presented. Free discussion was held on the future activity of delayed neutron data evaluation. The discussion was helpful for the future activity of the delayed neutron working group of JNDC aiming to the evaluation of delayed neutron data for JENDL-3.3.

Keywords: Proceedings, Nuclear Data, Delayed Neutron, Fission Yields, Evaluation

JAERI－Conf 99－007

INDC(JPN)-184/U

遅発中性子核データ専門家会合報文集
1999年1月28日～29日、日本原子力研究所、東海村

日本原子力研究所東海研究所
シグマ研究委員会
（編）片倉　純一

（1999年6月24日受理）

本報文集は、遅発中性子核データ専門家会合の報文を収録したものである。専門家会合は、1999年1月28日と29日の両日、日本原子力研究所東海研究所において、30名の専門家の出席のもとに開催された。遅発中性子は、核分裂で生成する中性子のうちわずか1％にも満たないものであるが、この遅発中性子があることにより原子炉の制御が可能となる重要なものである。この遅発中性子の評価済核データファイルにおける現状や評価法、FCA (Fast Critical Assembly) や TCA (Tank-type Critical Assembly) を用いた実験及び解析、高速炉における感度解析、アクチニド核種からの遅発中性子割合の測定等が報告された。また、関連する話題として消滅処理での遅発中性子や核分裂収率データについても報告された。また、JENDL-3.3に向けた取り組みについてのフリーディスカッションが行われ今後の方向性を議論した。シグマ委員会の遅発中性子WGでは、国際的な評価WG WPEC/SG6に寄与するとともに、JENDL-3.3用の遅発中性子データを整備するため活動しているが、本専門家会合での議論は、今後のWG活動にとっても有意義なものであった。

東海研究所：〒319-1195　茨城県那珂郡東海村白方白根2-4

Contents

目　次

JAERI－Conf 99－007

1. Precision of fission product yield and decay data required for practical delayed-neutron summation calculations

K. Oyamatsu*

Department of Energy Engineering and Science, Nagoya University

1. Introduction

This paper focuses on the precision of Fission Product (FP) yield and decay data required for delayed-neutron (DN) summation calculations. The DN data of interest are

$\overline{\nu}_d$ average delayed neutrons after a fission burst,

$n_d(t)$ delayed neutron activity after a fission burst.

Here, the latter gives the time dependence of the former;

$$\overline{\nu}_d = \int_0^\infty dt\, n_d(t) \ . \tag{1}$$

The target precision of these data is 5 % [1]. There are three methods of evaluating these data.

The DN summation calculation simulates actual decays of FP nuclei using FP yield and decay data for hundreds of FP nuclei. This method is often called "microscopic" because it calculates aggregate DN data from individual FP data.

The other evaluation methods of the delayed-neutron data are macroscopic measurement and integral-type measurement. In a macroscopic measurement, the delayed neutrons are counted after irradiation of a sample containing a fissile. The precision of this method is deteriorated by the limited neutron detection efficiency because the activity varies orders of magnitudes as a function of cooling time. An integral-type measurement is an essentially indirect way to obtain the DN data because neutronics enters into derivation of the DN data.

The DN data of contemporary use are evaluated from macroscopic and integral-type measurement data. However, "artificial" adjustments are needed inevitably because there are appreciable scatterings among these measurement data. There is no direct way to justify the adjustments without more fundamental summation calculation.

Ultimately, the summation calculation is desirable to sweep away the uncertainties due to the artificial adjustments. Unfortunately, the present DN summation calculations do not have sufficient accuracy for practical use because the input data (the FP yield and decay data) are not known in sufficient precision.

---

* present address : Department of Studies on Contemporary Society, Aichi-Shukutoku University, Nagakute-cho, Aichi, 480-1197, Japan.

are not known in sufficient precision.

In the following, we report the present uncertainties in the DN summation calculations and describe a strategy to improve the summation calculation up to practical level.

2. Delayed neutron summation calculation

The mechanism of DN emission is schematically shown in Fig. 1. Note that there can be more than one DN precursor in a decay chain.

The DN activity after a fission burst is given by

$$n_d(t) = \sum_i^{allFP} P_{n\,i}\,\lambda_i\,N_i(t) \quad . \tag{2}$$

Here, $P_{n\,i}$ and λ_i are the DN emission probability (per decay) and the decay constant of nuclide *i*, respectively. The population of nuclei *i* at cooling time *t*, $N_i(t)$, is the solution of coupled linear differential equations:

$$\frac{d}{dt}N_i(t) = -\lambda_i\,N_i(t) + \sum_{j\neq i} b_{j\to i}\,\lambda_j\,N_j(t) \quad . \tag{3}$$

Here,$b_{j\to i}$ is branching ratio from nuclide j to i. Note that Pn's are nothing but branching ratios that correspond with the β decays accompanying neutron emission. The initial population of nuclide *i* after a fission burst is the independent fission yield of the nuclide:

$N_i(0) = y_i$.

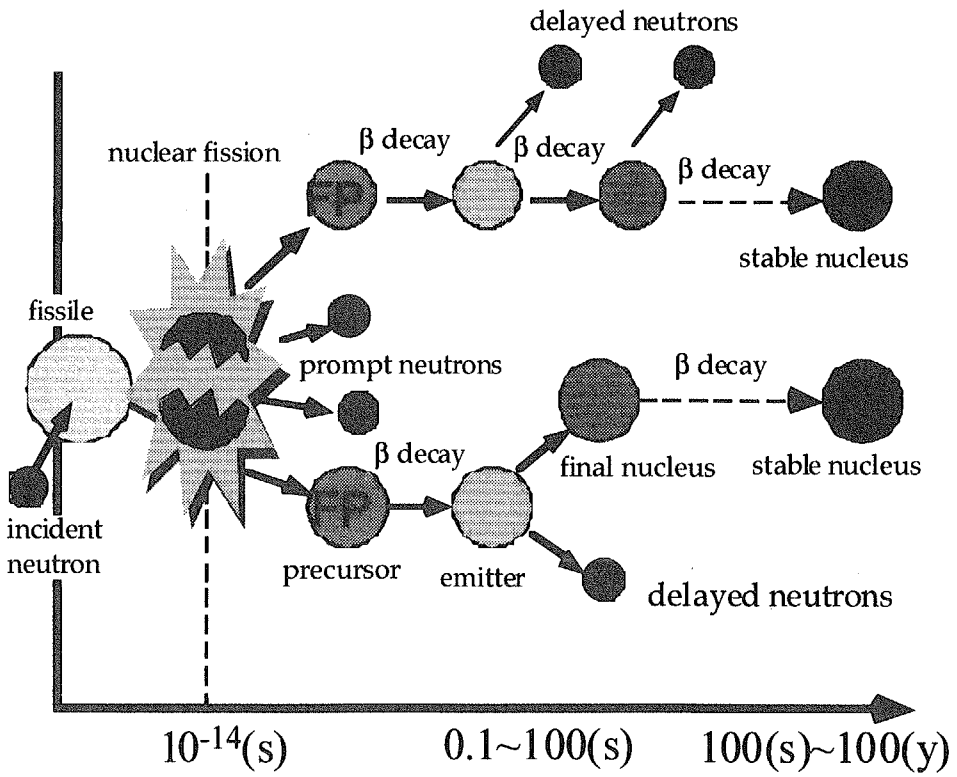

Fig. 1. Machanism of delayed neutron emission.

3. Difficulty in DN summation calculations

The inputs of the summation calculations are independent fission yields, the branching ratios and decay constants. However, it has been very difficult to obtain their precise values. The nuclides relevant to the DN calculations are so short-lived (Fig. 2) that precise measurements for these data have been prohibitingly difficult. This is the reason why DN summation calculations have had too large uncertainties to be used for practical reactor calculations.

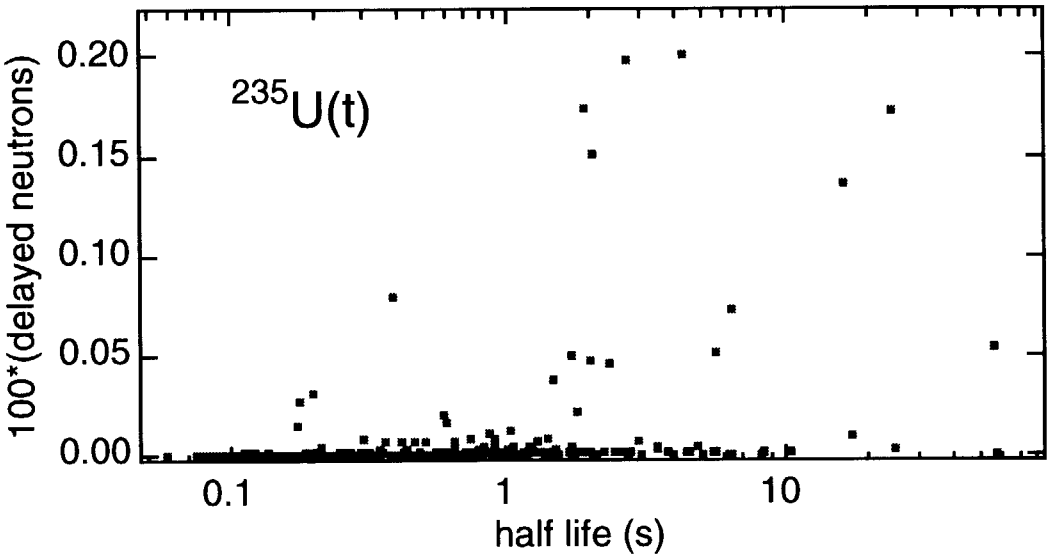

Fig. 2. Delayed neutron yields from indiviual precursors as a function of precursor half-life.

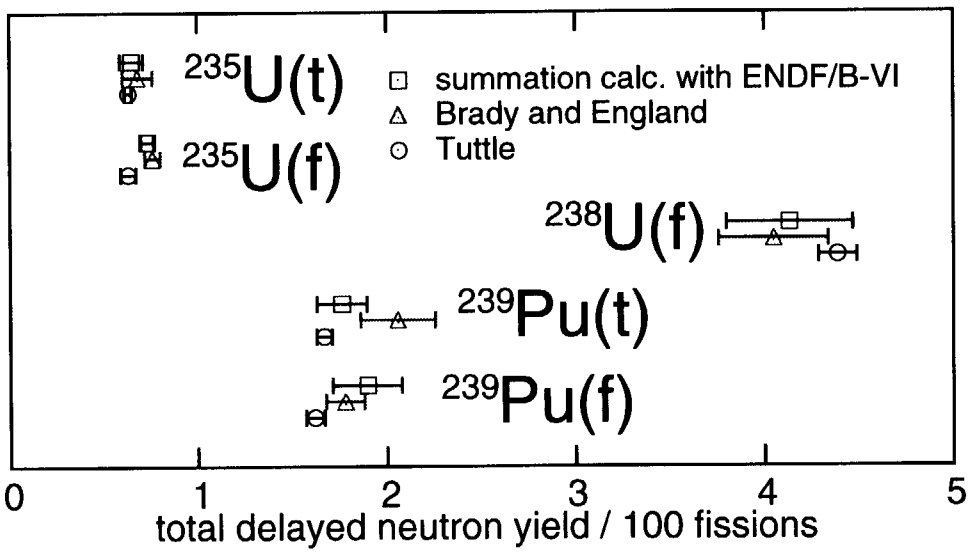

Fig. 3. Total delayed neutron yield $\overline{\nu}_d$ and its uncertainty. Results of two summation calculations are shown together with Tuttle's recommendation values[2]. The squares denote summation calculations using ENDF/B-VI [3,4]. The triangles denote summation calculations by Brady and England[5] with preliminary ENDF/B-VI data.

4. The present uncertainties in the delayed neutron summation calculations

4-1 Uncertainties in $\overline{\nu_d}$ values

At present, about 10 % uncertainties exist in summation calculations of $\overline{\nu_d}$ values as shown in Fig. 3. We also note the appreciable difference between the two summation calculations (squares and triangles) using preliminary and final ENDF/B-VI data. This also implies that there remains much room to improve the input database for the DN calculations.

4-2 Uncertainties in $n_d(t)$ values

Then, how about $n_d(t)$ values that give the time dependence of the DN emission? Figure 4 shows $n_d(t)$ for ^{235}U(thermal), ^{238}U(fast) and ^{239}Pu(fast) obtained from summation calculations and Tuttle's 6-group parameter sets[2,6].

The time dependent profiles agree fairly well between the summation calculations and Tuttle's in spite that the integrated values ($\overline{\nu_d}$) have about 10 % uncertainties. Except for ^{235}U(thermal), the better estimates of $n_d(t)$ seem to be obtained if the curves in Fig. 4 are renormalized with Tuttle's $\overline{\nu_d}$ values. This kind of renormalization procedure was actually adopted in preparing the ENDF/B-VI six-group parameter sets.

However, this renormalization does now work well. In Figs. 5-7, comparison of $n_d(t)$ values is made between summation calculation and Tuttle's recommendation for each fissioning system.

For ^{235}U(thermal), we see significant deviation at short cooling times. This is attributed to too large independent fission yield of ^{86}Ge[7,8]. It is also noted that the summation calculation gives too small values at about 30 s beyond expected uncertainties in the two evaluations.

The appreciable underestimate of the summation calculations is also seen for ^{238}U(fast) as shown in Fig. 6. The deviation between the two evaluations exceeds the sum of the 1 σ uncertainties, too.

For ^{239}Pu(fast), the two evaluations agree reasonably if we take into account 1 σ uncertainties. However, the uncertainty values associated with the summation calculation are much larger than those for ^{235}U(thermal) and ^{238}U(fast).

We conclude that the renormalization of summation values of $n_d(t)$ is too simple to obtain reliable values. Dominant FP data for $n_d(t)$ in the summation calculations varies much with cooling time. For ^{235}U(thermal), erroneous fission yield of ^{86}Ge resulted in the significant overestimate. However, the sources of the underestimate for ^{235}U(thermal) and ^{238}U(fast) should be found in other FP data.

We also remark that the above deviation at about 30 s is more important for practical use. The usual reactor conditions are close to infinite irradiation because the DN time scale (tens of seconds) is much shorter than the normal operation time scale. Figure 8 shows the

DN activity after infinite irradiation, $N_d(t)$. The deviation at 30 s for ^{238}U (and ^{235}U) is remarkable for infinite irradiation case although they do not look so for the burst case in Fig. 4.

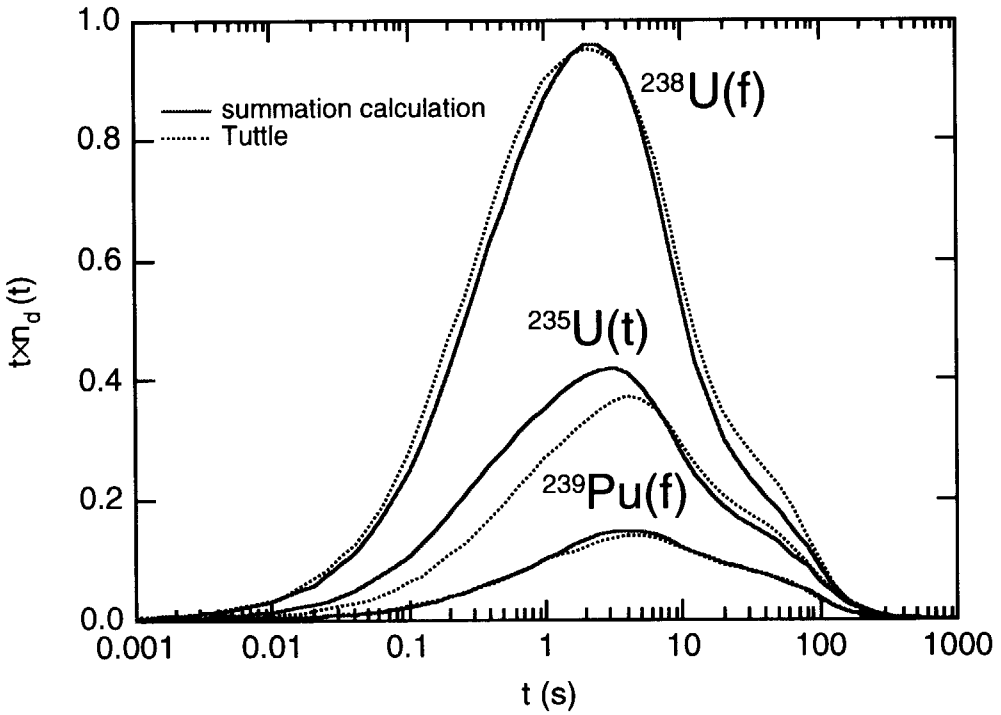

Fig. 4. Delayed neutron activity $n_d(t)$ after a fission burst.

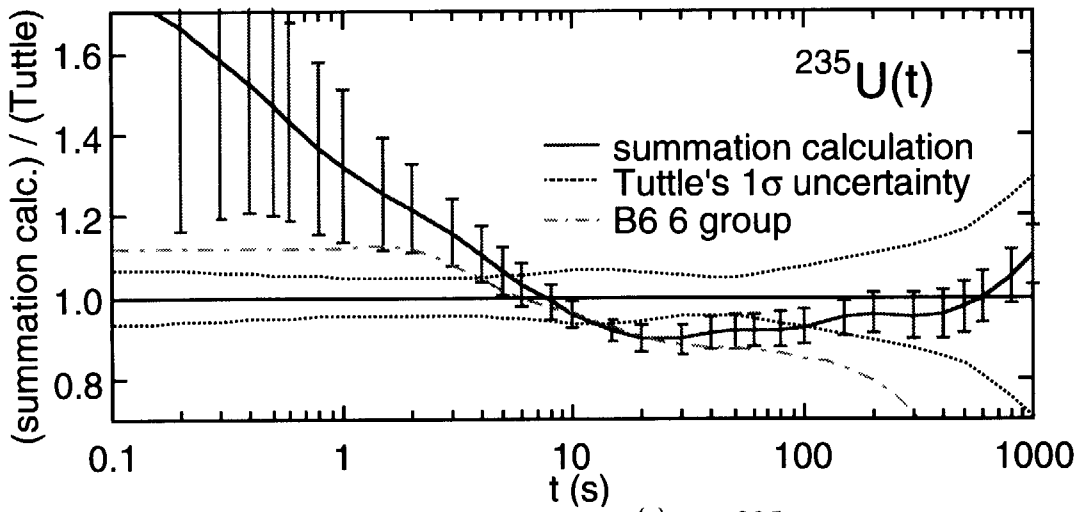

Fig. 5. Comparison of delayed neutron activity $n_d(t)$ for ^{235}U(thermal). The values plotted are ratios of the summation calculation to Tuttle's recommendation values. The error bars indicate 1 σ uncertainties in the summation calculation.

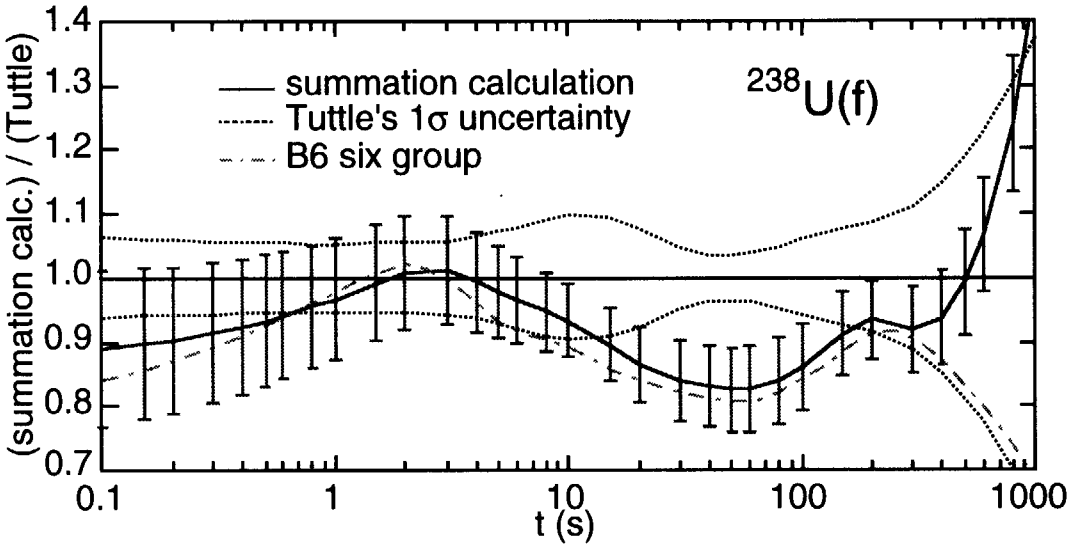

Fig. 6. Comparison of delayed neutron activity $n_d(t)$ for ^{238}U(fast). The values plotted are ratios of the summation calculation to Tuttle's recommendation values. The error bars indicate 1 σ uncertainties in the summation calculation.

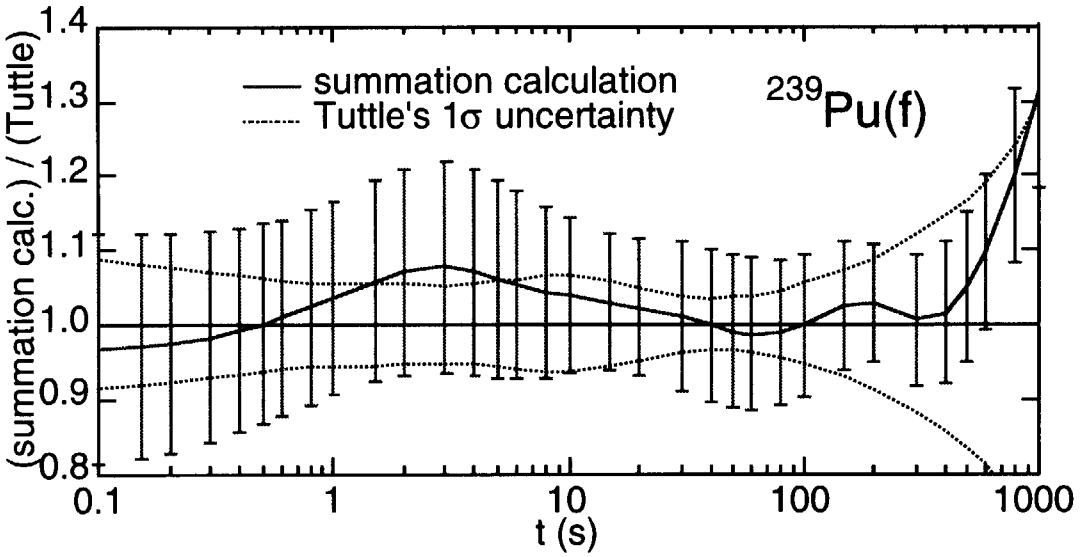

Fig. 7. Comparison of delayed neutron activity $n_d(t)$ for ^{239}Pu(fast). The values plotted are ratios of the summation calculation to Tuttle's recommendation values. The error bars indicate 1 σ uncertainties in the summation calculation.

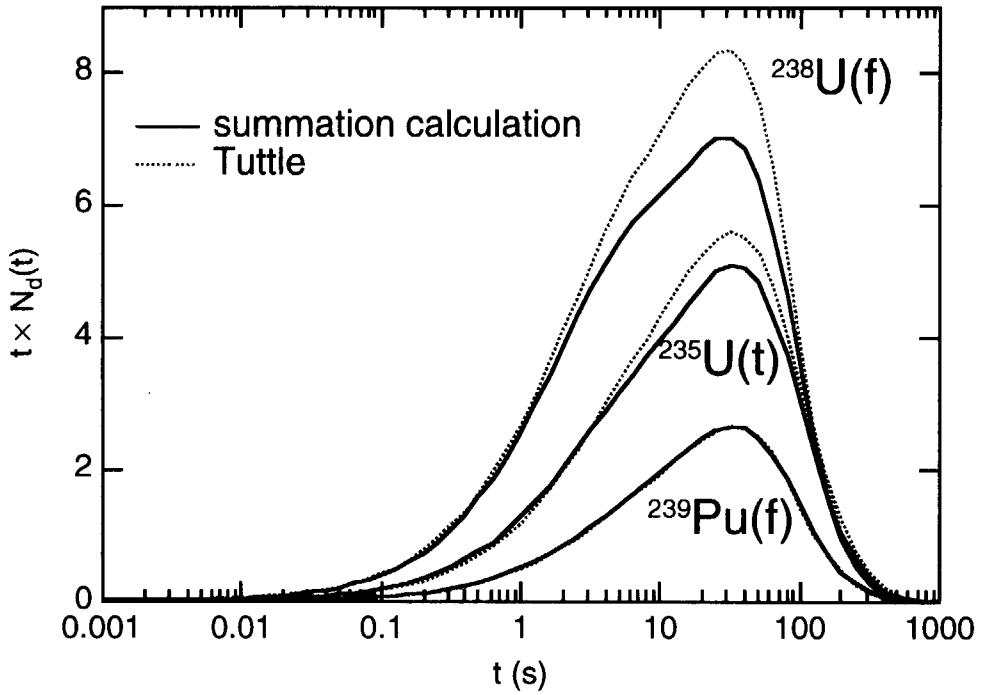

Fig. 8. Delayed neutron activity $N_d(t)$ after infinite irradiation at constant reaction rate 1 fission/s.

5. Key FP data to improve summation calculations at 30 s

A reasonable strategy to improve the summation calculations is to start with the deviation at 30 s after infinite irradiation.

First, we examine which precursor should be relevant to the deviation. Figure 9 shows delayed neutron yields from individual precursors after infinite irradiation for ^{238}U(fast). From half-lives, relevant precursors in question are limited to ^{87}Br, ^{137}I, ^{136}Te, ^{88}Br and ^{138}I. The (β-decay) parent nuclides of these precursors do not give appreciable contribution to the 30 s problem. As a result, the independent and cumulative fission yields are almost equal to each other for these nuclides.

The source of the problem should be found in fission yield or decay data of these 5 nuclides. Among these data, half-lives (or equivalently decay constants) of the precursors are known precisely within precision of about 1%.

The primary sources of the 30 s problem are marked uncertainties (6-23%) in fission yield data of the 5 nuclides (Fig. 10). Actually, if we adjust the independent fission yields of the five precursors, the summation calculation of $N_d(t)$ for ^{238}U(fast) can be fitted to Tuttle's values[9].

It is also noted that Pn values are also rather uncertain for these nuclides as shown in Fig. 11. Uncertainties of their Pn values are too large to satisfy the target accuracy (5 %) of $n_d(t)$ or $N_d(t)$. It is also noted that relatively small uncertainty values are stored in ENDF/B-VI compared with the latest evaluation in Table of Isotopes (8th ed.). In addition, Pn values themselves differ appreciably between the two evaluations.

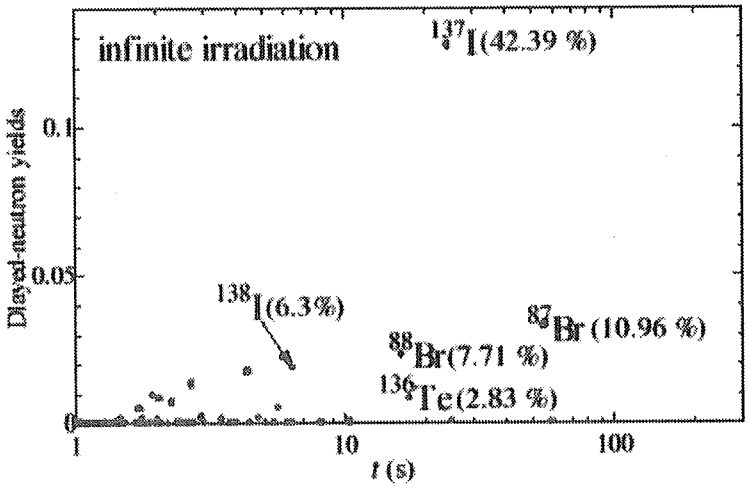

Fig. 9. Delayed neutron yields for ^{238}U(fast) after infinite irradiation at constant reaction rate 1 fission/s. The yields are plotted against half-lives of precursors.

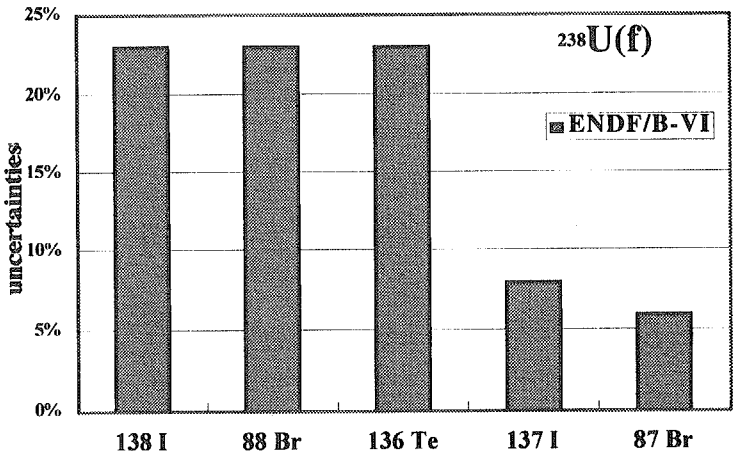

Fig. 10. Uncertainties in independent fission yields of ^{87}Br, ^{137}I, ^{136}Te, ^{88}Br and ^{138}I for ^{238}U(fast).

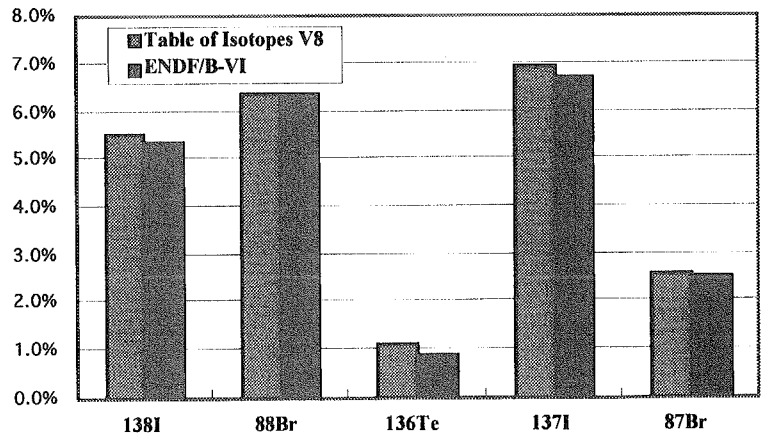

Fig. 11. Uncertainties in Pn values of ^{87}Br, ^{137}I, ^{136}Te, ^{88}Br and ^{138}I.

6. What can we do to improve delayed neutron summation calculation?

To achieve the 5 % target accuracy in summation calculations, it is necessary to improve precision of fission yield and Pn values down to about 4 % and 3 %, respectively. Uncertainties in the summation calculations essentially stem from these input data;

$$(\delta n_d(t) \text{ or } \delta N_d(t))^2 = (\delta \text{ fission yield})^2 + (\delta Pn)^2.$$

We may perform simple arithmetic;

$$(5\ \%)^2 = (4\ \%)^2 + (3\ \%)^2 \ .$$

Since the fission yields are more difficult to measure precisely, 4 % is assigned to the fission yield uncertainty.

As for Pn measurements, we can expect substantial progress in precision thanks to innovative RI beam facilities. The Pn measurements were difficult because precursor yields (production rates) were too small to have enough statistics. Furthermore, chemical isotope separations of these nuclides were also difficult because they are too short-lived. Now, RI beam facilities enable us to produce enough precursor yields with excellent in-flight isotope separations[10].

The Pn measurements can also made more precise using γ-spectroscopy instead of detecting neutrons directly[11]. It is very difficult to reduce uncertainties in Pn measurements by direct neutron detection because the detection efficiency deteriorates the precision. However, this drawback can be overcome if we count the number of nuclei which are formed after delayed neutron emission. This can be done by counting γ rays emitted in decays of these nuclei because they are also unstable against β decay.

As for fission yield measurements, no direct breakthrough can be anticipated at present. However, the progress in the Pn measurements may contribute indirectly for improvement of the yield data. First, fission yields of precursors will be better determined from cumulative fission yields of their daughter nuclides because the Pn values provide branching ratios of the precursor decays. Second, Pn measurements in RI facilities use photo fissions of actinides so that it might be possible to obtain some information about fission yields theoretically.

7. Remark

It is important to inform nuclear physicists of the importance of the DN properties in reactor physics. Innovative RI beam facilities have potential to improve Pn values required in the DN summation calculations. It is time to cooperate with nuclear physicists in Pn measurements. There still lays difficulty in determining fission yields precisely. However, I believe that we should take the plunge from Pn measurements to improve the DN summation calculations. There is no direct other way to justify the evaluation of DN data derived statistically from macroscopic and integral-type measurements.

References

[1] J.Rowlands, private communications.

[2] R.J. Tuttle, INDC(NDS)-107/G+Special (1979).

[3] T.R. England and B.F. Rider, LA-UR-94-3106 (1994).

[4] T. R. England et al., LA-UR-92-3785(1992).

[5] M.C. Brady and T.R. England, Nucl. Sci. and Eng. 103 (1989) 129-149.

[6] R.J. Tuttle, Nucl. Sci. and Eng. 56, (1975) 37-71.

[7] T.Miyazono et al., Proc. 1996 Sympo. on Nucl. Data, JAERI-Conf 97-005 (1997) 83-88.

[8] T.R.England, private communications.

[9] T.Sanami, K.Oyamatsu and Y.Kukita, Proc. 1998 Sympo. on Nucl. Data, JAERI-Conf 99-002, (1999) pp. 120-123.

[10] M. Bernas et al., Phys. Lett. B331 (1994) 19.

[11] K.Kawade, private communications.

JP9950500

2. Present Status of Delayed Neutron Data in the Major Evaluated Nuclear Data Libraries

Tsuneo NAKAGAWA
Nuclear Data Center

Japan Atomic Energy Research Institute
Tokai-mura, Naka-gun, Ibaraki-ken, 319-1195
e-mail: nakagawa@ndc.tokai.jaeri.go.jp

The status of delayed neutron data of ^{235}U, ^{238}U and ^{239}Pu was investigated. As major evaluated nuclear data libraries, we consider JENDL-3.2, ENDF/B-VI.5 and JEF-2.2. Quantities related with the delayed neutrons are the total number of delayed neutrons emitted per fission, ν_d, decay constants, λ_i, normalized abundance, α_i, and neutron spectra, χ_i, of six temporal groups.

1. Introduction

Delayed neutron data are very important for reactor performance. In this paper, the status of the data in the major evaluated nuclear data libraries was investigated for ^{235}U, ^{238}U and ^{239}Pu. The quantities considered here are the total number of delayed neutrons ν_d, decay constants λ_i, normalized abundance α_i, and delayed neutron spectra χ_i of temporal groups. JENDL-3.2[1], ENDF/B-VI.5[2] and JEF-2.2[3] were selected as the major libraries.

2. Format for delayed neutron data

Current evaluated nuclear data libraries are compiled in the ENDF-6 format[4]. The total number of delayed neutrons per fission, ν_d, is stored in MF=1 and MT=455 together with decay constants of temporal groups. The delayed neutron spectra χ_i and the normalized abundance α_i of temporal groups are given in the MF=5 and MT=455. The χ_i is usually represented in a tabular form. The data in MF=5 can be represented as energy dependent. On the other hand, the current ENDF-6 format is not capable to represent the energy dependence of the decay constants in MF=1.

3. Evaluations

Main evaluations are listed in Table 1 where year of publication, authors and evaluated quantities are given. "◎" indicates that the evaluation is adopted in the current evaluated nuclear data libraries.

The most famous early evaluation was made by Keepin[5] on the basis of the experiment performed with GODIVA. His results of 6 group parameters have been used for many years. Evaluation by Tomlinson[6] was adopted in JENDL-3.2. The fast and thermal energy parameters of the 6 groups are taken from the evaluation made by Keepin. The high-energy data are mainly based on the data of East[7].

Cox[8] made an evaluation for ENDF/B-VI. The ν_d was estimated on the basis of available experimental data. Energy dependence was taken into account around 4 to 7 MeV. The values of λ_i were the same as those at the fast energy of Tomlinson; that is the same as Keepin's data. For the neutron spectra, the data of Fieg[9] and Shalev and Cuttler[10] were adopted.

Tuttle[11] evaluated ν_d values by considering experimental data available by August 1974. He derived also a sytematics formula of ν_d. In his report, 6 group parameters were also

recommended by adopting Keepin's data at the fast energy. His ν_d values were reevaluated in Ref. [12], and the sytematics formula was also revised.

Saphier et al.[13] made the summation calculation to obtain delayed neutron spectra by considering 20 precursors. Their results are adopted in JENDL-3.2. After this summation calculation, Rudstam[14] performed more complete calculation for the wide range of fissioning nuclides by taking 67 precursors. Furthermore Brady and England[15] completed the summation calculation by considering 271 precursors. Their results of group parameters and neutron spectra were adopted in ENDF/B-VI.

Villani et al.[16] made an evaluation of delayed neutron spectra of ^{235}U by means of the least-squares method using measured composite neutron spectra.

Blachot et al.[17] obtained ν_d values by the summation calculation by using fission yield data in JEF-2.2 Fission Yield Library[18] and neutron emission probabilities for 158 precursors given in JEF-2.2 Radioactive Decay Data Libraray[19].

4. Total number of delayed neutrons

The ν_d values adopted in the major libraries are summarized in Table 2. Except JEF-2.2, old data in 1970s are used in the libraries. The ν_d values in the libraries for the three nuclides are compared with other evaluations at the certain energy in Fig. 1. The data in the libraries are shown with horizontal lines, and those of other evaluations with solid or open circles. Evaluation made by Manero and Konshin[20], and England[21] are also shown in the figure. Uncertainties of ±5 % are indicated for the line of JENDL-3.2. The data of the evaluated data libraries are those at 0.0253 eV (thermal) and 2 MeV (fast).

Figure 1 (a) shows the data for the ^{235}U thermal fission. The results of the summation calculations are too large and have relatively large uncertainties. Data in the three libraries are within the ±5% uncertainties. JENDL-3.2 is lower than others. As is shown in Fig. 2, JENDL-3.2 evaluation considers the energy dependence below 3 MeV, while the other evaluations are constant. Tutlle[12] recommended such energy dependence. All of JENDL-3.2 data for the major three nuclides has the energy dependence below about 3 MeV.

In the case of the ^{238}U fast fission of Fig.1 (b), the data of JENDL-3.2 are too large.

The data of ^{239}Pu fast fission are in good agreement with each other as is shown in Fig.1 (c). The summation calculations are rather discrepant. Figure 3 is a comparison of three evaluated data sets. In the resonance region, JEF-2.2 has fine structure which calculated with Lendel's formula[22] and the number of prompt neutrons ν_p in JEF-2.2.

In the JENDL-3.2 evaluation for the minor nuclides, sytematics of ν_d is frequently used to estimate the values at low and high energies. The following three systematics are adopted in JENDL evaluation:

$$Y_{DN} = \exp\left[13.81 + 0.1754(A_C - 3Z)\frac{A_C}{Z}\right] \qquad \text{by Tuttle[12],}$$

$$Y_{DN} = 0.01 \times \exp[16.698 - 1.144Z + 0.377A_C] \qquad \text{by Waldo et al.[23],}$$

$$Y_{DN} = \exp\left[14.268 + 0.1796(A_C - 3Z)\frac{A_C}{Z}\right] \qquad \text{by Benedetti et al.[24],}$$

where A_c and Z are mass and atomic numbers of a compound nucleus. These systematics give almost the same ν_d values.

5. Decay constants and normalized abundance of temporal groups

The references of decay constants and normalized group abundance are listed in Table 3. JENDL-3.2 adopted the evaluated data of Tomlinson[6] which are the same as Keepin's data[6] at thermal and fast energies, and based on the experimental data by East et al.[7] at the high energy. The data of ENDF/B-VI are the evaluation made by Brady and England[15].

Since the ENDF format cannot represent the energy dependence of the decay constants, JENDL-3.2 and ENDF/B-VI adopted the evaluated values for the fast fission. For the group abundance, JENDL-3.2 considers the energy dependence, but ENDF/B-VI gives constant values of the fast fission. As an example, Table 4 shows the parameters of ^{235}U comparing JENDL-3.2 and ENDF/B-VI. To show the discrepancies between the two libraries, the delayed neutron emission rates are illustrated in Fig. 3 together with those calculated from the parameters obtained by Brady and England. At 60 sec, discrepancies among ENDF/B-VI and JENDL-3.2 are about 10 %. The curve of Brady and England is almost the same as JENDL-3.2 above 30 sec, However discrepancies of about 20 % are found at 0 sec among JENDL-3.2 and Brady-England. In order to show the discrepancies at early times, the delayed neutron emission rate multiplied by time is shown in Fig. 5. The discrepancies between ENDF/B-VI and Brady-England, and between JENDL-3.2 and Keepin come from deferent ν_d values and the problem of ENDF-6 format, i.e. the energy dependence of decay constants cannot be represented.

6. Delayed neutron spectra

JENDL-3.2 adopted the results of summation calculation made by Saphier et al.[13] and ENDF/B-VI those of Brady and England[15]. Table 5 gives a comparison of important input data used in these two summation calculations. The calculation made by Brady and England is obviously superior to that by Saphier et al. Neutron spectra of individual groups of ^{235}U thermal fission are shown in Fig. 5 together with the evaluation by Villani et al.[16] The spectra originally given in JENDL-3.2 were in compilation error. Here the modified data are shown in Fig. 6. The spectra of group 2 are almost the same as each other, except below 1 MeV. However the large discrepancies exist among JENDL-3.2 and ENDF/B-VI in the case of other groups as shown in Fig. 6 (b). The results of Villani et al. are in good agreement with ENDF/B-VI.

7. Conclusion

As for the numbers of delayed neutrons, current evaluated libraries adopt old evaluations, but their accuracy seems to be better than 5 %. However, since more recent experimental data are available, re-evaluation is recommended, especially for the data of ^{238}U in JENDL-3.2.

The decay constants and group abundances are also old data. However, there are no particular problems. Delayed neutron spectra adopted in JENDL-3.2 are not good. They should be replaced with better evaluations.

Recent tendency of delayed neutron evaluation is the summation calculation. For the next version of JENDL, activities for new summation calculations of the 6 group parameters and spectra are required.

References

[1] Nakagawa T., Shibata K., Chiba S., Fukahori T., Nakajima Y., Kikuchi Y., Kawano T., Kanda Y., Ohsawa T., Matsunobu H., Kawai M., Zukeran A., Watanabe T., Igarasi S., Kosako K., and Asami T.: *J. Nucl. Sci. Technol.*, **32**, 1259 (1995).

[2] (Ed.) Rose P.F.: "ENDF-201, ENDF/B-VI Summary Documentation," *BNL-NCS*-17541, 4th Edition (1991).

[3] Nordborg C., and Salvatores M.: "Status of the JEF Evaluated Data Library", *Proc. Int.*

Conf. on Nuclear Data for Science and Technology, Gatlinburg, Teneessee, USA, May 9-13 May 1994, Vol. 2, p.680 (1994).
[4] McLane V., Dunford C.L., abd Rose P.F.: "ENDF-102, Data Formats and Procedures for the Evaluated Nuclear Data File, ENDF," BNL-NCS-44945 (1995), more recent version is available from http://www.nndc.bnl.gov/nndcscr/documents/endf/endf102/.
[5] Keepin G.R., Wimett T.F., and Zeigler R.K.: *Phys. Rev.*, **107**, 1044 (1957).
[6] Tomlinson L.: "Delayed Neutrons from Fission: A Compilation and Evaluation of Experimental Data," *AERE-R* 6993 (1972).
[7] East L.V., Auguston R.H., Menlove H.O., and Masters C.F.: *Trans. Am. Nucl. Soc.*, **13**, 760 (1970) cited in [6].
[8] Cox S.A.: "Delayed Neutron Data - Review and Evaluation," *ANL/NDM*-5 (1974).
[9] Fieg G.: *J. Nucl. Energy*, **26**, 58 (1972).
[10] Shalev S., and Cuttler J.M.: *Nucl. Sci. Eng.*, **51**, 52 (1973).
[11] Tuttle R.J.: *Nucl. Sci. Eng.*, **56**, 37 (1975).
[12] Tuttle R.J.: "Delayed-Neutron Yields in Nuclear Fission," *Proc. Consultants' Meeting on Delayed Neutron Properties*, Vienna, 26-30 Mar. 1979, *INDC(NDS)*-107/G+ Special, p.29 (1979).
[13] Saphier D., Ilberg D., Shalev S., and Yiftah S.: *Nucl. Sci. and Eng.*, **62**, 660 (1977).
[14] Rudstum G.: *Nucl. Sci. Eng.*, **80**, 238 (1982).
[15] Brady M.C., and England T.R.: *Nucl. Sci. Eng.*, **103**, 129 (1989).
[16] Villani M.F., Couchell G.P., Haghighi M.H., Pullen D.J., Schier W.A., and Sharfuddin Q.: *Nucl. Sci. Eng.*, **111**, 422 (1992).
[17] Blachot J., Chung C., and Storrer F.: *Ann. Nucl. Energy*, **24**, 489 (1997).
[18] Mills R.W., James M.F., and Weaver D.R.: "The JEF-2.2 Fission Product Yield Evaluation," Proc. Specialists' Meeting on Fission Product Nuclear Data, Tokai, Japan, 25-27 May, 1992, p.358 (1992).
[19] Blachot J., and Nordborg C.: "Decay Data Evaluation for JEF-2.2," *Proc. Int. Symposium on Nuclear Data Evaluation Methodology*, BNL, Upton, New York, 12-16 Oct. 1992, World Scientific, p.623 (1993).
[20] Manero F., and Konshin V.A.: *At. Energy Rev.*, **10**, 637 (1972) cited in [11].
[21] England T.R., and Rider B.F.: "Yield validation: Integral Comparisons," Proc. Specialists' Meeting on Fission Product Nuclear Data, Tokai, Japan, 25-27 May, 1992, p.378 (1992).
[22] LendelA.I., Marinets T.I., Sikora D.I., and Charnovich E.T.: *Sov. At. Energy*, **61**, 752 (1986).
[23] Waldo R.W., Karam R.A., Meyer R.A.: *Phys. Rev.*, **23**, 1113 (1981).
[24] Benedetti G., Cesana A., Sangiust V., Terrani M., and Sandrelli G.: *Nucl. Sci. Eng.*, **80**, 379 (1982).
[25] Evans A.E., and Thorpe M.M.: *Nucl. Sci. Eng.*, **50**, 80 (1973).
[26] Meak M.E., and Rider B.E.: "Compilation of Fission Product Yields," *NEDO*-12154 (1972) and *NEDO*-12154-1 (1974) cited in [13].
[27] Kaiser R., and Carpenter S.: private communication (1978).

Table 1 Evaluations of delayed neutron data

Year	Autors	ν_d	λ_i, α_i	χ_i	Comments
1957	Keepin et al.[5]	○	◎	－	
1972	Tomlinson[6]	○	◎	○	Adopted in JENDL-3.2
1974	Cox[8]	◎	◎	◎	Adopted in ENDF/B-IV and -V, and ν_d adopted in ENDF/B-VI
1975	Tuttle[11]	○	○	－	
1977	Saphier et al.[13]	－	－	◎	Summation calculation Adopted in JENDL-3.2
1979	Tuttle[12]	◎	－	－	Systematics of ν_d
1982	Rudstum[14]	－	○	○	
1989	Brady and England[15]	○	◎	◎	Summation calculation Adopted in ENDF/B-VI
1992	Villani et al.[16]	－	○	○	^{235}U only
1997	Blachot et al.[17]	○	－	－	Summation calculation

Table 2 Number of delayed neutrons ν_d in evaluated data libraries

Nuclide	Library	Adopted data
^{235}U	JENDL-3.2	Evaluation based on the experimental data in 1957 to 1979
	ENDF/B-VI.5	Evaluation by Cox[8] (same as ENDF/B-IV)
	JEF-2.2	?
^{238}U	JENDL-3.2	Based on the data of Evans[25] and evaluation by Tuttle[11]
	ENDF/B-VI.5	Evaluation by Kaiser[27]
	JEF-2.2	Same as JENDL-3.2
^{239}Pu	JENDL-3.2	Evaluation by Tuttle[12]
	ENDF/B-VI.5	Evaluation by Cox[8] (same as ENDF/B-IV)
	JEF-2.2	Calculated with Lendel's formula[22]

Table 3 Decay constants λ_i and normalized abundances α_i of temporal groups

Nuclide	Library	λ_i	α_i
^{235}U	JENDL-3.2	Tomlinson[6]	Tomlinson
	ENDF/B-VI.5	Brady and England[15]	Brady and England
	JEF-2.2	Tomlinson	Brady and England
^{238}U	JENDL-3.2	Tomlinson	Tomlinson
	ENDF/B-VI.5	Brady and England	Brady and England
	JEF-2.2	same as JENDL-3.2	?
^{239}Pu	JENDL-3.2	Tomlinson	Tomlinson
	ENDF/B-VI.5	Brady and England	Brady and England
	JEF-2.2	almost Brady and England	Tomlinson

Table 4 Decay constants λ_i and normalized group abundances α_i of ^{235}U

group	λ_i		α_i			
	JENDL-3.2	ENDF/B-VI	JENDL-3.2			ENDF/B-VI
			0 MeV	2 MeV	14 MeV	
1	0.0127	0.013336	0.33	0.038	0.057	0.035
2	0.0317	0.032739	0.219	0.213	0.192	0.1807
3	0.115	0.12078	0.195	0.188	0.190	0.1725
4	0.311	0.30278	0.395	0.407	0.357	0.3869
5	1.40	0.84949	0.115	0.128	0.120	0.1586
6	3.87	2.853	0.042	0.026	0.084	0.0664

Table 5 Summation calculations of delayed neutron spectra

	Saphier et al.[13]	Brady and England[15]
Fissioning nuclides	6	28
Precursors	20	271
Neutron emission probability (P_n)	Tomlinson[6] (average values of experimental data)	Measured values for 83 ground states and 3 meta-stable states. Systematics of Kratz-Herrmann adopted for others.
neutron spectra from each precursor	Experimental data for 20 precursors	Experimental data for 34 precursors with modification, and evaporation spectra for others
Fission yields	evaluation by Meak and Rider[26]	ENDF/B-VI

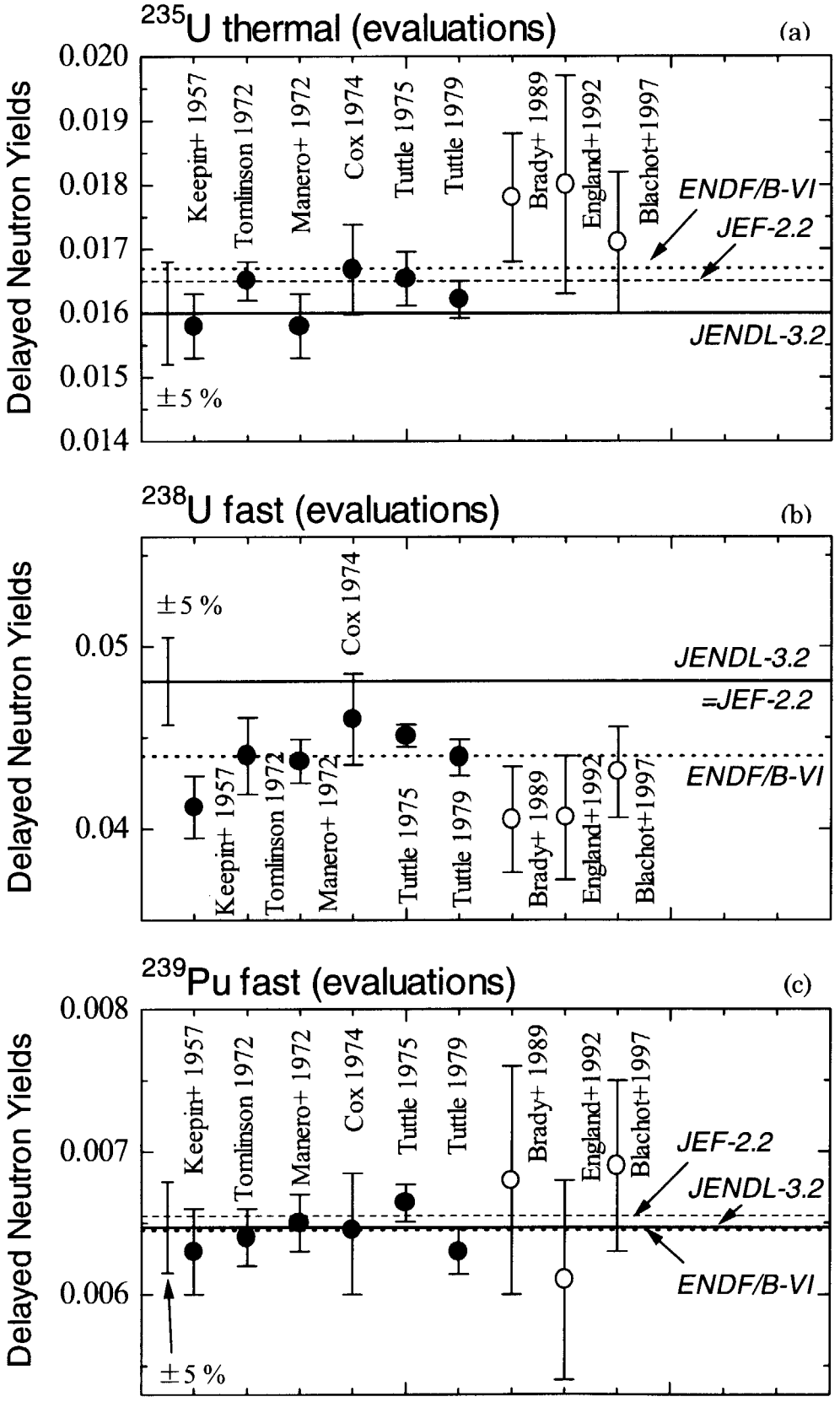

Fig. 1 Comparison of evaluated ν_d values

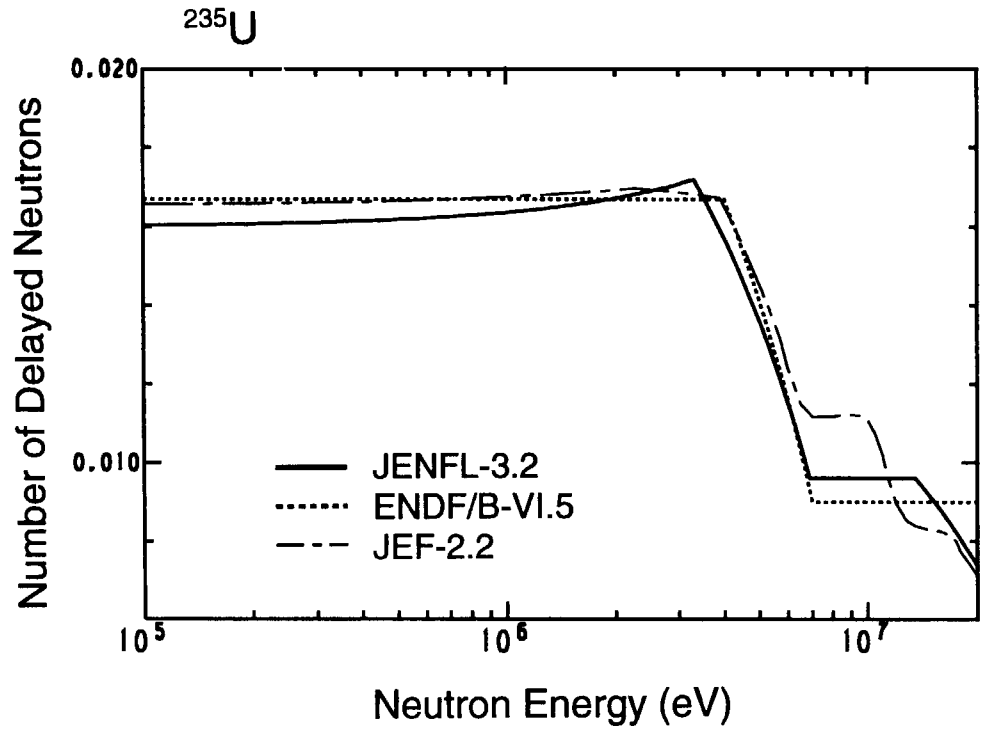

Fig.2 Total number of delayed neutrons (^{235}U)

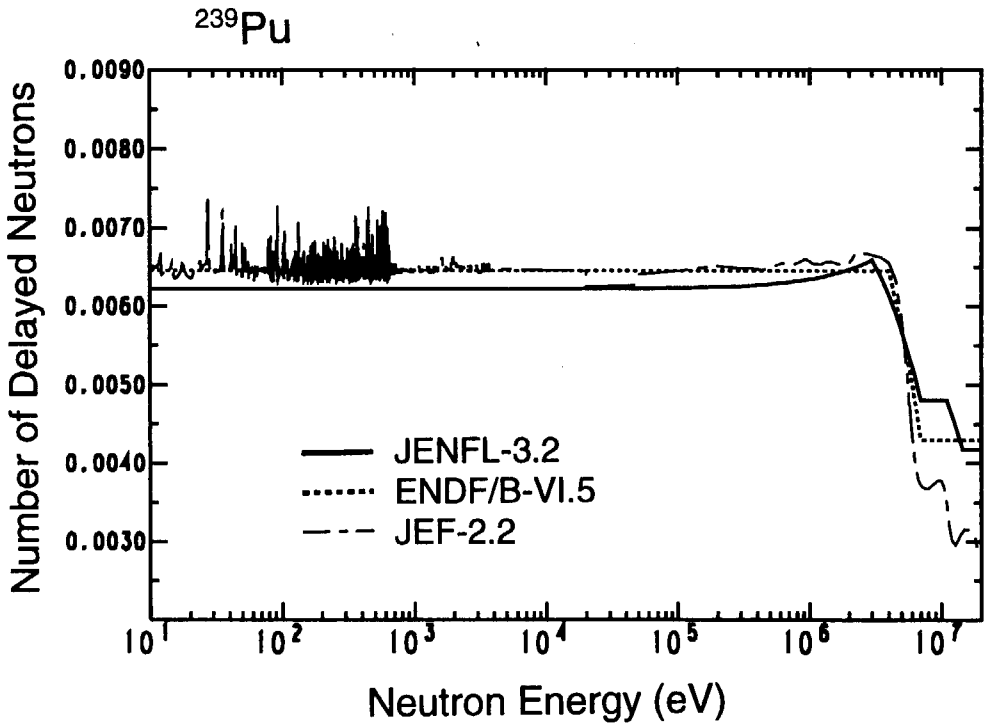

Fig.3 Total number of delayed neutrons (^{239}Pu)

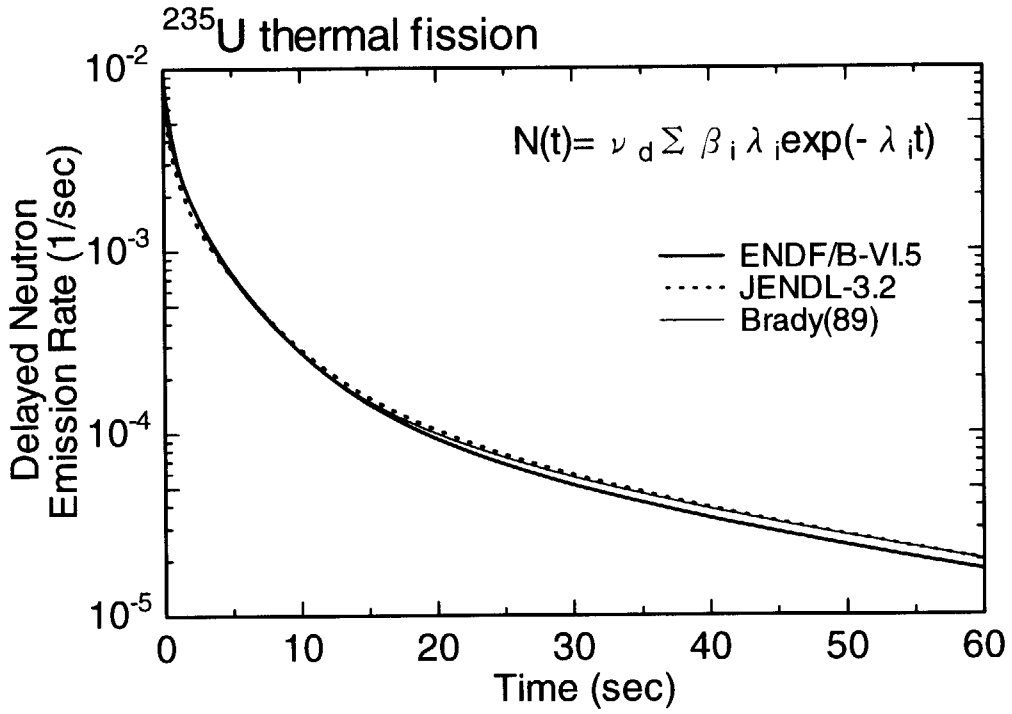

Fig.4 Calculated delayed neutron emission rate of ^{235}U thermal fission

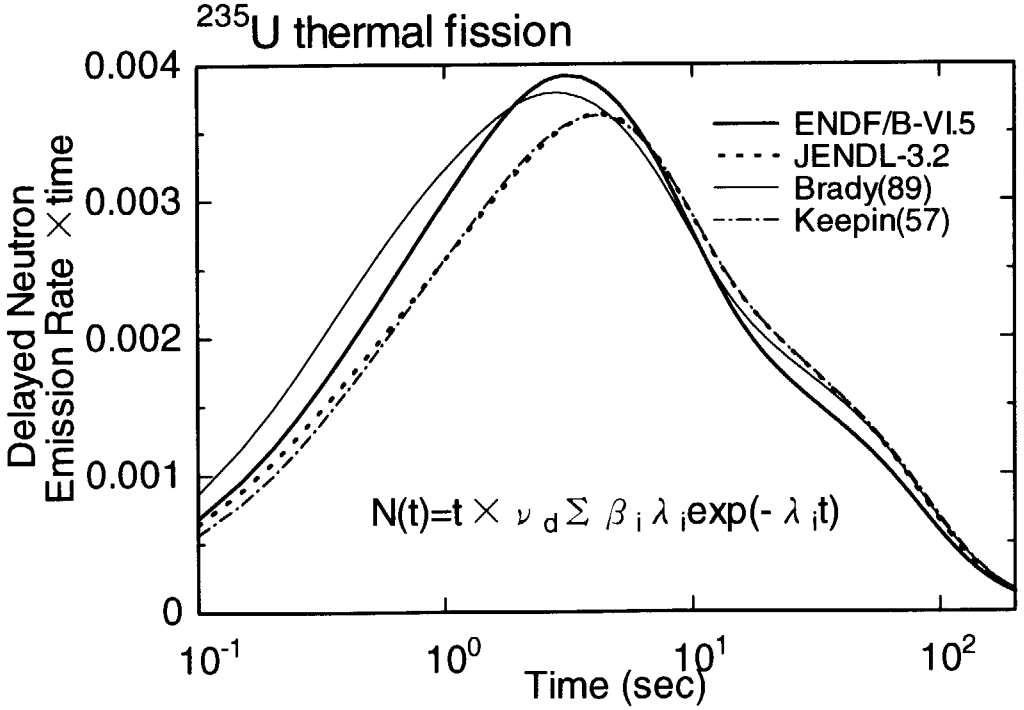

Fig.5 Calculated delayed neutron emission rate of ^{235}U thermal fission

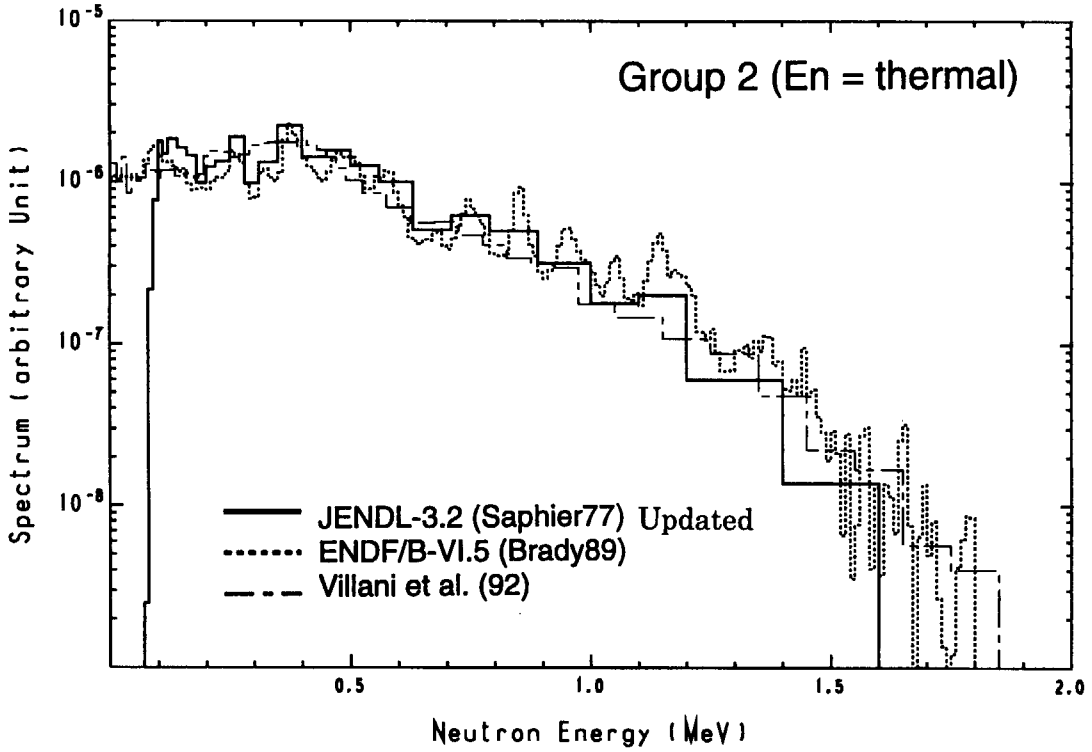

Fig.6 (a) Delayed neutron spectra from ^{235}U thermal fission (Group 2)

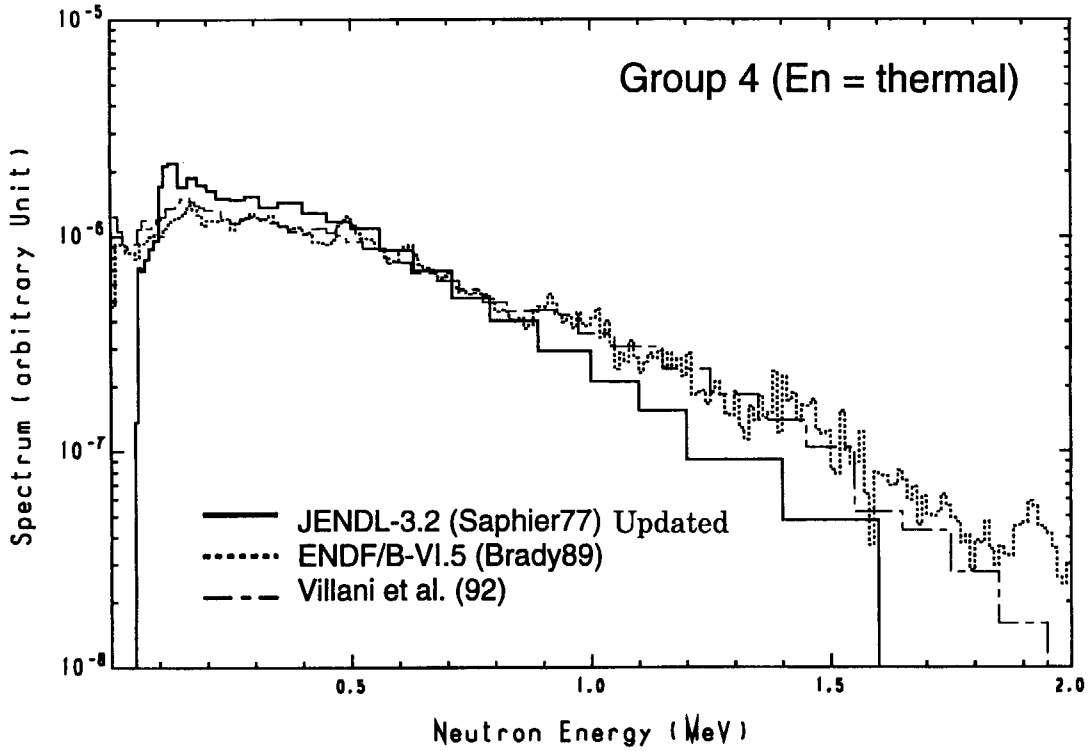

Fig.6 (b) Delayed neutron spectra from ^{235}U thermal fission (Group 4)

3. The Recent Measurements of Delayed Neutron Emission from Minor Actinide Isotopes Conducted at Texas A&M University

Masaki ANDOH

Reactor Physics Laboratory, Japan Atomic Energy Research Institute

Tokai-mura, Naka-gun, Ibaraki-ken 319-1195

e-mail: andoh@fca001.tokai.jaeri.go.jp

This paper summarizes resent measurements of delayed neutron emission from minor actinide isotopes using the Triga Reactor at the Texas A&M University (TAMU) Nuclear Science Center (NSC). Operating the Nuclear Science Center Reactor (NSCR) in a pulsed mode, a complete set of delayed neutron parameters were obtained for Np-237 and Am-243. Delayed neutron energy spectra following neutron induced fission were measured for U-235 and Np-237. These spectra were compared to those calculated using individual precursor P_n values, yields, and spectra from the ENDF/B-VI file.

1. Introduction

Texas A&M University (TAMU), in collaboration with Oak Ridge National Laboratory and Japan Atomic Energy Research Institute, has been actively studying the delayed neutron emission characteristics of the minor actinide isotopes using the Triga Reactor at the TAMU Nuclear Science Center (NSC).[1,2,3]

Due to a transfer time from core-to-detector of ~0.5 seconds, the previous experiments have been unable to measure the shortest-lived delayed neutron groups. The existing

experimental system has been modified to allow for pulsed experiments. One special feature of the NSCR is its ability to be operated in a pulsed mode. This feature allows the generation of extremely high neutron fluxes for very brief time periods. Thus, using the pulsing capabilities of the reactor, an irradiation could be performed that would accentuate the shorter-lived delayed neutron groups, allowing for a measurement of the complete the delayed neutron emission parameters. The "seven-group" structure[4] was used throughout the measurements.

Recently, a proton recoil detector system was designed, built, and characterized for use in measuring delayed neutron energy spectra following neutron induced fission. The system has been used to measure aggregate delayed neutron energy spectra from neutron induced fission of U-235 and Np-237.

2. Experimental Procedure

A. Actinide Samples

Two U-235 and Np-237 samples and three Am-243 samples (fabricated by Isotopes Products Laboratory in California) were used during the irradiations. The samples consisted of an inner pellet 4.88 mm in diameter and 0.92 mm thick. The pellet was composed of a matrix of aluminum powder and actinide oxide. The aluminum and actinide were mixed together and pressed under high pressure to form the disc-shaped pellets. The pellets were encapsulated in a thin (0.05 mm) titanium cover.

B. Measurement System

The TAMU delayed neutron measurement system is composed of several integrated components (a pneumatic transfer system, a detector array, a storage container, and sensors) controlled by a computer with an internal I/O card. The sample to be irradiated is transferred to the core, to the detector array, and to a remote storage box via a pneumatic transfer system.

A series of sensors transfer data to the computer relaying various information including sample position, permit control, and reactor pulse power. In a pulsing operation, the computer control system (CCS) can immediately return the sample following a pulse.

The sample to be irradiated is transferred to and from the core using a pneumatic system consisting of pressurized CO_2 gas, polyethylene tubing, a series of Swagelok Unions, and associated electronics and pneumatics. This pneumatic system connects all the individual components of the measurement system and provides a safe means of transporting the potentially radioactive samples to the detector array and to a remote storage location.

In the measurement of delayed neutron emission parameters, a BF_3 detector array is used. The detector array consists of three BF_3 proportional counters (N. Wood Model G-20-5) embedded in a block of paraffin. A lead sheath surrounds the sample tube to decrease the gamma-ray build-up in the detectors. Also, a thin cadmium sheet surrounds the detector array to eliminate any background sources of neutrons. The individual signals from the three detectors are combined using a dual-sum inverting amplifier. The signal then passes to the CCS computer that allocates the pulses to various time bins. The detector efficiency for delayed neutrons was estimated 2.17% using a Cf-252 source.

In the measurement of delayed neutron spectra, a proton recoil detector array consisting of three high-pressure proton recoil detectors (LND Model 28305) is used. The array consists of the detectors, a sample tube with a lead sheath and outer lead shielding. The array was characterized using several neutron and gamma-ray sources to check for efficiency, gamma-ray response, and reliability of the unfolding techniques. Resultant measured proton recoil distributions were unfolded using a modified version of the spectrum unfolding code PSNS (the new code was renamed SAC). SAC used response functions calculated using MCNP 4A.

C. Measurement of Delayed Neutron

Several measurements have been performed to determine the short-lived delayed neutron

group yields and half-lives for Np-237 and Am-243. The samples were irradiated in the NSCR core at 300 W for approximately 10 seconds; then, the reactor was pulsed by adding $1.50 reactivity. The pulses last for approximately 60 milliseconds. The CCS reads the power from the reactor console and removes the sample at the peak of the pulse. The sample is then transferred to the BF_3 detector array where the delayed neutrons versus time are counted. Due to the larger fission of U-235 by the pulsed irradiation, the U-235 samples could not be measured. It was estimated that the detector dead time would have been unacceptably high and disrupted the accuracy of the results.

A high-purity germanium detector was used to determine the total number of fissions in the sample by measuring the buildup of certain fission products (specifically Ba-140, La-140, Ru-103, I-131, Mo-99, Zr-97, Sr-91, Te-132, I-132, and I-135). The number of fissions were typically on the order of 10^9. In the fission rate determination, the yield data for the fission products was taken from the ENDF/B-VI file.

U-235 samples were irradiated in the NSC reactor at a power of 1 MW for 200 seconds. The delayed neutron spectrum was then acquired for up to 600 seconds. The resultant spectra were then unfolded using the SAC unfolding code. A similar technique was used to measure the delayed neutron spectra following a 200 second irradiation of a Np-237 sample; however, due to the lower fission rate in the Np-237 sample, multiple irradiations were required to generate sufficient statistics for unfolding. Within a period of 4 hours, two Np-237 samples were irradiated up to eight times each. The counts from each sample were added together to generate a composite spectrum.

The Am-243 samples contained Pu-239 0.19% as an impurity. Since Pu-239 has the extremely larger fission cross section than Am-243, there is a large contribution of Pu-239 to the Am-243 spectrum. To overcome the deficiency, a new sample of Am-243 with much higher purity should be used.

3. Results and Analysis

Parameters (yields and decay constants) for all seven groups of the alternate "seven-group" structure[4] were acquired from the measured emission rates using a graphical stripping procedure. The delayed neutron curves were fit using the following relation:

$$C(t) = N_f \varepsilon \sum_i Y_i \lambda_i \exp(-\lambda_i t)$$

where C(t) is the measured (dead-time corrected) delayed neutron count rates, N_f is the measured total number of fissions during the irradiation, ε is the detector efficiency, Y_i is the delayed neutron yield for group i, λ_i is the delayed neutron decay constant for group i, and t is the time after the end-of-irradiation. The pulsing technique was unable to produce enough counts to allow for accurate measurement of the group 1 and 2a values. Thus, the results determined previously[1,2] for group 1 were used to allow for a complete "seven-group" set. The group parameters determined in the experiments are presented in Table 1.

Table 1 Delayed neutron yields and decay constants for the pulsing experiments

Group	Np-237		Am-243	
	λ_i (sec^{-1})	Y_i (n/100 fissions)	λ_i (sec^{-1})	Y_i (n/100 fissions)
1	0.0124 ± 0.0003	0.035 ± 0.002	0.0124 ± 0.0004	0.014 ± 0.004
2a	0.0283 ± 0.0007	0.183 ± 0.012	0.0283 ± 0.0009	0.192 ± 0.009
2b	0.0411 ± 0.0008	0.095 ± 0.005	0.0415 ± 0.0009	0.075 ± 0.005
3	0.155 ± 0.002	0.325 ± 0.018	0.151 ± 0.002	0.175 ± 0.009
4	0.397 ± 0.006	0.368 ± 0.015	0.392 ± 0.006	0.285 ± 0.009
5	0.845 ± 0.03	0.100 ± 0.011	0.895 ± 0.04	0.075 ± 0.008
6	2.55 ± 0.03	0.037 ± 0.009	2.45 ± 0.04	0.035 ± 0.007
total		*1.14 ± 0.07*		*0.85 ± 0.05*

Figures 1 and 2 contain plots of the aggregate delayed neutron spectra from neutron induced fission of U-235 and Np-237, respectively. The figures also show the results from a

summation calculation involving the 18 most predominant precursors using P_n values, yields, and individual precursor spectra from ENDF/B-VI. The uncertainty on the measured data is generally within 5%. As can be seen, the measured and calculated spectra show reasonable agreement even though the summation calculation included only 18 of the 271 identified precursors (~87% of the total delayed neutrons emitted). It is expected that better agreement will be found when more precursors are added to this calculation. Because this measurement was simply an aggregate spectrum measurement, it is difficult to compare the result to the few previous measurements.

4. Conclusions

The recent research activities on the measurement of the delayed neutron data of the minor actinide isotopes conducted at Texas A&M University were summarized.

The measurements of the delayed neutron emission parameters were carried out using the Triga Reactor at the TAMU NSC with the pulsed operation. The data of the shortest-lived delayed neutron groups were obtained for Np-237 and Am-243. Experiments are planned to extend the above investigations to include other actinide isotopes (e.g., Pu-239, U-238, Am-241, etc..). Investigations to increase the number of detectors (and hence the detector array efficiency) are undergoing.

A series of the delayed neutron energy spectra measurements were made using the Np-237 and U-235 samples. These measurements showed agreement with ENDF/B-VI summation calculations. Experiments to measure time-dependent spectra are going to be performed in the future which will allow comparison to other results.

All the measured data and the results of the analysis described in this paper were offered by the research group at the TAMU.

References

[1] W. S. CHARLTON, *et al.*: *Proc. Int. Conf. on the Phys. of Reactors*, Mito, Japan, Sept. 16-20, 1996, p. F-11 (1996).

[2] W. S. CHARLTON, *et al.*: *Proc. Int. Conf. on Nucl. Data for Sci. and Tech.*, Trieste, Italy, May 19-24, 1997, p. 491 (1997).

[3] H. H. SALEH, *et al.*: *Nucl. Instr. and Methods in Phys. Res. B,* **103**, 393-400 (1995).

[4] T. A. Parish, *et al.*: *Nucl. Sci. Eng.*,**131**, 208(1999).

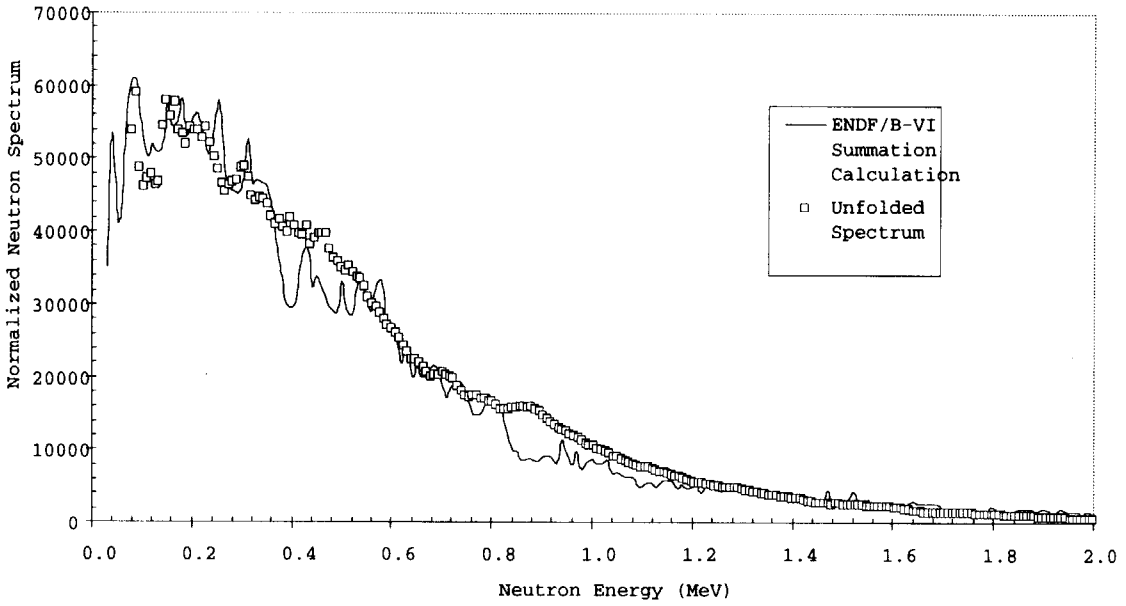

Fig. 1 Measured and calculated aggregate delayed neutron emission spectra for U-235

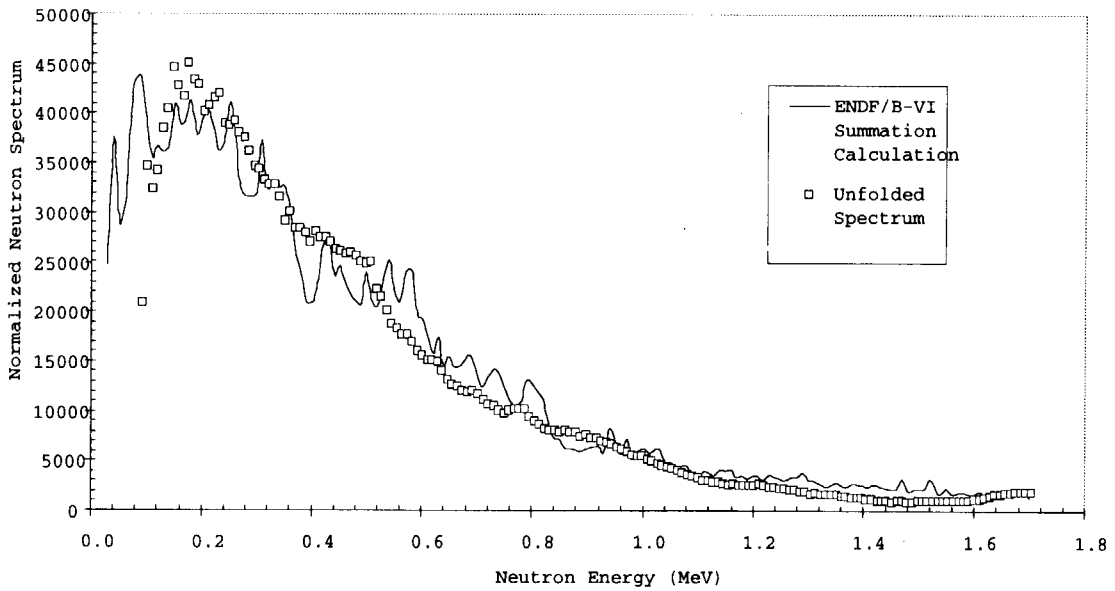

Fig. 2 Measured and calculated aggregate delayed neutron emission spectra for Np-237

JP9950502

JAERI－Conf 99－007

4. Benchmark Experiments of Effective Delayed Neutron Fraction β_{eff} at FCA

Takeshi Sakurai and Shigeaki Okajima
Reactor Physics Laboratory, Japan Atomic Energy Research Institute
Tokai-mura, Naka-gun, Ibaraki-ken 319-1195
e-mail: sakurai@fca001.tokai.jaeri.go.jp

Benchmark experiments of effective delayed neutron fraction β_{eff} were performed at Fast Critical Assembly (FCA) in the Japan Atomic Energy Research Institute. The experiments were made in three cores providing systematic change of nuclide contribution to the β_{eff} : XIX-1 core fueled with 93% enriched uranium, XIX-2 core fueled with plutonium and uranium(23% enrichment) and XIX-3 core fueled with plutonium(92% fissile Pu). Six organizations from five countries participated in these experiments and measured the β_{eff} by using their own methods and instruments. Target accuracy in the β_{eff} was achieved to be better than $\pm$3% by averaging the β_{eff} values measured using a wide variety of experimental methods.

1. Introduction

The effective delayed neutron fraction β_{eff} is an important parameter as a reactivity scale of a nuclear reactor. To validate delayed neutron data of ^{235}U, ^{238}U and ^{239}Pu which have large contribution to the β_{eff} of fast critical assemblies and fast power reactors, a program of benchmark experiments was performed in the Fast Critical Assembly(FCA) of the Japan Atomic Energy Research Institute(JAERI)[1].

Three cores were built for the benchmark experiments to provide a systematic change in ^{235}U, ^{238}U and ^{239}Pu contribution to the β_{eff}: XIX-1 core fueled with highly enriched uranium; XIX-2 core fueled with plutonium and natural uranium; XIX-3 core fueled with plutonium. Target accuracy of 3%(1σ) was requested for the experimental β_{eff}[2]. Six organizations from five countries(CEA/France, IPPE/Russia, KAERI/Korea, LANL/USA, Nagoya-University/Japan and JAERI/Japan)* participated in the experiments with their own measuremnt methods of the β_{eff}. Comparisons of the β_{eff}'s between the measurement methods were carried out to improve reliability of the measurements and to achieve the target accuracy.

This program was the complementary nature to the previous one in the MASURCA fast critical facility of CEA-Cadarache[3]. These programs in the FCA and the MASURCA were conducted under the NEA/NSC Working Party on International Evaluation Cooperation (WPEC), Subgroup 6 on delayed neutron data validation.

*KAERI: Korea Atomic Energy Research Institute,
CEA: Comissariat á l'Energy Atomic,
IPPE: Institute of Physics and Power Engineering,
LANL: Los Alamos National Laboratory

In this paper, characteristics of three cores are shown and the measurement results of the β_{eff} are summarized. Description of the FCA cores are shown in Chap.2. The β_{eff}'s by the individual methods are summarized in Chap.3. Finalization of the β_{eff} at each core is discussed in Chap.4.

2. Brief Description of the FCA Cores

Three cores for the β_{eff} measurements were chosen : XIX-1(U) core, XIX-2(Pu/U) core and XIX-3(Pu) core. Main characteristics of these cores are summarized in Table 1. A cylindrical model of these cores is shown in Fig.1. These cores were simple in geometry. Each core was composed of a core region and axial and radial blanket regions(SB and DUB regions in Fig.1).

Core fuel cells were composed of square plates of a dimension of 50.8mm by 50.8mm with thickness ranging from 1.59mm to 6.35mm. Plate arrangements in the unit cells are shown in Fig.2. The XIX-1 core is fueled with 93% enriched uranium plates. The XIX-2 core is fueled with plates of plutonium(92% fissile) and natural uranium. The XIX-3 core is fueled with the plutonium plates. The SB blanket cell is composed of depleted uranium oxide plates and sodium plates. The DUB blanket cell is composed of a depleted uranium metal block.

Figure 3 shows the systematic change of nuclide contribution to the β_{eff} in these cores together with those of the previous benchmark experiments at MASURCA: R2(30% enrichement uranium fuel) and Zona2(25% enrichement Mox fuel). The contributions of the principal nuclides to the β_{eff} in FCA XIX-2 core were similar to those in MASURCA Zona2 core.

3. β_{eff}'s by individual methods

Table 2 summarizes the experimental methods adopted by the participants. An overview of these β_{eff} measurement methods is given in reference[1]. These methods can not directly give the β_{eff}, but they yield it using several parameters as shown in Table 3. These parameters are categorized as shown in this table:

(a) Parameters that are peculiar to each method and were measured by each participant and

(b) Parameters that are common to several methods.

Table 4 shows the β_{eff}'s which were measured by the individual methods. Each method determined the β_{eff} with uncertainty of $\pm$1.8~2.8%.

4. Finalization of β_{eff}

The final value of β_{eff} in each core was obtained by taking the mean value of the individual β_{eff}'s. Table 3 shows that several parameters were used in different methods. Covariances of β_{eff}'s between different methods were therefore taken into account to determine the mean value of β_{eff}. For this purpose, the correlation coefficients of β_{eff}'s between the methods were estimated in each core. The correlation matrix in the XIX-1 core is shown in Table 5 as a typical example. The mean value m of the β_{eff} was determined by[4]

$$m = (\mathbf{u} \cdot \mathbf{C}^{-1} \cdot \mathbf{u}^{T})^{-1} \cdot \mathbf{u} \cdot \mathbf{C}^{-1} \cdot \mathbf{p}, \qquad (1)$$

where $\mathbf{p}$ is a column vector whose elements are the β_{eff}'s by the individual methods; $\mathbf{C}$ is

a covariance matrix of β_{eff}'s; $\mathbf{u}$ is a row vector with all elements equal to one; T means a transpose of vector. The statistical parameter χ^2 was estimated by

$$\chi^2 = (\mathbf{r} \cdot \mathbf{C}^{-1} \cdot \mathbf{r}^T), \quad (2)$$

where the $\mathbf{r}$ is a row vector whose elements are the residuals of the individual β_{eff}'s around the m. The internal uncertainty e_{int} of the m was estimated by the error propagation law:

$$e_{int} = \sqrt{(\mathbf{u} \cdot \mathbf{C}^{-1} \cdot \mathbf{u}^T)^{-1}}. \quad (3)$$

Furthermore, the external uncertainty e_{ext} was estimated by

$$e_{ext} = \sqrt{\chi^2/f} \cdot e_{int}, \quad (4)$$

where the f is the degrees of freedom. The e_{ext} reflects the scattering of the individual data around the mean value.

Table 6 shows the results for the mean value, the internal uncertainty of the mean value and the χ^2, where the estimated internal uncertainty was less than 2%. Figure 4 shows the residuals of individual β_{eff}'s around the mean with the range of internal uncertainty. The residuals were almost within the internal uncertainty in the XIX-3 core. On the other hand, the internal uncertainty was found to be too small to reflect the scattering of the data in the XIX-1 core.

A quantitative discussion for the scattering of these data can be made by using the parameter χ^2. The χ^2's were 23 and 2.1 for five and one degrees of freedom in the XIX-1 and XIX-2 cores respectively, while the χ^2 was 3.1 for three degrees of freedom in the XIX-3 core. The large χ^2's compared with the degrees of freedom indicate that the uncertainties of individual β_{eff}'s were underestimated in the XIX-1 and XIX-2 cores. To reflect the spread of the data, the external uncertainty of the mean value was adopted in the XIX-1 and XIX-2 cores. The external uncertainties are also shown in Table 6. No uncertainty exceeded 3%.

5. Summary

Measurements of the β_{eff} were performed using wide variety of the methods in three cores providing systematic change of nuclide contribution to the β_{eff}. The uncertainty of the β_{eff} by the individual method was ±1.8~2.8%. The mean values of the β_{eff} were 742pcm, 364pcm and 250pcm at the cores of XIX-1, XIX-2 and XIX-3 respectively. The uncertainties of these mean values were estimated by taking account of the spread of the individual β_{eff}'s and were found to be not more than 3%. The measured β_{eff} in this work can be used in future to validate the delayed neutron yields of the principal nuclides of ^{235}U, ^{239}Pu and ^{238}U.

Acknowledgements

We would like to thank Dr. T. Mukaiyama of JAERI for his contribution to initiate this experimental program. We would also like to thank all the participants in the present benchmark experiments. The authors are grateful to the FCA operating staff for their support to perform the present experiments.

References

[1] Sakurai T., *et al.*: "Benchmark Experiments of Effective Delayed Neutron Fraction β_{eff} at FCA-JAERI", Proc. Int. Conf. on the Physics of Nuclear Science and Technology, Oct. 5-8, 1998, Long Island, USA, p.182 (1998, American Nuclear Society, Inc.).

[2] Blachot J., *et al.*: "Status of Delayed Neutron Data - 1990", OECD NUCLEAR ENERGY AGENCY(NEA), NEACRP-L-323, 1990.

[3] Bertrand P., *et al.*: "BERNICE -Interlaboratory Comparison of β_{eff} Measurement Techniques at MASURCA", Proc. Int. Conf. on the Physics of Reactors, Sept. 16-20, 1998, MITO, JAPAN, E-190.

[4] Brandt S.: "Statistical and Computational Methods in Data Analysis", Second revised edition, (1976, North-Holland Publishing Company, New York, USA).

Table 1 Main characteristics of FCA cores

Core	XIX-1	XIX-2	XIX-3
Fuel	Enriched uranium	Plutonium /Natural uranium	Plutonium
Fuel enrichment	93%	23%	(92% fissile Pu)
Moderator	Graphite	Sodium	Stainless steel
Core dimensions(cm) Radius(R_C) x Height(H_C)	33.0 x 50.8	35.7 x 61.0	35.1 x 61.0
β_{eff}(pcm)*	774	376	251

*Calculated value

Table 2 Participants and measurement methods of β_{eff} in FCA cores

Core	XIX-1	XIX-2	XIX-3
JAERI/KAERI (Japan/Korea)	^{252}Cf source method	^{252}Cf source method	^{252}Cf source method
JAERI (Japan)	Covariance-to-mean method	— —	Covariance-to-mean method
CEA (France)	Noise method	— —	Noise method
IPPE (Russia)	Rossi-α method ^{252}Cf source method	^{252}Cf source method	^{252}Cf source method
LANL (USA)	Nelson-number method	— —	— —
Nagoya University (Japan)	Covariance method	Covariance method	Covariance method

Table 3 Principal parameters used in the β_{eff} measurement methods

Method†	Covariance -to-mean	Covari -ance	Noise	Rossi -α	Nelson -number	^{252}Cf source
(a) Parameters that were peculiar to each method						
Covariance-to-mean ratio	○					
Local covariance		○				
Cross power spectrum density			○			
Rossi-α correlation amplitude				○	○	
Cf source intensity					○	○
Apparent reactivity worth of ^{252}Cf source (in dollars)						○
Reactivity (in dollars)†					○	
(b) Parameters that were common to several methods						
Central fission rate of core material per volume	○	○	○	○		○
Reactivity (in dollars)‡	○	○	○	○		
Relative fission integral	○	○	○	○		
Normalization integral						○
Diven factor	○	○	○	○	○	
Spatial correction factor D_S	○	○	○	○	○	
Spatial correction factor g*					○	

† Reactivity determined by Rossi-α measurements
‡ Reactivity determined by calibrated control rods

Table 4 Experimental β_{eff}'s by different methods

Core	XIX-1	XIX-2	XIX-3
Covariance-to-mean	724±13*(1.8%)†	—	251±5(2.0%)
Covariance	782±16(2.1%)	368±6(1.7%)	256±4(1.6%)
Noise	730±15(2.0%)	—	248±5(2.0%)
Rossi-α	771±17(2.2%)	—	—
Nelson-number	737±20(2.7%)	—	—
Cf source	727±20(2.7%)	354±10(2.8%)	247±7(2.9%)

* Unit : pcm
† Values in parentheses : relative uncertainty

Table 5 Correlation matrix* of the β_{eff} between different methods

Method	(a)	(b)	(c)	(d)	(e)	(f)
(a) Covariance-to-mean	1.00					
(b) Covariance	0.47	1.00				
(c) Noise	0.47	0.43	1.00			
(d) Rossi-α	0.43	0.39	0.39	1.00		
(e) Nelson-number	0.58	0.53	0.53	0.48	1.00	
(f) Cf source	0.21	0.18	0.18	0.23	-0.32	1.00

* Symmetrical matrix

Table 6 Mean value and uncertainty of β_{eff}

Core	XIX-1	XIX-2	XIX-3
Mean value of β_{eff}	742pcm	364pcm	250pcm
Internal uncertainty	±11pcm(1.4%)	±7pcm(1.9%)	±4pcm(1.6%)
Degrees of freedom	5	1	3
χ^2	23	2.1	3.1
External uncertainty	±22pcm(3.0%)	±10pcm(2.8%)	±4pcm(1.6%)

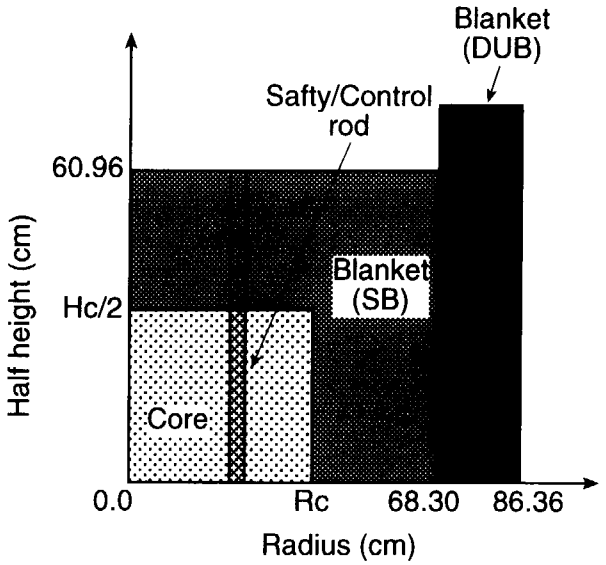

Fig.1 Cylindrical model of FCA cores for benchmark experiments of β_{eff}. Core dimensions are shown in Table 1.

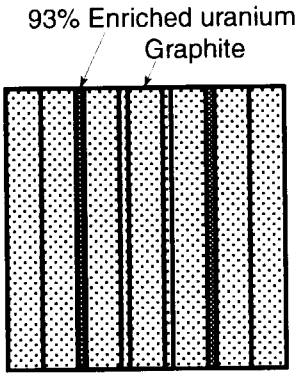

(a) XIX-1 core fuel cell

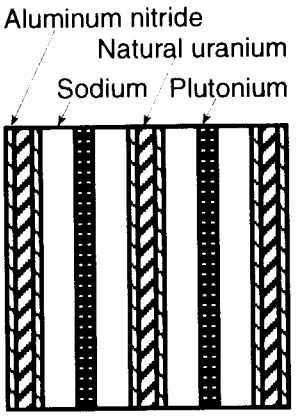

(b) XIX-2 core fuel cell

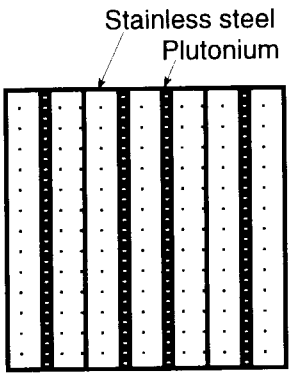

(c) XIX-3 core fuel cell

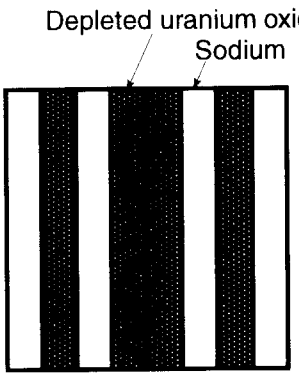

(d) SB blanket cell

Fig.2 Plate arrangements in fuel cells of FCA cores

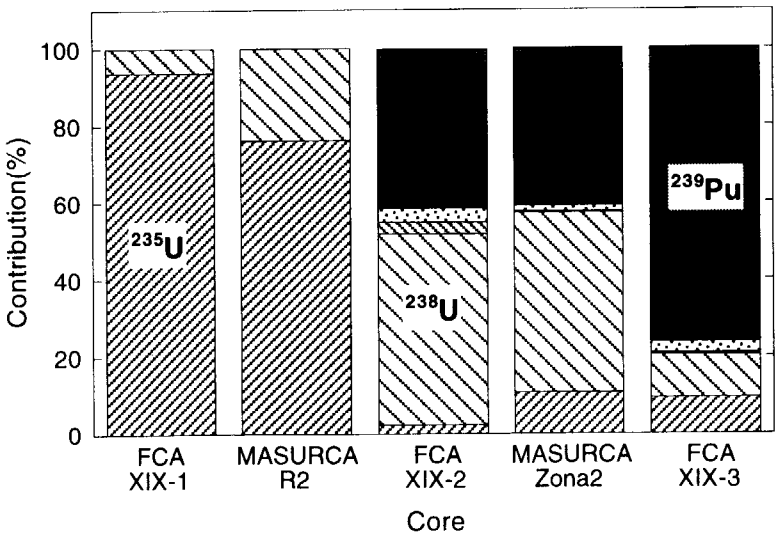

Fig.3 Comparison of nuclide contribution to the β_{eff} of five cores in FCA and MASURCA[3]

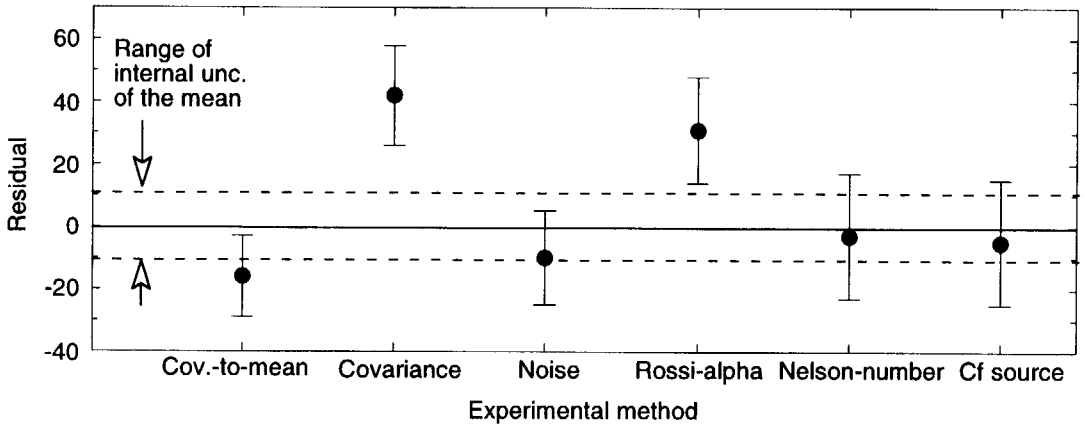

(a) XIX-1 core

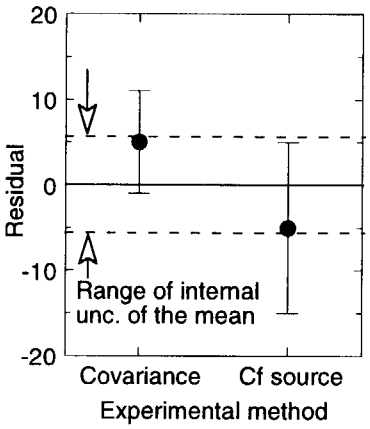

(b) XIX-2 core

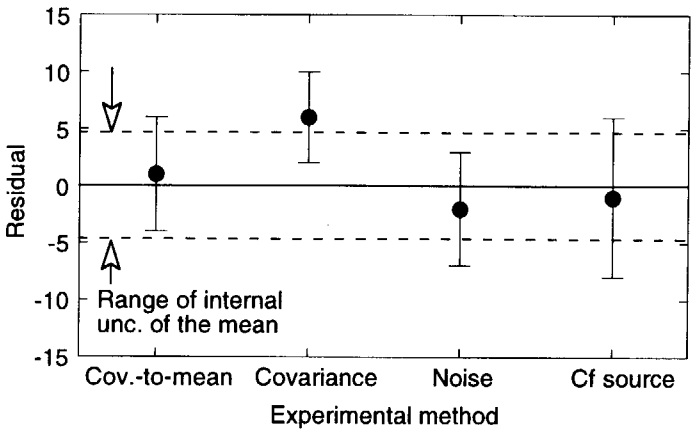

(c) XIX-3 core

Fig.4 Residuals of β_{eff}'s by individual methods around the mean value of β_{eff}. Range of internal uncertainty estimated by Eq.(3) is shown by dotted lines in each core.

5. Measurement of the effective delayed neutron fraction for the TCA cores

Ken NAKAJIMA
Criticality Safety Laboratory
Department of Fuel Cycle Safety Research
Japan Atomic Energy Research Institute
Tokai-mura, Naka-gun, Ibaraki-ken 319-1195 JAPAN
email: nakajima@melody.tokai.jaeri.go.jp

The effective delayed neutron fraction, β_{eff}, was measured for light-water moderated low-enriched UO_2 cores using the following two methods.

1) Substitution method,

2) Method using the buckling coefficient of reactivity (K-method).

The results of both methods agreed well each other. The K-method was, then, applied for three MOX cores to obtain their β_{eff} values. All the results of experiments showed good agreements with the calculations employing the JENDL-3.2 library, although the experiments were slightly larger than the calculations for all cases.

1. Introduction

The effective delayed neutron fraction, β_{eff}, is used to convert the unit of the measured reactivity to that of the calculated one. Recently, it is required to improve the accuracy in β_{eff} calculations in order to reduce the uncertainty of reactor designing work[1].

The present paper describes the results of β_{eff} measurements for the light-water moderated UO_2 and MOX cores of the TCA[2,3]. Comparisons with the calculated results are also presented.

2. Measurement Techniques

2.1 Substitution method[4,5]

According to the perturbation theory, the reactivity change caused by substituting absorber rods for all fuel rods in the core is given by the following equation.

$$\sum_i \rho_i = -\frac{1}{\beta_{eff}}(1-\delta A) \equiv -\frac{1}{\beta_{eff}}\left\{1-\frac{\left\langle\left(\Sigma_a-\Sigma_a{}^P\right)\phi\phi^*\right\rangle}{\left\langle\nu\Sigma_f\phi\phi^*\right\rangle}\right\}, \qquad (1)$$

where ρ_i : Reactivity change of the substitution at position i,

Σ_a, $\Sigma_a{}^P$: Absorption cross section of fuel and absorber rods,

$\nu\Sigma_a$: Production cross section,

ϕ, ϕ^* : Forward and adjoint flux.

The brackets < > in the last term of right-hand in Eq.(1) indicate the integration overall energy range and whole core volume. The β_{eff} is obtained by measuring the substitution reactivities for all fuel rods. The reactivity change for the substitution is evaluated from the change of critical water level between the clean and the substituted cores. The term δA in Eq.(1) is a factor to correct the difference of absorption cross sections between the fuel and the absorber rods.

2.2 Method using the buckling coefficient of reactivity (K-method)[6]

The buckling coefficient of reactivity, K, is defined as the ratio of the reactivity change to the vertical buckling change of the core. Practically, the measured coefficient, K_{EXP}, has the unit of \$·cm^2, and the calculated K_{CAL} has the unit of dk/k·cm^2. The β_{eff} is then obtained as the ratio of the calculated to the measured K's, as shown in Eq.(2).

$$\beta_{eff} = K_{CAL}/K_{EXP} . \qquad (2)$$

In the measurements, the vertical buckling change is produced by a change of core water level, and the reactivity change is measured by using the reactivity-meter.

3. Measurements for UO_2 cores

3.1 Substitution method[3,4,7]

The specifications of the UO_2 experiment core are shown in Fig.1. A closed circle in Fig.1 corresponds to the position in which the absorber rod was substituted for the fuel. An SB-Cd-Pb alloy absorber was used in the present experiments. The correction factor δA was calculated using the SRAC code system[8] with the JENDL-3.2 nuclear data library[9]. The results of the measurements are listed in Table 1.

Table 1 Measurement of β_{eff} for the UO_2 core by the substitution method[7]

Sum of the substitution reactivities	-129.0 \$
Correction factor δA	-0.0104
Effective delayed neutron fraction β_{eff}	0.00767

3.2 K-method[6]

The buckling coefficient of reactivity K was measured for five UO_2 cores with different core sizes, in order to obtain the precise value of K. The specifications of these experiment cores are shown in Fig.2. The continuous energy Monte Carlo code, MCNP[10], with the JENDL-3.2 library was used to obtain the calculated coefficient, K_{CAL}. The results are shown in Table 2.

As seen from Tables 1 and 2, the β_{eff} values obtained with the above two methods agree well each other, and this indicates that the present measurements are considered to be reliable.

Table 2 Measurement of β_{eff} for the UO_2 core by the K-method[6]

Measured coefficient K_{EXP}	4309 \$ δm^2
Calculated coefficient K_{CAL}	32.65 dk/k δm^2
Effective delayed neutron fraction β_{eff}	0.00758

4. Measurements for MOX cores by the K-method

The β_{eff} for MOX cores were measured by the K-method[11]. The specifications of the MOX cores are shown in Fig.3. The results of measurements including that for the UO_2 core are shown in Fig.4 in comparison with the calculations. In these calculations, the correction factors for the energy group collapsing and for the transport effects were multiplied to the β_{eff} values that were calculated with the diffusion code CITATION in the SRAC code system employing the JENDL-3.2 library[7]. All the experimental results show good agreements with the calculations, although the experiments are slightly larger than the calculations for all cases as shown in Fig.4. The maximum difference is about 3% which is observed for the UO_2 core.

5. Summary

The effective delayed neutron fraction β_{eff} for the light-water moderated UO_2 core of the TCA has been measured with the two methods, the substitution and the K-methods. The results of these measurements agreed well each other. Then, the β_{eff}'s for the light-water moderated MOX cores have been measured using the K-method. Although the experiments were slightly larger than the calculations for all cases, the experimental results agreed well with the calculations employing the JENDL-3.2 library. The maximum difference was about 3% which was observed for the UO_2 core.

References

[1] J. Rowlands, "Requirements for Delayed Neutron Data and the Current Status,"

Presentation at *Colloquy on delayed neutron data*, Obninsk, Russia, April 9-10, 1997.

[2] H. TSURUTSA et al., "Critical Sizes of Light-Water Moderated UO_2 and PuO_2-UO_2 Lattices," JAERI 1254 (1978).

[3] S. OKAJIMA et al., "Status and Future Program of Reactor Physics Experiments in JAERI Critical Facilities, FCA and TCA," *Proc. 1998 Symposium on Nuclear Data* (JAERI-Conf 99-002), Tokai, Japan, November 19-20, 1998.

[4] T. HAGA, I. KOBAYASHI, "Space Dependent Reactivity Effect of Fission and Absorption," *J. Nucl. Sci. Technol.*, **1** [7], 246 (1964).

[5] F. AKINO et al., "Measurement of Effective Delayed Neutron Fraction of VHTRC-1 Core," *J. Nucl. Sci. Technol.*, **31** [8], 861 (1994).

[6] T. SUZAKI et al., "Evaluation of β_{eff} by a Method Using Buckling Coefficient of Reactivity – (1) Methodology and Results on Uranium Core of TCA," *Preprint 1996 Fall Meeting AESJ*, A29 (1996), [in Japanese].

[7] K. NAKAJIMA, *Private Communication* (1999).

[8] K. OKUMURA et al., "SRAC95 ; General Purpose Neutronics Code System," JAERI-Data/Code 96-015 (1996), [in Japanese].

[9] T. NAKAGAWA et al., "Japanese Evaluated Nuclear Data Library Version 3 Revision-2 : JENDL-3.2," *J. Nucl. Sci. Technol.*, **32**, 1259 (1995).

[10] J. F. Briesmeister (Ed.), "MCNP – A General Monte Carlo N-Particle Transport Code, Version 4A," LA-12625 (1993).

[11] T. SUZAKI et al., "Evaluation of β_{eff} by a Method Using Buckling Coefficient of Reactivity – (4) Results on Pu-U 2-Regional Cores," *Preprint 1998 Annual Meeting AESJ*, G20 (1998), [in Japanese].

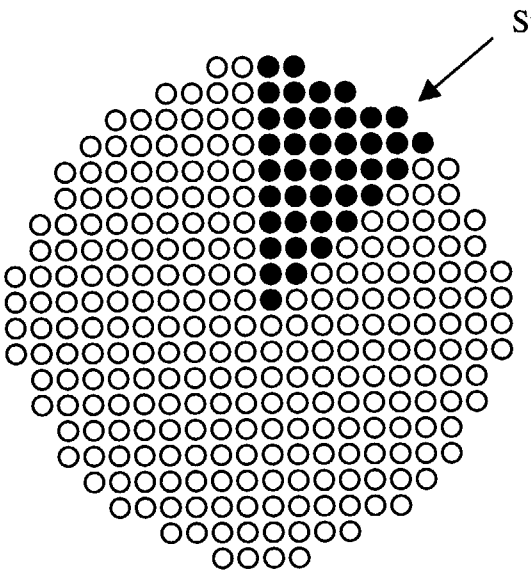

1.83U Cylindrical Core (292 rods)
Lattice pitch : 19.56mm
Water to Fuel Volume Ratio : 1.83
Critical Water Level : 92.24cm

Fuel Rod : 2.6wt% enriched UO_2

Absorber Rod : Sb-Cd-Pb rod
(Sb:48, Cd:0.184, Pb:51.8wt%)

Fig.1 Specifications of UO_2 core (1)

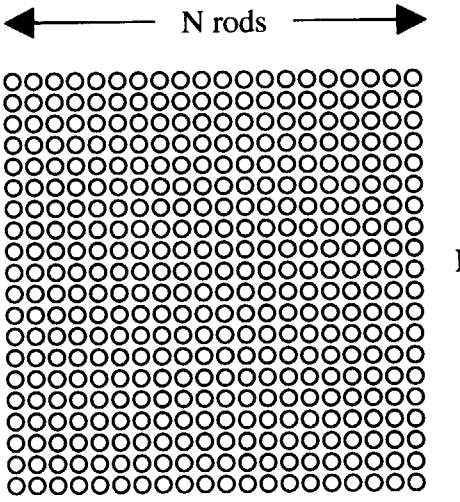

1.83U Square Core
Lattice pitch : 19.56mm
Water to Fuel Volume Ratio : 1.83

Fuel Rod : 2.6wt% enriched UO_2

Critical Water Level : H_c

N (rods)	H_c (cm)
17	113.03
18	75.42
19	60.21
20	51.10
21	45.71

Fig.2 Specifications of UO_2 core (2)

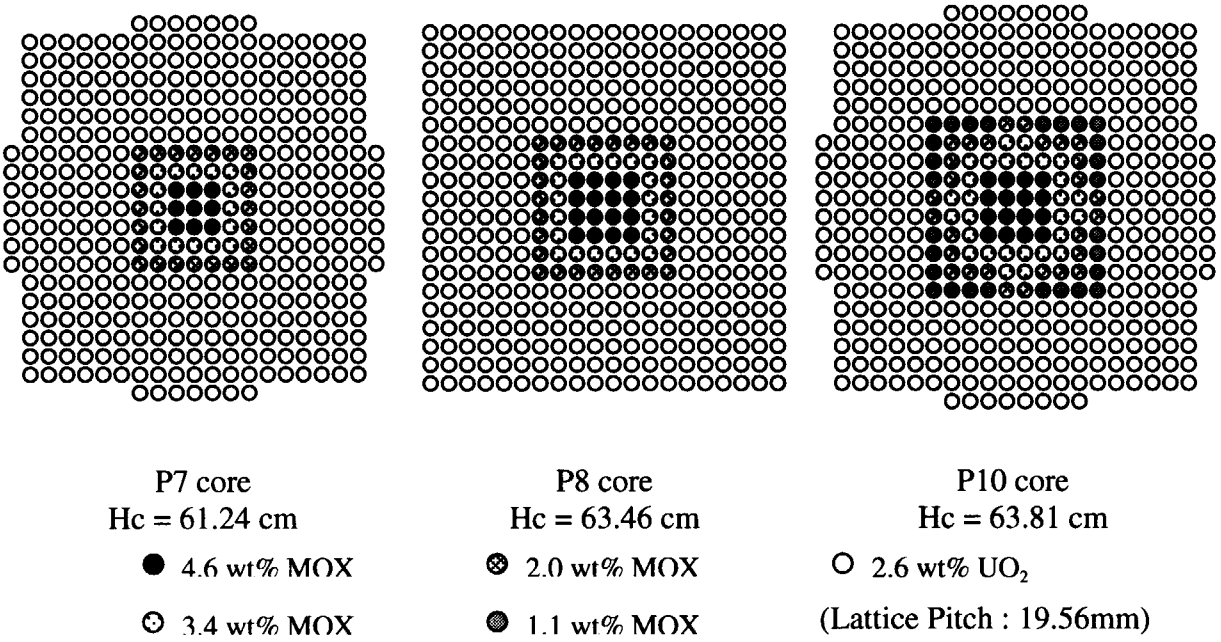

Fig.3 Specifications of MOX cores

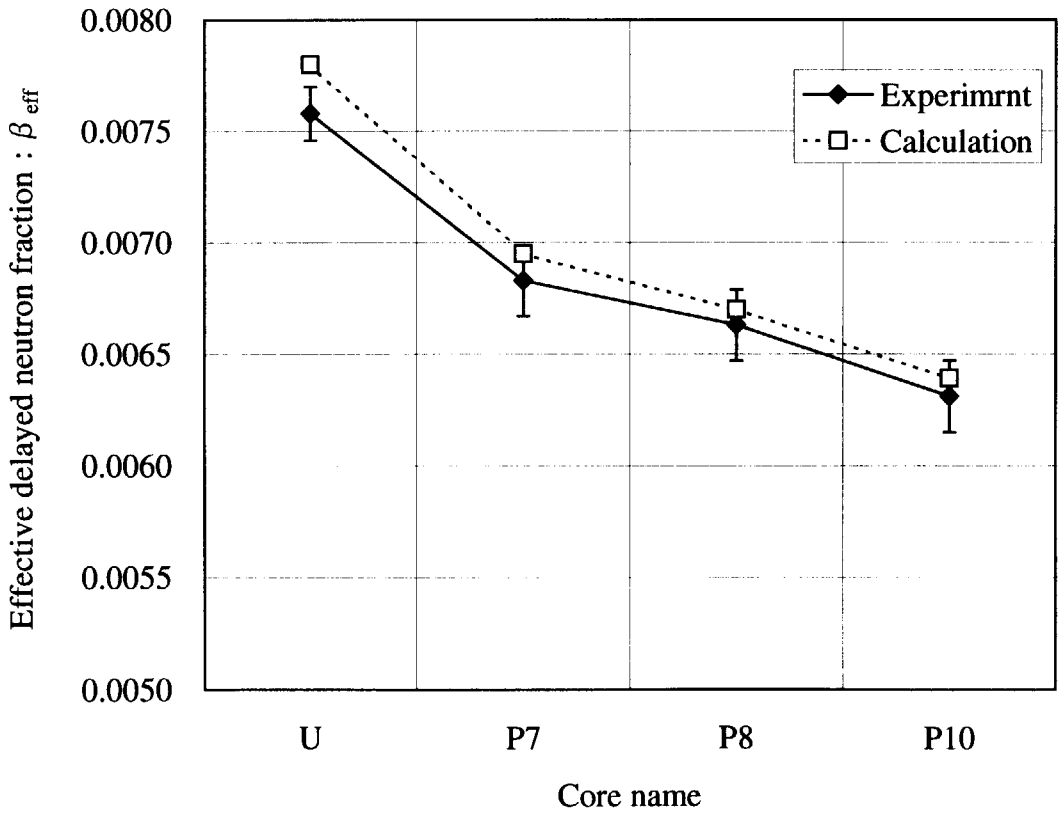

Fig.4 Results of β_{eff} measurements

6. Possible Fluctuations in Delayed Neutron Yields in the Resonance Region of U-235

Takaaki OHSAWA and Tomoyo OYAMA*

Department of Nuclear Engineering, Faculty of Science and Technology, Kinki University
3-4-1 Kowakae, Higashi-osaka, Osaka 577-8502, Japan
E-mail: ohsawa@mvg.biglobe.ne.jp

Abstract: An estimate of the delayed neutron yield in the resonance region of U-235 was made on the basis of the measurement of fragment mass and kinetic energy distributions and their analysis in terms of multimadal fission model performed at Geel. In contrast to the evaluation adopted in JEF-2.2, the calculated delayed neutron yield showed local dips at resonances.

1.Introduction

It is known that the delayed neutron (DN) yield remains almost constant in the energy range below 4 MeV. However, it has been pointed out by reactor physicists[1] that the DN yield data in the near-thermal region might be smaller than the constant value. In fact, some of the experimental data on DN yield in the lower end of the region tends to be lower than the plateau value (**Fig.1**). Reflecting these facts, evaluated data of the absolute DN yield for U-235 in JENDL-3.2 have a slight positive slope in the energy region concerned, and JEF-2.2 evaluation has some structures in the eV-region. (In contrast, ENDF/B-VI adopted a constant value. See **Fig.2**.) However, the physical reason for the decrease in the lower end of the region has not been clear so far, because, according to the conventional theory of fission, it was hard to consider that the precursor yields were changed in such a small energy range.

This report proposes a possible interpretation for the decrease, on the basis of multimodal analysis of fragment mass distribution in the resolved resonance region of U-235.

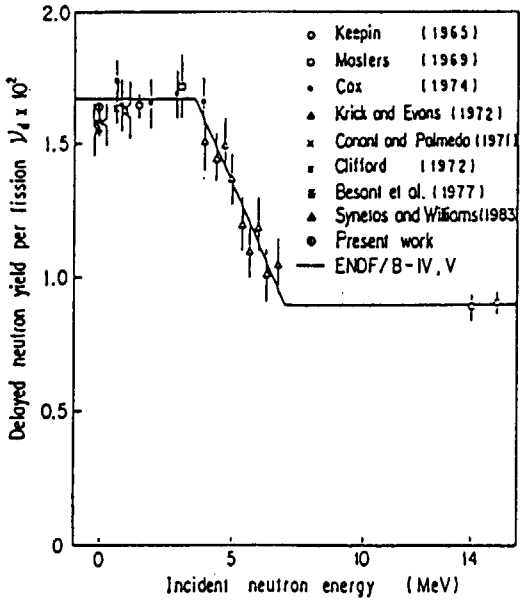

Fig.1 Experimental and evaluated data of delayed neutron yield for U-235 (taken from Ref.[1]).

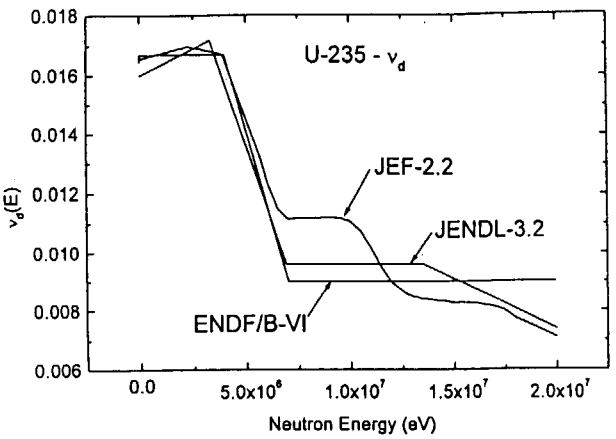

Fig.2 Comparison of evaluated DN yield data for U-235 in JENDL-3.2, JEF-2.2 and ENDF/B-VI.

*Present address: Graduate School of Engineering, Osaka University. Yamada-oka, Siuta-shi, Osaka.

2. Fission Mode Fluctuations at Resonances

Difference was observed by Hambsch *et al.* [2] in the fission fragment mass distributions from resonance to resonance for U-235, which are correlated with fluctuations of the reaction Q-value and also with the total kinetic energy averaged over all fragments. These data were analyzed in terms of multimodal fission model [3] and it was found that the mode branching ratios (w_{S1}, w_{S2}, *etc.*) differ from resonance to resonance, the observed changes of the ratios $(w_{S1}/w_{S2})_{res}/(w_{S1}/w_{S2})_{th}$ ranging up to 20% (the subscript S1, S2 refer to Standard-1 and Standard-2 mode, respectively). This amounts to a decrease of fission yields of the outside wings (A = 84–96, 140–152) and an increase of the inside wings (A = 96–108, 128– 140) of the mass distribution (**Fig.3**).

On the other hand, precursors of delayed neutrons lie the region where a nucleus has a few excessive neutrons just outside of the closed shell, because such a nucleus has higher neutron emission probability after beta-decay due to the lower neutron binding energy of the DN-emitter nucleus. These precursor regions are denoted in Fig.3 with bold horizontal lines. It can readily be seen that these regions overlap with the regions where substantial changes of mass yield are observed in the resonance-neutron fission. This implies that the yields of DN precursors fluctuate in the resonance region, resulting in local variation of DN yield. In order to verify this reasoning, estimation of possible changes in DN yield was made using the data of Hambsch *et al.* [2] as the basis.

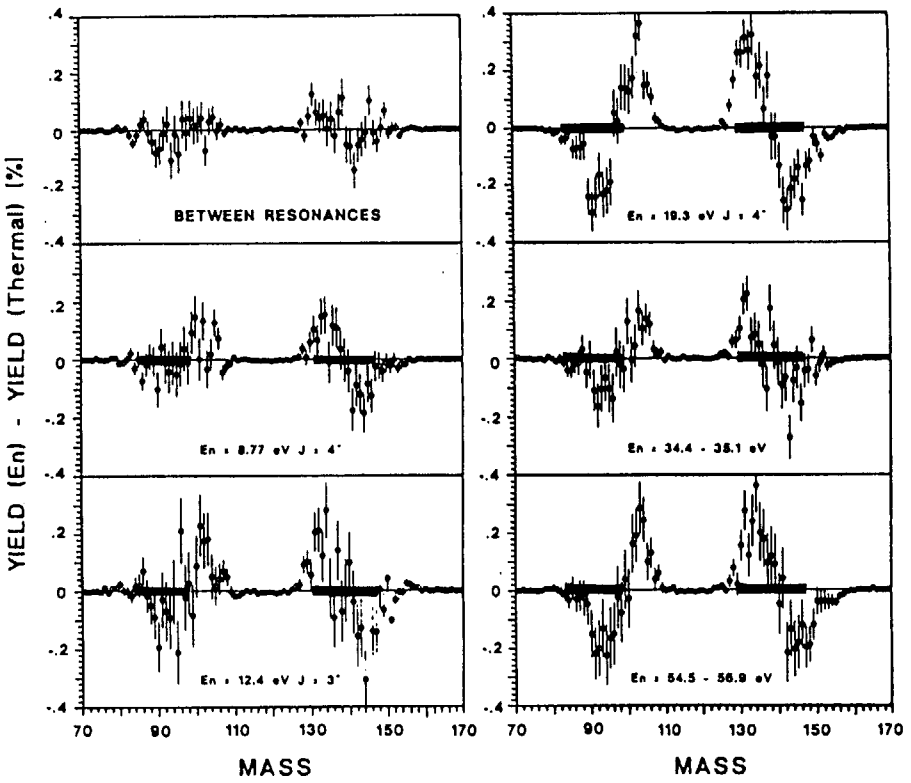

Fig. 3 Fragment yield differences at resonances with respect to the thermal values. (After F.-J.Hambsch *et al.* [2]. The bold horizontal lines, indicating the precursor regions, were added by the present author.)

3. Method

The total DN yield was calculated using the summation method:

$$\nu_d = \sum_i Y_i P_{ni}, \quad (1)$$

where Y_i is the fission yield and P_{ni} is the neutron emission probability of a precursor i. The fission yield Y_i was calculated by using the five-Gaussian representation with parameters given by Hambsch *et al.*, together with the data of Nishio *et al.* [4] on the prompt neutron multiplicity $\nu_p(A^*)$ as a function of the preneutron-emission mass of the fragment. Fragment charge distribution of Gaussian shape with the standard deviation σ =0.56 and the most probable charge

$$Z_p = Z_{UCD} \pm 0.5 \quad (2)$$

was used to obtain the independent fission yields, where Z_{UCD} is the charge predicted with the UCD (unchanged charge distribution) hypothesis. The even-odd effect of the proton number on the fission yield, defined by

$$X = (Ze - Zo)/(Ze + Zo), \quad (3)$$

was considered, using the formula proposed by the present author :

$$X = -0.1033 + 0.6907/(Z^2/A - 33.8486). \quad (4)$$

Two sets of data for the neutron emission probability were used: the set of Mann *et al.* [5], comprising 79 precursors, and the set of Wahl [6], comprising 271 precursors.

4. Results

The difference of the DN yield at 10.18 eV-resonance with respect to the thermal values as a function of precursor mass are shown in **Figs.4a** and **b** where Mann's and Wahl's P_n-data were used, respectively. In the heavy fragment (HF) region, a structure similar to Fig.3 is observed, which means that positive and negative contributions almost cancel out. In the light fragment (LF) region, however, the positive contribution is much less than the negative contribution, thus resulting in negative total value in this region. The same applies to other resonances, except 4.85, 38.41 and 81.9-86.2eV resonances where the opposite tendency is observed in mode branching ratios. Therefore the total DN yield at resonances is decreased compared with the thermal value, except for the three cases. This tendency is more emphasized for Fig.4b, because much more precursors are considered in Wahl's data set.

The relative variation of the DN yield ν_d(E)/ ν_d(thermal) simulated using the resonance parameters in [7] is shown in **Fig.5**. The degree of decrease differs from one resonance to another, the maximum decrease being about 2.3% in the region less than 100 eV. The effect of these dips in ν_d(E) on reactor physics will be amplified many times more than this value due to locally enhanced fission cross section at the resonances.

Two comments should be added here:

(1) The present result is only a preliminary one. The fragment charge distribution used in this work is just a rough approximation. Since the precursor nuclides lie in the tail region of the charge distribution curve, a slight change in the most probable charge Zp, given by eq.(2), and the standard deviation σ will change the fission yield considerably. Mass-dependent deviation of Zp from eq.(2) and possible fluctuation of σ, as was reported in [6], should be included. Refinement is required also for even-odd effect on fission yield; its dependence on the fragment mass and on the excitation energy should further be investigated.

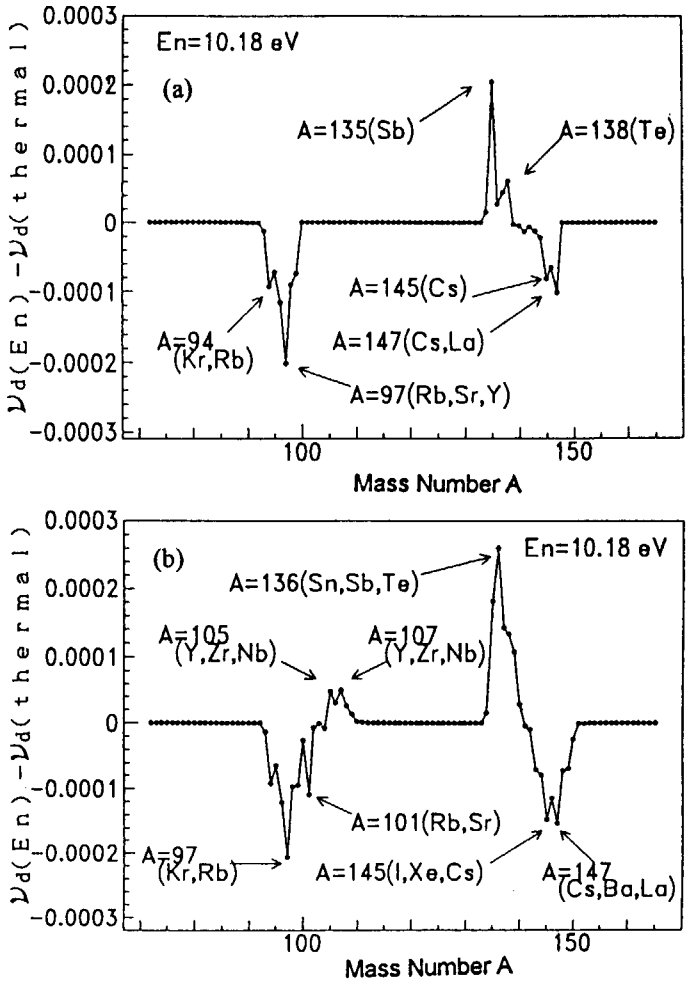

Fig.4 The difference of the DN yield at 10.18 eV-resonance with respect to thermal values as a function of precursor mass, calculated by using Mann's (a) and Wahl's data set (b).

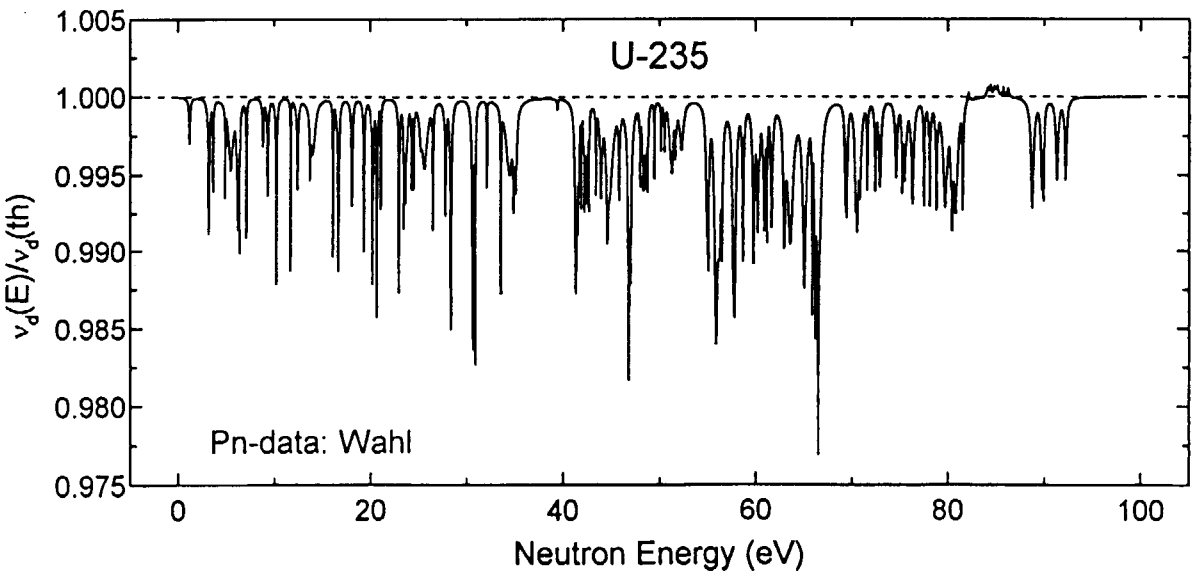

Fig.5 The relative variation of the DN yield vd(E)/ vd(thermal) simulated using the resonance parameters in [7].

(2) Figure 5 reminds us of the local dips at resonances observed in the average *prompt* neutron multiplicity $\nu_p(E)$ in ^{239}Pu. Fort *et al.* [8] analyzed these dips in terms of spin effect and (n,γf)-effect and this evaluation was reflected in JEF-2.2 file. They applied the model of Lendel *et al.* [9], which took into account the $\nu_p(E)$-dependence of the most probable charge, to evaluate the DN yield at resonances. This resulted in prominent local 'spikes' in the DN yield $\nu_d(E)$ at resonances where prompt neutron multiplicity shows dips, as can be seen in **Fig.6**, and consequently more pronounced peaks in the relative DN fraction β ($=\nu_d / \nu_p$) at resonances in JEF-2.2 data. In a word, the two quantities $\nu_d(E)$ and $\nu_p(E)$ are *anti-correlated.*

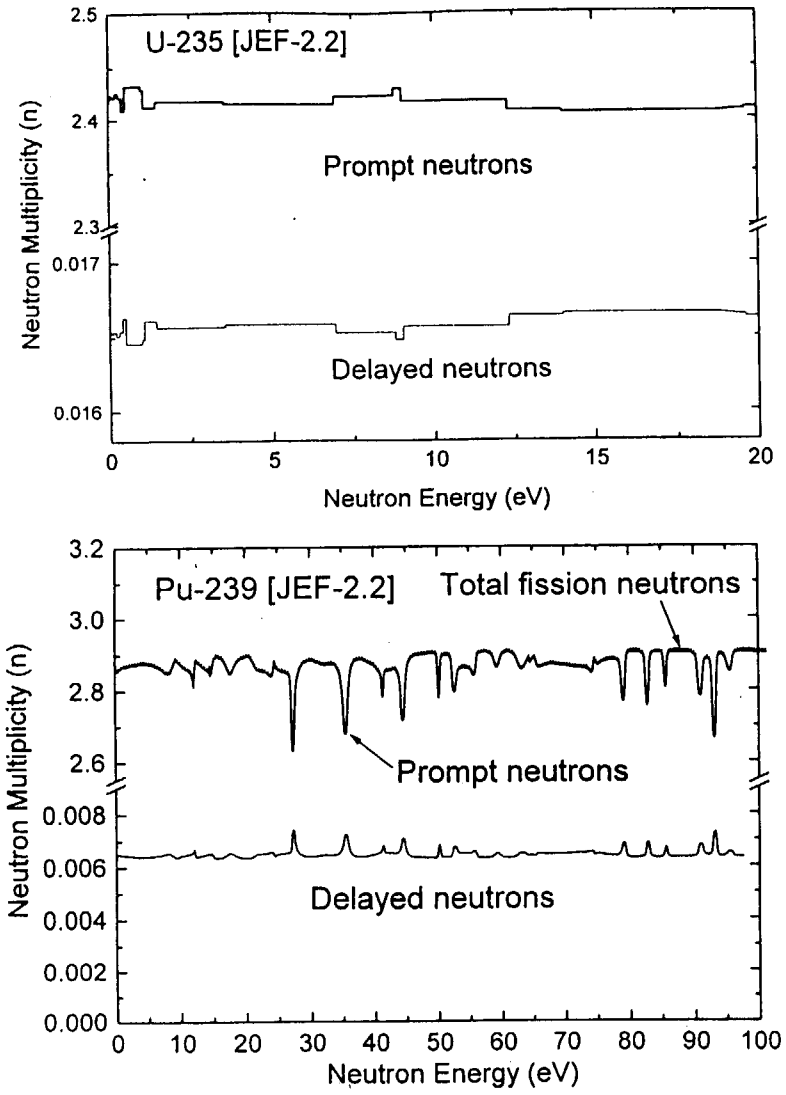

Fig.6 Evaluated data in JEF-2.2 of the prompt and delayed neutron yields in the resonance region of ^{235}U (a) and ^{239}Pu (b).

In contrast, the present analysis predicts a *positive correlation* between $\nu_p(E)$ and $\nu_d(E)$. For lack of experimental data on the DN yield at individual resonance, it is not possible at present to judge if there is a positive or negative correlation between the two quantities. However, the authors believe that the present result is probable for two reasons:

(a) Although there is no direct experimental evidence for local decrease of $\nu_d(E)$ at resonances, there is an evidence that, at resonances, the fission yield decreases just in the fragment mass region where important precursors exist.

(b) Local dips in the DN yield in the resonance region give a possible explanation to the slight decrease of $\nu_d(E)$ in the near-thermal region for which physical ground was not clear thus far.

Hambsch *et al.*[2] pointed out that the dips in ν_p are due to local changes in mode branching ratios w_i and that these changes are not correlated with the spin of the resonance. This interpretation is different from the previous one [8]. A new approach to a unified treatment of $\nu_p(E)$ and $\nu_d(E)$ on the basis of the multimodal fission model is under way.

5. Concluding Remarks

Detailed measurements of the fragment mass and kinetic energy distributions and their analyses in the 'language' of multimodal fission model performed during the last decade revealed many interesting features of the fission process. These studies have brought a new insight into the interpretation of variation of the DN yield in the resonance region. However, one should note that Hambsch's measurement is on ^{235}U and Fort's evaluation mainly concerns ^{239}Pu. It is thus highly desirable that measurements of fluctuation in the fragment mass distribution in the resonance region of ^{239}Pu will be made with high precision. Consistent simultaneous evaluation of prompt and delayed neutron multiplicity in terms of the multimodal fission model on the same nucleus would help to solve the problem.

References

[1] Kaneko, Y., F.Akino and T.Yamane, J. Nucl. Sci. Technol. **25**, 673 (1988)

[2] Hambsch, F.-J., H.-H.Knitter and C.Budtz-Jorgensen, Nucl. Phys. **A491**, 56 (1989).

[3] Brosa, U., S. Grossmasnn and A. Müller, Phys. Reports **197**, No.4, 167 (1990).

[4] Nishio, K., Y. Nakagome, I. Kanno and I. Kimura, J. Nucl. Sci. Technol. **32**, 404 (1995).

[5] Mann, F.M., M.Schreiber and R.E.Schenter, Nucl. Sci. Eng. **87**, 416 (1984).

[6] Wahl, A.C., Atomic and Nuclear Data Tables, **39**, 1 (1988).

[7] Mughabghab, S.F., Neutron Cross Sections, Vol.1, Part B, Academic Press (1984).

[8] Fort, E., J.Fréhaut, H.Tellier and P.Long, Nucl. Sci. Eng. **99**, 375 (1988).

[9] Lendel, A.I., T.I.Marinets, D.I.Siroka and E.I.Charnovich, Soviet At. Energy, **61**, 752 (1986)

7. Estimation of Delayed Neutron Emission Probability by Using the Gross Theory of Nuclear β–Decay

Takahiro Tachibana
Senior High School of Waseda University
3-31-1, Kamishakujii, Nerima-ku, Tokyo 177-0044
e-mail: ttachi@mn.waseda.ac.jp

The delayed neutron emission probabilities (P_n-values) of fission products are necessary in the study of reactor physics; e.g. in the calculation of total delayed neutron yields and in the summation calculation of decay heat. In this report, the P_n-values estimated by the gross theory for some fission products are compared with experiment, and it is found that, on the average, the semi-gross theory somewhat underestimates the experimental P_n-values. A modification of the β-decay strength function is briefly discussed to get more reasonable P_n-values.

1. Introduction

Either in the 2nd generation of the gross theory [1] (referred to as GT2 hereafter) or in the semi-gross theory [2] (referred to as SGT hereafter), the strength function of the β-decay $|M_\Omega(E)|^2$ is assumed to be given as

$$|M_\Omega(E)|^2 = \int_{\varepsilon_{\min}}^{\varepsilon_{\max}} D_\Omega(E,\varepsilon) W(E,\varepsilon) \frac{dn_1}{d\varepsilon} d\varepsilon, \qquad (1)$$

where Ω denotes the type of β-transition (Fermi, Gamow-Teller, or the 1st forbidden transition), ε the single-particle energy, and E the transition energy measured from the parent state. The function $D_\Omega(E,\varepsilon)$ is the one-particle strength function, $W(E,\varepsilon)$ a weight function to take into account the Pauli exclusion principle, and $\frac{dn_1}{d\varepsilon}$ the one-particle energy distribution of the decaying nucleon.

The characteristics of GT2 in comparison with SGT are as follows.

(1) The function $D_\Omega(E,\varepsilon)$ is a superposition of two parts. For example, in the case of the Gamow-Teller transition, one is a function with a large peak corresponding to the giant resonance, and the other is a widely-spreading distribution with long tails.

(2) The Fermi gas model with an effective mass is used for the calculation of the function

$\frac{dn_1}{d\varepsilon}$, and pairing gaps are taken into account for the nucleons near the Fermi surface.

(3) The UV factor of the BCS model is taken into account by a somewhat crude method.

In the case of GT2, the shell effect is taken into account only through the Q-value which is an input data of the model.

On the contrary, the characteristics of SGT are as follows.

(1) The function $D_\Omega(E,\varepsilon)$ is assumed to be a superposition of several functions which reflect the effects of spin-flip and change of the oscillator quanta by the transitions.

(2) The energy distribution $\frac{dn_1}{d\varepsilon}$ is a non-uniform and discrete function taking into account the shell effects and pairing effects in the parent nucleus.

(3) The UV factor is calculated by using this energy distribution $\frac{dn_1}{d\varepsilon}$.

In the case of SGT, having the above characteristics, some shell effects are taken into account in the strength function around the ground state of the daughter nucleus.

The delayed neutron emission probability, P_n, is calculated with the use of the total β-strength function, S_β, which is the sum of the allowed-equivalent strengths of all transitions $|M_\Omega(E)|^2$:

$$P_n = \frac{\lambda_n}{\lambda}, \tag{2}$$

with

$$\lambda_n = \int_{-Q+S_n}^{0} S_\beta(E)\ f(-E)\ \frac{\Gamma_n}{\Gamma_n+\Gamma_\gamma} dE\ , \tag{3}$$

and

$$\lambda = \int_{-Q}^{0} S_\beta(E)\ f(-E)\ dE = \frac{\ln 2}{T_{1/2}}. \tag{4}$$

Here, Q is the β-decay Q-value, S_n the neutron separation energy of the daughter nucleus, f the integrated Fermi function, $T_{1/2}$ the β-decay half-life, and $\Gamma_n/(\Gamma_n+\Gamma_\gamma)$ the competition factor with γ-radiation. In this report, we put this factor to unity for simplicity.

2. Calculated P_n-values and modified strength function

The calculated P_n- and λ_n - values are compared with experimental data [3] in fig. 1. In order to get the 'experimental' λ_n - values, we adopt the experimental $T_{1/2}$ [4] and P_n-values [3] in the equations (2) and (4). The calculated λ_n - values, on the average, somewhat overestimate the experimental values. This tendency is not bad if we notice that real competition factor should be less than unity. In GT2, reasonable P_n- and λ_n - values are

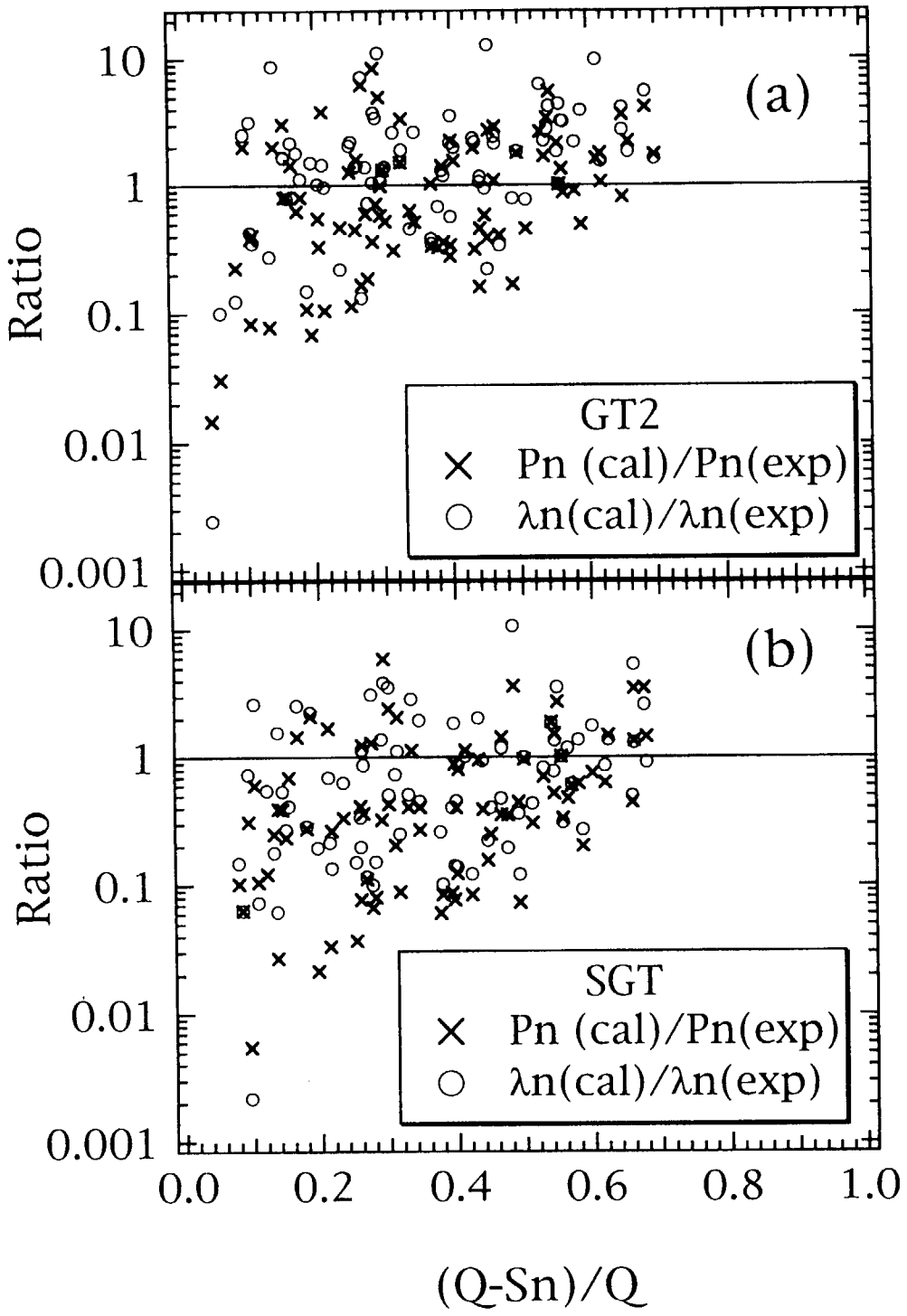

Fig. 1 Comparison between the calculated P_n-values (λ_n - values) and experimental ones. Figure (a) is for GT2 and (b) is for SGT.

obtained on the average except for the nuclei with small $(Q\text{-}Sn)/Q$ values. On the other hand, in the case of SGT, many P_n-values and λ_n - values are lower than the experimental ones. This means that the strength functions estimated by using SGT are smaller than the experimental strengths in the delayed neutron window.

In order to get more reasonable P_n - and λ_n - values in SGT, we introduce the spreading function $G(E-E_0;\ E_0+Q)$ [see Ref. [5] for more detail]. The β-strength function of SGT is spread in each small interval around the energy E_0 with the use of this function $G(E-E_0;\ E_0+Q)$. The modified strength function is obtained as

$$S_\beta(E)=\int_{-Q}^{\infty} S_\beta^{SGT}(E_0)\ G(E-E_0;\ E_0+Q)\ dE_0, \qquad (5)$$

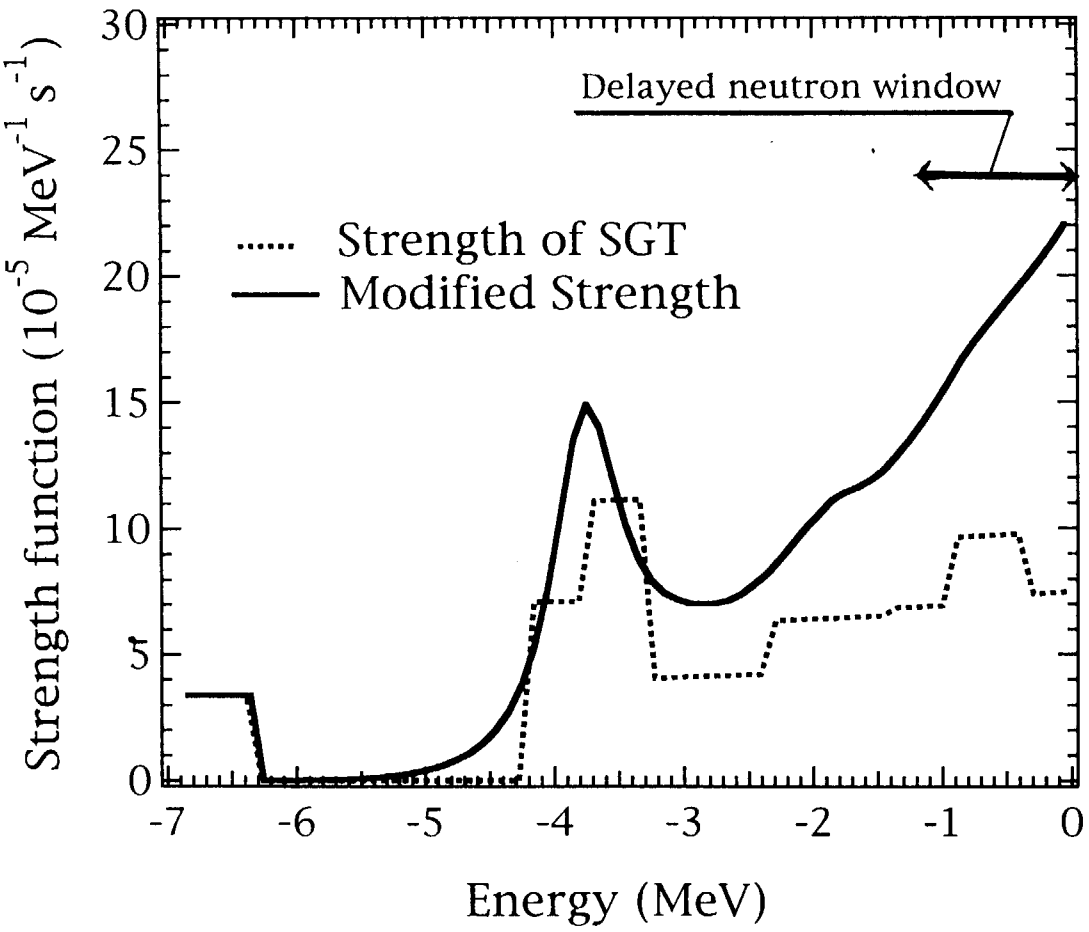

Fig. 2 The Gamow-Teller strength function of ^{87}Br. The delayed neutron window is between −1.3 (MeV) and 0 (MeV). δ-functions in the strengths are drawn with a half-width of 0.5 MeV.

with

$$G(E-E_0;\ E_0+Q)=\frac{C\ \exp(-[E-E_0]^2/2a_G^2[E_0+Q]^2)}{\sqrt{2\pi}a_G(E_0+Q)}\times \frac{a_L(E_0+Q)}{2\pi([E-E_0]^2+a_L^2[E_0+Q]^2/4)} \tag{6}$$

where S_β^{SGT} is the strength function calculated by SGT. This spreading function G is the product of a Lorentzian function with a parameter a_L and a Gaussian function with a normalization constant C and a parameters a_G. The parameters a_L and a_G define the absolute values of the widths and are fixed to reproduce reasonable half-lives and P_n-values in the whole nuclidic region. After some examinations, we have taken a_G=0.3 and a_L=0.2. The example of the modified strength function shown in fig. 2 has been obtained in this way. It should be noted that the strength function at the ground state of the daughter nucleus does not change because the function G is a δ-function at $E=-Q$. As seen in fig. 2, the modified strength function increases very much in the delayed neutron window but does not change so much around the ground state of the daughter nucleus.

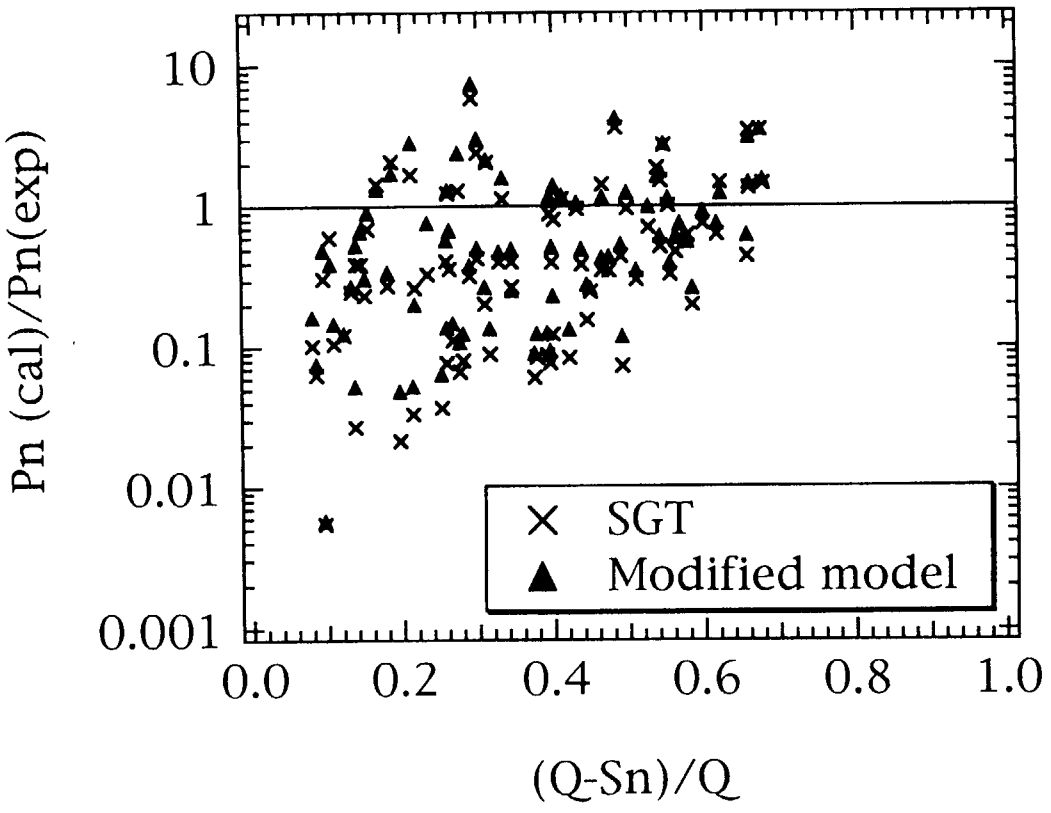

Fig. 3 The ratios between calculated and experimental P_n-values.

In fig. 3, we show how the calculated P_n-values change with the use of the modified strength functions. Almost all the new P_n-values have increased to the right direction, but the magnitudes of the modification are not sufficient. In the case of λ_n - values, the effect of the modification is more clearly seen [5].

3. Conclusion

The P_n-values calculated with the use of GT2 are, on the average, in fairly good agreement with the experiment, although, in the case of SGT, the P_n-values are somewhat underestimated. We have proposed a method to modify the strength function to get more reasonable P_n-values.

Acknowledgments

The author gratefully acknowledges Prof. M. Yamada for helpful discussions. This work was financially supported, in part, by Grant Special Research Projects, Waseda University (98A-176).

References

[1] Tachibana T., Yamada M., and Yoshida Y.; Progress of Theoretical Physics, **84**, 641 (1990);
Tachibana T. and Yamada M.; Proc. Inc. Conf. on exotic nuclei and atomic masses (ENAM95) p. 763, (Editions Frontueres, Gif-sur-Yvette, 1995).

[2] Nakata H., Tachibana T. and Yamada M.; Nuclear Physics **A625**, 521 (1997);
Tachibana T., Nakata H. and Yamada M.; Tours Symposium on Nuclear Physics III, AIP Conference Proceedings 425, p.495 (1998).

[3] Rudstam G., Aleklett K., and Sihver L.; Atomic Data and Nuclear Data Tables **53**, 1 (1993).

[4] Evaluated Nuclear Structure Data Files (ENSDF), communicated through Nuclear Data Center, Japan Atomic Energy Research Institute.

[5] Tachibana T. and Yamada M.; Exotic Nuclei and Atomic Masses (ENAM98), AIP Conference Proceedings 455, p.805 (1998).

8. Activity of the Delayed Neutron Working Group of JNDC and the International Evaluation Cooperation - WPEC/SG6

Tadashi YOSHIDA
Faculty of Engineering, Musashi Institute of Technology
Mamazutsumi 1-28-1, Setagaya-ku, 158-8557 Tokyo
e-mail: yos@ph.ns.musashi-tech.ac.jp

The Delayed Neutron Working Group was established in April 1997 within the Nuclear Data Subcommittee of JNDC. It has two principal missions. One is to coordinate the Japanese activities toward the WPEC/Subgroup-6 efforts, and the other is to recommend the delayed neutron data for JENDL-3.3. The final report of Subgroup-6, which is one of the subgroups of the NEA International Evaluation Cooperation(WPEC) and is in charge of the delayed neutron data, is to be completed in 1999. Here in Japan, JENDL-3.3 is planned to be released in early 2000. Delayed Neutron Working Group is, then, going to finalize its activity by the end of the fiscal year 1999 after recommending appropriate sets of data as coherently as possible with the of Subgroup-6 efforts.

1. Introduction

The delayed neutron (DN) plays a crucial role in nuclear reactor in all senses. The DN data are, therefore, essential in various areas of the nuclear technology from a conceptual design of future reactors to daily operation of the power reactors. Here in Japan, various recommended sets of the DN data and the spectra of foreign-origin[1 ~ 5] had long been used rather occasionally in each company or laboratory. In generating JENDL-3 (Japanese Evaluated Nuclear Data Library version 3), the average numbers of DNs emitted per fission, ν_d, were critically reviewed among the evaluations to be included in it[6]. The six-group structure and the related constants, however, were simply taken from Tomlinson's work[4], and the energy spectra from Saphier's work[5].

2. WPEC Effort

In 1989 an international working group was set up as a co-effort of the NEA Committee of Reactor Physics and the NEA Nuclear Data Committee in order to activate the world cooperation of nuclear data evaluation. Two years later, in 1992, the working group was reorganized into WPEC, the Working Party on International Evaluation Co-operation, under the NEA Nuclear Science Committee. Subgroup 6 of WPEC, coordinated by G. Rudstam and monitored by R. D. McKnight, was given a mission to improve the DN data to meet the

required accuracy standard in predicting the reactivity scales of the fast and the thermal reactors. Subgroup 6, or SG6, classified their activities into the following three levels[7]. Key words in the parentheses may help in grasping the idea.

Level 1: the individual precursor, or microscopic, level (Pn-values, fission yields, summation calculations)

Level 2: the aggregate precursor, or macroscopic, level (fissile-wise DN data, group constants)

Level 3: the integral or reactor level (criticality experiments, reactor kinetics, validation of β_{eff})

After several years of low-key activity, SG6 was reactivated in accordance with the progress of the FCA-MASURCA joint experiments of β_{eff} in Level 3 [8]. They organized a Colloquy on Delayed Neutron Data at Obninsk, Russia, in April 1996 under the new coodinatorship of A. D'Angelo. In this Obninsk meeting they concluded that they had better concentrate on the activities of Level 2 and 3 in order to propose a new set of improved DN data within several years. Spriggs proposed to extend the group structure of DN representation from the current 6-groups to 8-groups[9] on the basis of the extensive survey[10] of the existing experimental data categorized to Level 2. In ref.[10], 238 sets of DN parameters for 20 different fissionable isotopes are listed and reviewd, but no Japan-origin data is given. This reflects the historical weakness of the Japanese domestic activity in the research field of Level 2. Figure 1 is a brief mapping of the WPEC/SG6-related, current activities in the world after D'Angelo's survey[7].

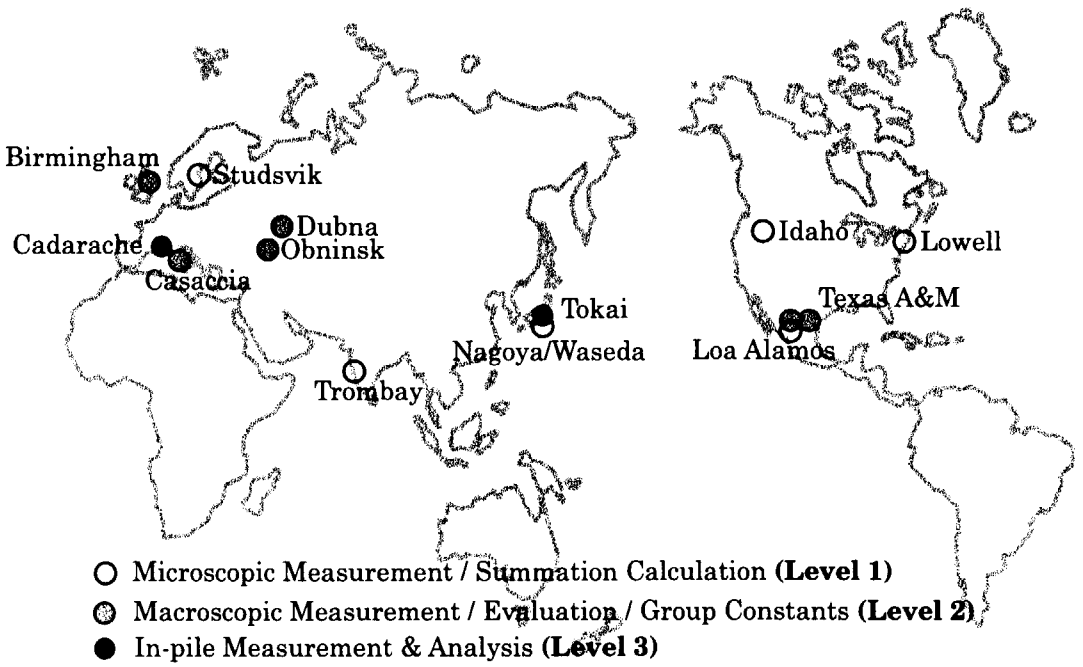

Fig. 1 WPEC/SG6-Related Activities in the World

At the Obninsk Colloquy, the SG6 members summarized the discussion as follows[11]: "The session devoted to a general discussion started with a presentation of the Japanese view[12] on the future programme of work for the subgroup. In summary, it was proposed that a state-of-the-art report, recommending the best delayed neutron data for the major actinides, should be written and published in 1998. The present subgroup should then be closed, and a new subgroup created for new interest areas, such as minor actinides". This recommendation met with general approval by the participants. Presently SG6 is working in accordance with this summary and the final report will be presented at the WPEC meeting to be held at Brookheaven National Laboratory on April 1999.

3. JNDC Effort

The Delayed Neutron Working Group was established in April 1997 with 9 members as a part of the Nuclear Data Subcommittee of the Japanese Nuclear Data Committee(JNDC). At the beginning, the mission of DNWG was to coordinate our domestic activities toward the WPEC/Subgroup-6 efforts and to avoid duplication in the work for SG6 and for JENDL-3.3. For this purpose DNWG made a proposal to SG6 at the Obninsk meeting[12] and it was approval by the participants there in principle as was described above. Soon after the Obniksk meeting, DNWG formally accepted the mission to recommend the DN data of major actinides, ^{235,238}U and ^{239}Pu, for inclusion in JENDL-3.3 upon a request from Heavy Nuclear Data Evaluation WG of JNDC.

The DNWG recommendation for JENDL-3.3 should be as coherent as possible with the coming SG6 recommendation. The latter, however, may possibly be given in a novel 8-group structure proposed by Spriggs[9]. G.D.Spriggs made a presentation on his 8-group structure at a DNWG meeting in Tokai in October 1997 [13], and the DNWG members studied his idea. Though it seemed to be a clear improvement from the conventional 6-group in a scientific sense, the DNWG members concluded that it is not appropriate to change the group structure from 6 to 8 in the coming JENDL-3.3 from the view point of the technological continuity. DNWG is, therefore, prepared to collapse the possible SG6 recommendation in 8-groups into a 6-group set for inclusion in JENDL-3.3 in case it becomes necessary. It may also help us to learn the effect of changing from 6 to 8. Anyway, we have to validate the DN data set on the basis of the integral, or Level 3, data from FCA and MASURCA [8], and from other two Japanese facilities; TCA and VHTRC. By the end of the year 1999 DNWG is to propose the best DN data sets for inclusion in JENDL-3.3.

4. Concluding Remarks

The three-year activity (1997-2000) of the Delayed Neutron Working Group is rather limited in its scope. It is, however, the first domestic working group concentrating on the delayed neutron in the 36-year history of JNDC, and we have to leave much to be experienced and studied in the future. In fact DNWG is to be closed in 2000, but a new working

group can be set up if we need the improved DN data for minor actinides, for example. In addition, the method-and-data for summation calculations, which is categorized to Level 1 in the SG6 classification, must be improved much further, not only for obtaining better DN data, but for all other technical goals concerning the aggregate behavior of the fission products; the decay heat, for example. After closing of DNWG, one of the working groups of JNDC will take over the works related to DN summation calculation putting it in an appropriate place in the wider range of the fission-product study, which is of common interest of both JNDC and WPEC.

References

[1] Keepin G.R.: Physics of Nuclear Kinetics, Addison-Wesley (1965)
[2] Tuttle R.J.: "Delayed-Neutron Yields in Nuclear Fission". Proc. Consultants' Mtg. on D.N. Properties, IAEA, Vienna (1979)
[3] Krick M.S. and Evans A.E.: Nucl. Sci. Engn., **47**, 311(1972)
[4] Tomlinson L.: "Delayed Neutron from Fission: A Compilation and and Evaluation of Experimental Data". AERE-R6993, Harwell (1972)
[5] Saphier D., Ilberg D., Shalev S. and Yiftah S.: Nucl. Sci. Engn., **62**, 660(1977)
[6] Shibata, K. and Narita T.(eds): "Descriptive Data of JENDL-3.2 (Z=51-100)", JAERI-Data/Code 98-006 (part II) (1998)
[7] D'Angelo, A.: Final Reprt of Subgroup 6 to WPEC, being prepared
[8] for example, Okajima S, Zuhair, Sakurai T and Song H.: J. Nucl. Sci. Technol., **35**, 963(1998); see also Sakurai K.: Nuclear Data News, **52**, 1 (1995) (in Japanese)
[9] Spriggs G.D., Campbell J.M. and Piksaikin V.M.: "An 8-Group Delayed Neutron Model Based on a Consisten Set of Half-Lives", LA-UR-98-1619 (1998)
[10] Spriggs G.D. and Campbell J.M.:"A Summary of Measured Delayed Neutron Group Parameters", LA-UR-98-918, Rev.1 (1998)
[11] D'Angelo, A.: "Status Report of the WPEC Subgroup 6 activities", a report to WPEC (May,1997)
[12] Okajima S., Oyamatsu K., Yoshida T., Katakura J. and Tanihata I.: "Japanese Comment on the Future Program in Sub-group 6", Colloquy on Delayed Neutron Data , Obninsk (1997)
[13] Spriggs G.D. and Campbell J.M.: "An 8-Group Delayed Neutron Model ", Meeting of the DNWG/JNDC, Tokai, October (1997)

9. Evaluation Method for Uncertainty of Effective Delayed Neutron Fraction β_{eff}*

Atsushi ZUKERAN
Power & Industrial System R & D Laboratory, Hitachi, Ltd.
7-2-1 Omika-cho, Hitachi-shi, Ibaraki-ken, 319-12 Japan

May 6, 1999

Abstract

Uncertainty of effective delayed neutron fraction β_{eff} is evaluated in terms of three quantities; uncertainties of the basic delayed neutron constants, energy dependence of delayed neutron yield ν_d^m, and the uncertainties of the fission cross sections of fuel elements. The uncertainty of β_{eff} due to the delayed neutron yield is expressed by a linearized formula assuming that the delayed neutron yield does not depend on the incident energy, and the energy dependence is supplemented by using the detailed energy dependence proposed by D'Angelo and Filip. The third quantity, uncertainties of fission cross section, is evaluated on the basis of the generalized perturbation theory in relation to reaction rate ratios such as central spectral indexes or average reaction rate ratios. Resultant uncertainty of β_{eff} is about 4 to 5 %s, in which primary factor is the delayed neutron yield, and the secondary one is the fission cross section uncertainty, especially for ^{238}U. The energy dependence of ν_d^m systematically reduces the magnitude of β_{eff} about 1.4 % to 1.7 %, depending on the model of the energy vs. ν_d^m correlation curve.

1 Introduction

Effective delayed neutron fraction β_{eff} is a key safety parameter. Uncertainties of control rod, sodium-void and Doppler reactivity worths have a high priority from the reactor safety point of view. While, the verification of β_{eff} as a conversion factor from measured reactivity worth to the difference in the effective multiplication factor δk is required in reactor physics.

Required accuracies for the β_{eff} and its components were recommended by Hammer and Tuttle[1,2], and were 3 % for critical experiments and 5 % for an operating power reactor. The uncertainties of the β_{eff} were ±2.0 % from neutron flux $\phi(E,\vec{r})$ and adjoint fluxes $\phi^\dagger(E,\vec{r})$, ±1.5 % from fission $\sigma_f(E)$ and neutron production cross sections $\nu\sigma_f$, and ±0.5% from delayed neutron spectra[3] χ_{di}^m.

*The outline and supplements for "Uncertainty Evaluation of Effective Delayed Neutron Fraction β_{eff} of Typical Proto-type Fast Reactor" published as Jr. of Nucl. Sci. and Tech., vol. 36, No.1, p.61-80 (1999)

Recently, D'Angelo et al.[4] evaluated the β_{eff} uncertainty from overall uncertainty sources and they found the uncertainty was about 5 % for a typical fast reactor core, which is consistent with the uncertainty reviewed by Hammer[3]. However, the uncertainty components due to fission cross sections were intuitively estimated in relation to the uncertainties of central spectral indexes such as ^{238}U fission to ^{239}Pu fission reaction rate ratio.

D'Angelo and Filip[5] estimated the effect of the energy dependence of delayed neutron yield in the lower energy side below 50 keV as well as the higher energy side as usually expected, and obtained around 2 % uncertainty for a typical fast reactor. In their parametric study, two energy ranges in the lower energy side, namely below 10 keV and 50 keV, were tested.

Theoretical interpretations had been attempted by Alexander and Krick[7] based on the partial fission cross sections derived graphically by Davey[6],[8] and Gardner[6], and interpreted the energy dependence of delayed neutron yield as being due to depression of the pairing energy in a fissioning nucleus with the excitation energy, which are discussed in 2.2.

The present work aims at emphasizing uncertainty evaluation methd of the effective delayed neutron fraction β_{eff} based on a firm theoretical formula for uncertainty evaluation and giving an example of the application to a fast reactor. In particular the uncertainties due to the fission cross sections are emphasized. In Section 2, the basic formula for uncertainty evaluation is discussed, and the Section 3 is devoted to the sensitivity analysis and evaluation of the uncertainty components. In the Section 4 overall uncertainty of β_{eff} is evaluated.

2 Evaluation Method for β_{eff} Uncertainty Components

2.1 β_{eff} Uncertainty due to Delayed Neutron Parameters

The effective delayed neutron fraction β_{eff} is the sum of the delayed neutron the contributions from individual fuel elements and delayed family[9],[10],[11].

$$\beta_{eff} = \sum_m \sum_i [\beta_i \gamma_i]^m. \tag{1}$$

The component $[\beta_i \gamma_i]^m$ and perturbation denominator D_p are defined by

$$[\beta_i \gamma_i]^m = \frac{\int_V \int_{E'} \chi^m_{d,i}(E') \phi^\dagger(E', \vec{r}) dE' \int_E \nu^m_{d,i}(E) \Sigma^m_f \phi(E, \vec{r}) dE dV}{D_p}, \tag{2}$$

$$D_p = \sum_n \int_V \int_{E'} \chi^n(E') \phi^\dagger(E', \vec{r}) dE' \int_E \nu^n(E) \Sigma^n_f \phi(E, \vec{r}) dE dV \tag{3}$$

$$\simeq \sum_n \int_V \int_{E'} \chi^n_p(E') \phi^\dagger(E', \vec{r}) dE' \int_E \nu^n_p(E) \Sigma^n_f \phi(E, \vec{r}) dE dV, \tag{4}$$

where the delayed neutron contribution to the perturbation denominator D_p is dropped in Eq.(4) for simplicity since its magnitude (at most 0.65 %) is negligibly small relative to

the total neutron yield about 2.49. The other parameters or variables are as follows,

E	: incident neutron energy (eV),
V	: reactor volume,
ν_p^m	: prompt neutron yield of fuel element m ,
ν_{di}^m	: delayed neutron yield of fuel element m and family i ,
ν^m	: total neutron yield, i.e., $\nu^m = \nu_p^m + \sum_i \nu_{di}^m$,
χ_p^m	: prompt neutron spectrum of fuel element m,
χ_{di}^m	: delayed neutron spectrum of fuel element m and family i ,
χ^m	: average neutron spectrum, i.e., $\chi^m = \chi_p^m(1-\beta^m) + \sum_i \chi_{di}^m \beta_i^m$,
β^m	: total β, i.e., $\beta^m = \sum_i \beta_i^m$,
$\phi, \phi^\dagger$	: neutron and adjoint fluxes,
Σ_f^m	: macroscopic fission cross section of fuel element m,
$\vec{r}$	: spatial position,
D_p	: perturbation denominator.

Evaluated total delayed neutron yields ν_d^m of principal fuel elements are listed in **Table 1**. Fractional yields a_{di}^m and decay constants λ_i^m are shown in **Table 2**. These values are used for the present work as the reference data.

The delayed neutron mean energy is about 0.5 MeV which is about 1.5 MeV far from the peak position of the prompt neutron spectrum, as shown in **Fig. 1** where the energy dependence of the ^{238}U fission cross section and β_{eff} related quantities are superposed as an example.

A typical delayed neutron yield curve, for instance ^{235}U's, is shown in **Fig. 2** as a function of incident neutron energy. As the distribution of the experimental data for ^{235}U implies, the delayed neutron yield is nearly constant below about 4 MeV. Therefore, at least for energies below several MeV, the delayed neutron yield can be assumed to be constant as a first order approximation. At high energy, a drop of the yield is clearly found in the experimental data. However, the non-linearity (decreasing trend) is not so important for estimation of the β_{eff} uncertainty using sensitivity coefficients, since the sensitivity coefficient is defined by the derivative with respect to the delayed neutron parameter. While, in the high energy region, the fission reaction rates decrease with the neutron energy due to neutron flux depression, where some threshold fission reactions such as those of ^{238}U take an important role for governing β_{eff}.

In the present work, the first order approximation is adopted by omitting the energy dependence of the delayed neutron yield, i.e.,

$$\nu_d^m(E) \simeq \nu_{d0}^m \qquad \ldots\ldots \text{constant value.} \tag{5}$$

and the effect of the energy dependency is treated as a separate term of systematical error. The effect of this approximation was examined by direct comparison of the calculated β_{eff}-values based on the exact treatment with the approximated yield, and the difference was about 1.7 %, as shown in Section 3.2. Therefore, this is seemed to be acceptable for the present work since the approximation is used only for estimating the sensitivity coefficient defined by Eq.(11).

By using the approximation Eq.(5), $[\beta_i\gamma_i]^m$ defined by Eq.(2) takes a simplified form as the result of variable separation,

$$[\beta_i\gamma_i]^m \simeq \nu_{d0}^m \cdot \frac{\gamma_i^m}{D_p}, \tag{6}$$

where the factor γ_i^m is defined by

$$\gamma_i^m = \int_V \int_{E'} \chi_{d,i}^m(E')\phi^\dagger(E',\vec{r})dE' \int_E \Sigma_f^m \phi(E,\vec{r})dEdV. \tag{7}$$

The γ_i^m has the same dimensions as the perturbation denominator (D_p) defined by Eq.(3) and means the fractional importance of the delayed neutrons relative to whole (prompt and delayed) neutrons in a reactor as implied by the second term of the right-hand side of Eq.(6). The component β_i^m is defined by,

$$\beta_i^m = \frac{\nu_{di}^m}{\nu_d^m} \tag{8}$$

Finally, the effective delayed neutron fraction β_{eff} can be shown as a linear sum of fuel element m and family i components $[\beta_i\gamma_i]^m$s as follows,

$$\beta_{eff} = \frac{\sum_{m=1}^M \sum_{i=1}^I \nu_i^m \gamma_i^m}{D_p} \tag{9}$$

where M and I ($\simeq 6$) indicate the numbers of fuel elements and delayed neutron families. By using this simplified expression, the error of β_{eff} due to errors of delayed neutron parameters can be expressed in terms of several error sources as,

$$\frac{\delta\beta_{eff}}{\beta_{eff}} = -\frac{\delta D_p}{D_p} + \frac{\sum_{m=1}^M \sum_{i=1}^6 \{\frac{\delta\nu_{d,i}^m}{\nu_{d,i}^m} + \frac{\delta\gamma_{d,i}^m}{\gamma_{d,i}^m}\} \cdot \nu_{d,i}^m \gamma_i^m}{\sum_{m=1}^M \sum_{i=1}^6 \nu_{d,i}^m \gamma_i^m}. \tag{10}$$

Sensitivity coefficient $S_{\nu_{di}^m}^{\beta_{eff}}$ of β_{eff} with respect to the change of delayed neutron yield ν_{di}^m can be defined by,

$$S_{\nu_{di}^m}^{\beta_{eff}} = \frac{\nu_{di}^m}{\beta_{eff}} \cdot \frac{\partial\beta_{eff}}{\partial\nu_{di}^m} = \frac{\nu_{d,i}^m \gamma_i^m}{\sum_{m=1}^M \sum_{i=1}^6 \nu_{d,i}^m \gamma_i^m}. \tag{11}$$

This implies that the sensitivity coefficient is the fractional contribution of ν_{di}^m to the β_{eff} and can be obtained as a part of the calculated β_{eff}-values.

The error of ν_{di}^m is the sum of errors due to total delayed neutron yield ν_d^m and due to fractional delayed neutron yield a_{di}^m; i.e.,

$$\nu_{di}^m = \nu_d^m \cdot a_{di}^m, \tag{12}$$

therefore

$$\frac{\delta\nu_{di}^m}{\nu_{di}^m} = \frac{\delta\nu_d^m}{\nu_d^m} + \frac{\delta a_{di}^m}{a_{di}^m}. \tag{13}$$

The error components $\delta\nu_d^m/\nu_d^m$ and $\delta a_{di}^m/a_{di}^m$ are taken from the recommended values by Tuttle[12] shown in **Tables 1** and **2**, respectively. Since the family sum of a_{di}^m $(i = 1\ to\ 6)$ is unity, the error $\delta a_{di}^m/a_{di}^m$ has an anti-correlation with the other $\delta a_{dj}^m/a_{dj}^m$ $(i \neq j)$. However, the anti-correlation is omitted and thus the resultant error tends to be overestimated, which is preferred from a statistical viewpoint.

The statistical error of β_{eff}, denoted by $\delta\beta_{eff}/\beta_{eff}$, as functions of generalized parameters x_{di}^ms of delayed neutron parameters and fission cross sections is estimated by error propagation law as,

$$\frac{\delta\beta_{eff}}{\beta_{eff}} = \sqrt{\sum_m \sum_i \{W_{di}^m \cdot S_{x_{di}^m}^{\beta_{eff}} \cdot (\frac{\delta x_{di}^m}{x_{di}^m})\}^2} \quad + \quad (\frac{\delta\beta_{eff}}{\beta_{eff}})^{st.}, \tag{14}$$

where $(\frac{\delta\beta_{eff}}{\beta_{eff}})^{st.}$ means some systematical error but the mutual correlation, i.e. the off-diagonal term in the covariance matrix in the assemblage $\{x_{di}^m\}$ of all delayed neutron related quantities , is neglected. Uncertainties due to calculational methods are generally systematical errors which do not obey a normal distribution of errors. The weight W_{di}^m defined by the fractional contribution $[\beta_i\gamma_i]^m$ to β_{eff} is introduced for the uncertainty due to the fission cross section (discussed in Section 2.4),i.e.,

$$W_{di}^m = \frac{[\beta_i\gamma_i]^m}{\sum_m [\beta_i\gamma_i]^m} \cdot \frac{1}{\sum_g S_{\sigma_g^m}^{[\beta_i\gamma_i]^m}} \tag{15}$$

where $S_{\sigma_g^m}^{[\beta_i\gamma_i]^m}$ is sensitivity coefficient for g-group fission cross section of isotope m as shown in Section 2.4 in detail. While, magnitude for the basic delayed neutron parameters discussed in this section are unity since their weights are automatically introduced into the second term of Eq.(10).

The error of the perturbation denominator $\delta D_p/D_p$ is mainly due to uncertainties of the fission cross sections as will be discussed in Section 3.4. Generalized perturbation theory is unavoidable for such a reaction rate ralated quantity as used in 2.4.

Using the same approach to the β_{eff}, the error evaluation formula of reactivity worth ρ for a step insertion of reactivity as a function of period T can be obtained. The final forms are shown below,

$$\begin{aligned} \rho &= \rho_p + \sum_{m=1}^{M} \sum_{i=1}^{I} \rho_i^m, \\ \frac{\delta\rho}{\rho} &= \frac{\rho_p}{\rho} \cdot (\frac{\delta l_p}{l_p} - \frac{\delta k}{k} - \frac{\delta T}{T}) \end{aligned} \tag{16}$$

$$+ \frac{\sum_{m=1}^{M}\sum_{i=1}^{6}\{-\frac{\delta D_p}{D_p}+\frac{\delta\nu_{d,i}^m}{\nu_{d,i}^m}+\frac{\delta\gamma_i^m}{\gamma_i^m}-\frac{\lambda_i^m T}{1+\lambda_i^m T}\cdot(\frac{\delta\lambda_i^m}{\lambda_i^m}+\frac{\delta T}{T})\}\rho_i^m}{\rho_p+\sum_{m=1}^{M}\sum_{i=1}^{6}\rho_i^m}, \quad (17)$$

$$\rho_p = \frac{l_p}{kT}, \quad (18)$$

$$\rho_i^m = \frac{\gamma_i^m \beta_i^m}{1+\lambda_i^m \cdot T}, \quad (19)$$

where newly introduced parameters have the following meanings.

k : effective multiplication factor,
l_p : prompt neutron life-time (s),
λ_i^m : decay constant of fuel element m and family i (s^{-1}),
T : reactor period (s),
ρ_p : reactivity worth component for prompt neutrons,
ρ_i^m : reactivity worth component for fuel element m and family i.

The sensitivity coefficient for the reactivity worth ρ with respect to the variation of the delayed neutron parameters can also be obtained. The uncertainty of ρ is evaluated in Section 4 in comparison with that of β_{eff}.

2.2 Uncertainty of Delayed Neutron Spectrum

Saphier et al.[13] estimated the influence of the evaluated delayed neutron spectra on the β_{eff}, and obtained about 0.5 % difference among three evaluated spectra. Moberg and Kockum[14] measured the effective delayed neutron fraction in three different cores of the fast assembly FRO, and in addition to the measurement, they studied the influence of the replacement of evaluated delayed neutron spectra, and the root-mean-square difference of 0.4 % was obtained. The above reports show the choice of the delayed neutron spectra gives around a 0.5 % difference to β_{eff}. Therefore, in the present work, the β_{eff} uncertainty due to the delayed neutron spectrum is assumed to be 0.5 %.

2.3 Energy Dependence of Delayed Neutron Yield

The energy dependence of the delayed neutron yield ν_d^m has been evaluated by several reports[5],[6],[7]. Sensitivity analysis on the energy dependence of ν_d^m to β_{eff} was made by D'Angelo and Filip[5].

As theoretically discussed by Alexander and Krick[7], at the higher energies above about 4 MeV, the pairing effect to nuclear fission is "washed out" with increasing excitation energy of a fissioning nucleus and consequently the delayed neutron yields decrease. The decrease can be found in the experimental data of all fuel elements. In the lower energy region, however, increasing of the ν_d^m beyond the experimental error with incident neutron energy can not be definitely observed (**Fig. 3**[15],[16]). As shown in **Fig. 3** with a open circle ($\odot$) linked to the Tuttle's 0 MeV point by the solid line, the increasing

Tuttle's thermal value by 3.3 % given by D'Angelo and Filip, as shown below in detail, is consistent with the experimental point, but it is within the experimental error. Therefore, it may be concluded that no obvious energy dependence can be found in the low energy side although the theoretical estimations mentioned above (**Fig. 2**) show clear increasing of $\nu_d^m(E)$. The energy dependencies of ^{238}U and ^{239}Pu delayed neutron yields as shown in **Figs. 4** and **5**

Recently, the resonance effect to the delayed neutron yield has been studied by T. Osawa[30], and the fine structure of the fractional total delayed neutron yield, defined by $\frac{\nu_d(E)}{\nu_d(th)}$, was derived from the F.-J. Humbsh et al. experiemtal data and Wahl's P_n-data, as shown in the insert of Fig. 3 where the energy range limited to the top resoance energy falls into the span between the first and second experimental data evaluated by Turttle. Osawa concluded that the depression of total delayed neutron yield $\nu_d(E)$ is about 2.3% as maximum which is in the same order to the D'Angelo's vales.

In order to study the resonace effect to β_{eff}, the neutron and adjoint fluxes should be prepared in an ultra-fine group structure so as to reveal the resonance effects in both fluxes and ν_d-value. However, such a fine-structure effect is left to be as further problems which are seemed to be important for thermal reactor kinetics parameters.

2.4 Uncertainties of Fission Cross Sections

The first term of Eq. (10) is due to the uncertainty of the perturbation denominator, which was substantially from the uncertainties of the fission cross sections characterizing the neutron and adjoint fluxes through the reactor spectral calculation.

The generalized perturbation theory[17],[18],[19] is usually focused on the reaction rate ratio or breeding ratio as one of the reaction rate ratios. The definition of β_{eff} can be interpreted as a macroscopic reaction rate ratio. Consequently, to use the generalized perturbation theory, the sensitivity coefficient for the fission cross section weighted by delayed neutron importance should be expressed in terms of the reaction rate ratios.

Detailed formulation of the sensitivity coefficient $S_{\sigma_f^j}^{[\beta_i\gamma_i]^m}$ for the fission cross section σ_f^j is shown in the APPENDIX-*I* of Ref. 29, and only an outline is shown here.

Reaction rates in the numerator and perturbation denominator D_p of the Eq.(2) can be rewritten by a reaction rate ratio R_k^m of the m to k reactions as shown below,

$$R_k^m(\vec{r}) = \frac{\int_E \sigma_f^m(E)\phi(E,\vec{r})dE}{\int_E \sigma_f^k(E)\phi(E,\vec{r})dE}, \tag{20}$$

$$\int_E \nu_p^n(E)\Sigma_f^n(E)\phi(E,\vec{r})dE = \overline{\nu_p^n}\cdot N^n \cdot R_k^n(\vec{r})\int_E \sigma_f^k(E)\phi(E,\vec{r})dE, \tag{21}$$

$$\int_E \nu_{di}^m(E)\Sigma_f^m(E)\phi(E,\vec{r})dE = \overline{\nu_{di}^m}\cdot N^m \cdot R_k^m(\vec{r})\int_E \sigma_f^k(E)\phi(E,\vec{r})dE, \tag{22}$$

$$\Sigma_f^n(E) = N^n\sigma_f^n(E), \tag{23}$$

where $\overline{\nu_p^n}$ and $\overline{\nu_{di}^m}$ mean average prompt and delayed neutron yields. The integrations in the right-hand sides of Eqs.(21, 22) are proportional to the power density $P_m(\vec{r})$, i.e.,

$$P_m(\vec{r}) = \Lambda_p^m \cdot \int_E \Sigma_f^m(r)\phi(E,\vec{r})dE, \tag{24}$$

where Λ_p^m ($\simeq$ 200 MeV/fission) means total energy release per fission which is approximately constant within a few percent deviation among fuel elements.

In general, the neutron energy spectrum in the core region has milder spatial change and the reaction rate distribution $R_k^m(\vec{r})$ can be approximated by the constant value of $R_k^m(0)$ at the core center, or an average reaction rate ratio over a core region $\overline{R_k^m}$ as defined by,

$$\overline{R_k^m} = \frac{\int_V \int_E \sigma_f^m(E)\phi(E,\vec{r})dEdV}{\int_V \int_E \sigma_f^k(E)\phi(E,\vec{r})dEdV}, \tag{25}$$

In this work, the average reaction rate ratio $\overline{R_k^m}$ is adopted since this quantity is based on the integrated reaction rates over core regions giving an effective multiplication factor k_{eff} as well as fractional powers.

Then, the component $[\beta_i\gamma_i]^m$ can be approximately expressed in terms of the average fission reaction rate ratio $\overline{R_k^m}$, and importance maps Ω_{di}^m and Ω_p^n as functions of average adjoint flux $\overline{\phi^\dagger}(E')$ as shown below

$$[\beta_i\gamma_i]^m \simeq \frac{\Omega_{di}^m \cdot \overline{\nu_{di}^m} \cdot N^m \cdot \overline{R_k^m}}{\sum_n [\Omega_p^n \cdot \overline{\nu_p^n} \cdot N^n \cdot \overline{R_k^n}]}, \tag{26}$$

$$\Omega_{di}^m = \int \chi_{di}^m \overline{\phi^\dagger}(E')dE', \tag{27}$$

$$\Omega_p^n = \int \chi_p^n \overline{\phi^\dagger}(E')dE'. \tag{28}$$

Finally, the sensitivity coefficient $S_{\sigma_f^j}^{[\beta_i\gamma_i]^m}$ of the β_{eff} component $[\beta_i\gamma_i]^m$ can be expressed by the sensitivity coefficient $H_{\sigma_f^j}^{\overline{R_k^m}}$ for the average fission reaction rate ratio $\overline{R_k^m}$ as,

$$S_{\sigma_f^j}^{[\beta_i\gamma_i]^m} = (1-\omega_p^m) H_{\sigma_f^j}^{\overline{R_k^m}} - \sum_{n\neq m} \omega_p^n H_{\sigma_f^j}^{\overline{R_k^n}}, \tag{29}$$

$$\omega_p^m \simeq \frac{P_m}{\sum_n P_n}, \tag{30}$$

$$H_{\sigma_f^j}^{\overline{R_k^m}} = \frac{\sigma_k^j}{\overline{R_k^m}} \cdot \frac{\partial}{\partial \sigma_f^j} \overline{R_k^m}, \tag{31}$$

where Ω_p^n is assumed to be constant since in ordinary flux calculations an average or representative fission spectrum is approximately used. Volume effect is included in the ω_p^ns.

3 β_{eff} Uncertainty Evaluation

3.1 Specification of Proto-type Fast Reactor and Calculation Model

In the present work, a typical sodium cooled fast breeder reactor is adopted for a numerical evaluation of the β_{eff} uncertainty. Specifications are as follows[20].

A core loading map is shown in **Fig. 6**. For the present analysis, the hexagonal core is replaced by a cylinder under the volume conservation law, and then the control and sodium channels are replaced by an annular geometries. In the reference core, all control rods are withdrawn and the control rod follower channels are filled with sodium.

3.2 β_{eff} Uncertainty due to Basic Delayed Neutron Data Uncertainties

Delayed neutron yield data are adopted from the evaluated data by Tuttle[6] with the attached errors as shown in **Table 1**. The fractional delayed neutron yields, a_i^m values, are also from the evaluated data by Tuttle[12] as shown in **Table 2**, and the delayed neutron spectrum data are adopted from Saphier's evaluation[13]. Uncertainties of fission cross section of ^{238}U, the major contributor to β_{eff} uncertainty, are shown in **Fig. 7** together with the experimental data, in which average uncertainties[21] in the 18 group structure are shown at the bottom of the figure. The fission cross section uncertainties of the other fuel element are shown in **Fig. 8**.

Contributions of individual fuel elements in reactor region are shown in **Table 3** as function of delayed neutron families. The ^{238}U's family 4 with an average half-life of 2.3 s is the largest contribution over all fuel elements. The dominant contribution of ^{238}U arises from its large fuel content and delayed neutron yield. The major contributions of ^{239}Pu and ^{241}Pu come from their large fission reaction rates.

The sensitivity coefficients defined by Eq.(11) are shown in **Fig. 9**. As expected from the definition of the sensitivity coefficient, the delayed neutron yield of ^{238}U of family 4 is the most sensitive to the variation of the yield and the next most sensitive is the ^{239}Pu also of family 4. The uncertainty of the β_{eff} due to uncertainties of the delayed neutron yields can be obtained by the statistical sum as shown by Eq.(14). Resultant uncertainty of the β_{eff} due to the basic delayed neutron data is 2.5 %.

The effect of the energy dependence of the delayed neutron yield is evaluated by the difference between the resultant β_{eff}-value based on the energy dependent yield and the constant yield over the whole energy range from 0 to 10 MeV, where the constant value is assumed to be Tuttle's recommended value at the lowest energy, i.e., 0 MeV for ^{235}U and ^{239}Pu, and to be the plateau-value above the threshold energy (about 0.5 MeV) for ^{238}U.

In the case of D'Angelo and Filip's parametric study[5] for ^{235}U, ^{238}U, and ^{239}Pu, two kinds of energy dependencies below 10 keV and below 50 keV in the lower energy region are assigned for ^{235}U and ^{239}Pu, as well as in the high energy region up to 15 MeV. Therefore, these cases are independently treated under the same high energy dependencies. Larger effects to β_{eff} are obtained as shown below.

(a) Below 10 kev $\frac{\delta\beta_{eff}}{\beta_{eff}} = -1.4$ %, (b) Below 50 kev $\frac{\delta\beta_{eff}}{\beta_{eff}} = -1.7$ %,

where the energy dependency of ^{238}U in the high energy region was also simultaneously considered. These results are used for the β_{eff} uncertainty evaluation as the recommended component for the present work.

The fission cross sections of ^{238}U as a function of incident neutron energy[23] were shown in **Fig. 7** together with their uncertainty. The resultant sensitivity coefficients defined by Eq.(29) are shown in **Fig. 10** for five fuel elements and renormalized sensitivity coefficient are shown in **Table 4** . The β_{eff} uncertainties due to the fission cross sections are summarized as,

(a)	^{238}U and ^{239}Pu fission cross section uncertainties	1.50	%,
(b)	The other fission cross section uncertainties	0.05	%,
(c)	All fission cross section uncertainties	1.55	%.

As discussed in the previous section, the dominant contributions come from ^{238}U and ^{239}Pu. Considering the spatial change of $R_n^m(\vec{r})$ of about 5 % relative to the average reaction rate $\overline{R_k^m}$, the above uncertainties have about 5 % deviations, i.e. 1.55 ± 0.08 % for case (c), since the sensitivity coefficient $H_{\sigma_f^j}^{R_k^m}$ is proportional to $\delta\overline{R_n^m}/\overline{R_n^m}$ as shown by Eq.(48) in the APPENDIX-*I* of Ref. 29.

The Delayed neutron spectrum χ_d^m, in general, is very complicated function since actual spectrum is a mixture of about 72 β-decay precursor's spectra, but in practice, an average spectrum is used by many authors. As shown by Eq.(3), the delayed neutron spectrum in β_{eff} is used as the neutron importance and integrated over the whole energy range. Consequently, the partial fluctuation of the spectrum seems to give a minor effect to the β_{eff}. According to the work by Moberg and Kockum[14], the effect of the uncertainty of the delayed neutron spectrum to β_{eff} is at most about 0.5 %. Therefore, in the present work, their result of 0.5% is adopted as the uncertainty due to the error of the delayed neutron spectrum.

3.3 β_{eff} Uncertainty due to Uncertainties of Calculational Models

The effective cross section of the hexagonal fuel assembly is prepared by the collision probability cell calculation code SLAROM[24] using 70 group cross section library JFS-3-J2[25], and collapsed into 18 groups by the 70 group neutron flux. The energy group structure of the 70 group JFS-3-J2 cross section library is defined by constant lethargy width of 0.25 from the top energy 10 MeV. The 18 group structure can be seen in Fig. 8. This 18 group set is used for the overall β_{eff} uncertainty estimation. Reference calculation for the cylindrical core by an annular radial blanket and disc axial blankets is performed by the diffusion code CITATION[26]. Control rods are also simulated by the annular geometry, i.e. clean core mock-up, and the control rod effect is treated as a correction factor to the β_{eff} uncertainties. However, the uncertainties due to the fission cross section

errors are estimated by the generalized perturbation theory code SAGEP[17] in terms of the sensitivity coefficients of the reaction rate ratios $H^{R_k^m}_{\sigma_f^j}$, and then the coefficients are applied to Eq.(29) for the sensitivity coefficient of the β_{eff}.

The resultant neutron and adjoint fluxes are shown in **Fig. 11**. As a special case, the two-dimensional transport code TWOTRAN[27] is used for the estimation of transport correction of the β_{eff}.

The β_{eff}-values are obtained by the first order perturbation code PERKY[28] coupled with the 18 group cross section library, and the uncertainties of the β_{eff} are estimated by mean of the error propagation law using the sensitivity coefficients multiplied by the uncertainties of delayed neutron data and of fission cross sections. The sensitivity coefficients can be obtained from the β_{eff}-values given as PERKY output (Eq. (11)).

The evaluated β_{eff} uncertainties due to the fission cross sections are shown in **Table 5** as the percentage uncertainties. Significant contribution can be found in the ^{238}U's 4 energy group where the fission cross rapidly rises as shown in **Fig. 7** .

Transport effect is estimated for the RZ geometry by the two dimensional transport code TWOTRAN[27] using the 18 group cross section library with the optional terms S_4 and P_1. The difference, defined by (Transport - Diffusion) calculations, of some typical kinetic parameters are obtained as shown below.

1) $\frac{\delta\beta_{eff}}{\delta\beta_{eff}} = 0.31$ %, 2) $\frac{\delta l_p}{l_p} = 0.81$ %, 3) $\frac{\delta Inhour}{Inhour} = 0.23$ %,

where $\frac{\delta Inhour}{Inhour}$ means the error of Inhour, i.e., the relative error obtained by setting T=1 hour for Eqs.(16,17,18,19). The transport effect to β_{eff} is significantly small in comparison with the uncertainty due to the delayed neutron yield. In the present work, the above $\delta\beta_{eff}/\beta_{eff}$ is adopted as a systematical error of 0.31 % and it is added to the statistical sum of random errors.

The effect of the number of energy groups to β_{eff} was studied by D'Angelo and Filip[5] by comparison of 25 and 6 groups, and the result of 1.3 % enhancement was obtained. In the present work, an investigation of the group number effect is made by comparison between 18 and 6 group calculations, and the same enhancement 1.3 % is also obtained.

Control rod effect to β_{eff} is also assumed to be small since the flux perturbation by control rod insertion is generally spread over a wide region of the whole core, and thus a local flux depression in the perturbed region necessarily induces an enhancement on the opposite side so as to conserve the total power of the reactor. Besides, β_{eff} is an integrated reactivity worth of delayed neutrons over the whole reactor, and compensation of a reactivity loss near the perturbed region by the control rod with an increment on the unperturbed region can be expected. Therefore, the resultant effect is reduced in general. According to the work by D'Angelo and Filip[5], the control rod effect is at most 0.3 %. To validate the above consideration for the present work, the strongest perturbation takes place by full insertion of the B_4C control rod into the central position of the inner core in **Fig. 6**. Even in such a extreme case, the change of β_{eff} is 0.02 % relative to the clean core without the control rod. Therefore, the control rod effect can be neglected.

The cell homogenization effect to obtain the effective cross sections equivalent with homogeneous cores was about 0.3 % as a maximum in D'Angelo and Filip's study[5], which

is a minor contribution to the total β_{eff} uncertainty.

4 Overall Evaluation of β_{eff} Uncertainty

In this section, net uncertainty of the β_{eff} by taking into account all components is evaluated by judging the statistical nature of each component, i.e., if it is to a systematical or a random error. For random errors, a statistical sum is estimated by Eq.(14) and systematical errors can be treated as an additive or subtractive term according to their statistical nature.

The overall uncertainty components calculated in the previous sections are shown in **Table 6** together with the statistical treatments. Two models are considered as Model-1 and Model-2 which are distinguished as follows.

Model-1	has a smaller energy dependence, and excludes the control rod and cell homogenization effects.
Model-2	has a larger energy dependence, and includes the control rod and cell homogenization effects.

"Stat." and "Syst." stand for the statistical and systematical errors, respectively.

The major component is due to the uncertainty of the delayed neutron yield. The second and third main components are the energy dependence, and uncertainty of the fission cross sections (both are the same order). The energy dependencies have 1.4 % and 1.7 % uncertainties for below 10 keV and below 50 keV, respectively, as proposed by D'Angelo et al.[5], which have a difference of about 0.3 % depending on the range of energy considered in the lower energy side. The transport effect is about 0.3 % whose diffusion calculation gives larger β_{eff}.

Uncertainty of reactivity worth ρ due to the uncertainty of delayed neutron parameters can also be obtained by using Eq.(17). Resultant uncertainties are shown in **Fig. 12** for the ν_d^m's energy dependence of case-1 (up to 10 keV) and that of case-2 (up to 50 keV), respectively, as a function of reactor period. In this ρ-uncertainty evaluation, the errors of decay constants λ_i^m's and period T are additionally considered for the β_{eff} uncertainty evaluation. The error of the decay constant is adopted from Tuttle's recommendation[12] as shown in **Table 2** and the period error is assumed to be 1.5 %.

The magnitudes of the reactivity uncertainties $\delta\rho/\rho$'s are nearly same to those of the β_{eff}'s, but it is reduced by amount of about 10 % relative to β_{eff}'s, since the weighting functions differ from those of β_{eff}'s, i.e., the sensitivity coefficients of the β_{eff} are 0.40 for ^{238}U and 0.38 for ^{239}Pu while those for $\delta\rho/\rho$ are 0.28 and 0.4, respectively. Consequently, the reduction of the contribution from ^{238}U reduces $\delta\rho/\rho$ in comparison with $\delta\beta_{eff}/\beta_{eff}$. The uncertainty of the delayed neutron yield ν_d^m is still major a contribution to ρ.

5 Conclusion

The uncertainties of the effective delayed neutron fraction β_{eff} and the reactivity worth ρ for a step insertion of reactivity as a function of period T were evaluated based on the theoretically derived uncertainty evaluation formula. Total delayed neutron yield ν_d^m, its fraction a_{di}^m, energy dependence of ν_d^m, and fission cross sections of ^{235}U, ^{238}U, ^{239}Pu, ^{240}Pu and ^{241}Pu were considered. For the fission cross sections, a sensitivity calculational model was developed from the sensitivity coefficients of the reaction rate ratios based on the generalized perturbation theory. The following conclusions were obtained.

(1) Uncertainty of the effective delayed neutron fraction β_{eff} for the proto-type sodium cooled fast reactor was about 4-5 %, and that of the reactivity worth ρ is nearly the same order over whole practical range of reactor periods T.
(2) The largest component of the uncertainty, about 2.5 %, was due to the uncertainty of total delayed neutron yield ν_d^m, and its main contribution came from family 3 of ^{238}U. The second contribution was due to ^{239}Pu's and its magnitude was about 29 % compared to 35 % for ^{238}U's.
(3) The uncertainties of the energy dependency of ν_d^m, based on the parametric study used by D'Angelo and Filip, was about 1.55 ± 0.15 %, (i.e. 1.4 % and 1.7 %) with the deviation width depending on the energy range considered.
(4) The uncertainties of fission cross sections gave about a 1.6 % uncertainty to β_{eff}.

The uncertainty of the delayed neutron spectrum was not investigated since a calculational model for the sensitivity coefficient is not yet available. However, the uncertainty of about 0.5 % to the β_{eff}'s has been given by Moberg and Kockum.

Acknowledgments

The author wish to acknowledge Drs. A. D'Angelo and J.C. Cabriliat for their information which was incorporated into the supplements of the present work. For this work, the author had many discussions with his coworkers, Dr. T. Suzuki of Operations Engineering Section, Monju Construction Office, Japan Nuclear Cycle Development Institute, Dr. S. Sawada and Mr. H. Hanaki of Hitachi Works, Hitachi Ltd. Their contributions to this work have been very great and the author takes pleasure in acknowledging the important part played by them.

- References -

(1) *Proc. IAEA The Consultants Meeting on Delayed Neutron Properties*, Vienna, 1979.
(2) Hammer Ph. and Tuttle R.J.: *Proc. IAEA Consultants Meeting on Delayed Neutron Properties*, Vienna, 1979, P.277, (1979).
(3) Hammer Ph.: *Proc. IAEA Consultants Meeting on Delayed Neutron Properties*, Vienna, 1979, p.1 (1979).
(4) D'Angelo A., Vuillemin B. and Cabrillat J.C.: *NEAXRP-A-766*, (1987).
(5) D'Angelo A. and Filip A.: *Nucl. Sci. Eng.*, **114**, 332 (1993).
(6) Tuttle R.J.: *Proc. IAEA Consultants Meeting on Delayed Neutron Properties*, Vienna, 1979, p.29 (1979).
(7) Alexander D.R. and Krick M.S.: *Nucl. Sci. Eng.*, **62**, 627 (1977).
(8) Davey W.G.: *Nucl. Sci. Eng.*, **44**, 345 (1971).
(9) Bohn E.H.: *ANL-75-14* (1975).
(10) Foell W.K.: *"Small-Sample Reactivity Measurements in Nuclear Reactors"*, American Nuclear Society, (1972).
(11) Kobayashi K.: *Nuclear Reactor Physics,* Corona Publishing Co., Ltd., Tokyo Japan (1996) [in Japanese]
(12) Tuttle R.J.: *Nucl. Sci. Eng.*, **56**, 37 (1975).
(13) Saphier D., Ilberg D., Shalev S. and Yiftah S.: *Nucl. Sci. Eng.*, **62**, 660 (1977).
(14) Moberg L. and Kockum J.: *Nucl. Sci. Eng.*, **52**, 343 (1973).
(15) Krick M.S. and Evans A.E.: *Nucl. Sci. Eng.*, **47**, 311 (1972).
(16) Evans A.E., Thorpe M.M. and Krick M.S.: *Nucl. Sci. Eng.*, **50**, 80 (1972).
(17) Hara A. and Takeda T.: *JAERI-M-84-027*, (1984).
(18) Gandini A., Salvatores M. and Dal Bono I.: *Fast Reactor Physics,* **Vol. I**, p.241, International Atomic Energy Agency, Vienna (1968).
(19) Stacy Jr W.M.: *Nucl. Sci. Eng.*, **40**, 444 (1972).
(20) Ohmori Y. and Inoue T.: *Gensiryoku Kougyou*, **40**, 17, (1994), [in Japanese], and Suzuki T.: *Gensiryoku Kougyou*, **40**, 19 (1994), [in Japanese].
(21) Ishikawa M. et al.: *Proc. Int. Conf. on Mathematical Method and Super Computing in Nuclear Applications, (M&C + SNA'93)*, Karlsruhe, **Vol. 1**, 593 (1993).
(22) Keepin G.R.: *"Physics of Nuclear Kinetics"*, Addison-Wesley Publishing Co., Inc., Reading, Massachusets (1965).
(23) Nakajima Y.: JEF REPORT 9, (Nov. 1986), OECD NEA Data Bank (1986).
(24) Nakagawa M. and Tsuchihashi K.: *JAERI 1249*, (1984).
(25) Nakagawa T.: *JAERI-M 84-103(1984)*, and Takano M.: *JAERI-M 89-141*, (1989), [in Japanese].
(26) Fowler T.F., Vondy D.R. and Cunningham G.W.: *ORNL-TM-2496*, Revision 2, (1971).
(27) Lathrop K.D. and Brinkley F.W.: *LA-4432*, April 1970.
(28) Iijima S., Yoshida H., and Sakuragi H.: *JAERI-M 6993*, (1977).
(29) Zukeran A. et. al., Nucl. Sci. Tech., **36**,1,61-80 , (1999).
(30) Osawa T. et. al., Japan Atomic Energy Society Annual Meeting, C28,, (1977).
(31) Mills R.W., "Review of Fission Product Yields and Delayed Neutron Data for The Actinides Np-237, Pu-242, Am-242m, Am243, Cm-243 and Cm-245", NEANDC-300-U, (1990).

Table 1 Total delayed neutron yields by Tuttle[6] and Mills[31] as functions of fuel elements and incident neutron energy. The recommended values by Tuttle are used as the reference delayed neutron yield data and the relative errors are in used to evaluate the β_{eff} uncertainty in the present work.

Fuel Element	Themal	Fast	14 MeV
Tuttle*)			
^{231}Pa	－	(0.0111 ± 0.0011) 10.0%	0.0080 ± 0.0026
^{232}Th	－	0.0531 ± 0.0023 4.2%	0.0285 ± 0.0013 4.6%
^{233}U	0.00667 ± 0.00029 4.3%	0.00731 ± 0.00036 4.9%	0.00422 ± 0.00025 5.2%
^{234}U	－	(0.0105 ± 0.0011) 10.7%	(0.0062 ± 0.0008) 13.3%
^{235}U	0.01621 ± 0.00050 3.1%	0.01673 ± 0.00036 2.1%	0.00927 ± 0.00029 3.1%
^{236}U	－	(0.0221 ± 0.0024) 10.7%	(0.013 ± 0.002) 13.3%
^{238}U	－	0.0439 ± 0.0010 2.3%	0.0273 ± 0.0008 2.9%
^{238}Pu	－	(0.0047 ± 0.0005) 10.7%	(0.0028 ± 0.0004) 13.3%
^{239}Pu	0.00628 ± 0.00038 6.0%	0.00630 ± 0.00016 2.5%	0.00417 ± 0.00016 3.7%
^{240}Pu	－	(0.0095 ± 0.0008) 7.9%	0.00671 ± 0.00050 7.5%
^{241}Pu	(0.0152 ± 0.0011) 7.3%	(0.0152 ± 0.0011) 7.3%	0.00834 ± 0.00070 8.4%
^{242}Pu	－ －	(0.00221 ± 0.0026) 11.8%	(0.0084 ± 0.0011) 13.3%
Mills#)			
^{237}Np	0.01779$^{s)}$ ± 0.00146	0.01207$^{s)}$ ± 0.0005	0.00970$^{s)}$ ± 0.0011
^{242}Am	0.00688$^{E)}$ ± 0.0005	0.00565$^{s)}$ ± 0.00092	
^{243}Am	0.00870$^{s)}$ ± 0.00143	0.00833$^{A)}$ ± 0.00118	
^{243}Cm	0.00209$^{s)}$ ± 0.00044	0.002297$^{s)}$ ± 0.00066	
^{245}Cm	0.00592$^{E)}$ ± 0.0004	0.004887$^{s)}$ ± 0.00109	

*): Values influenced by empirical estimation are shown in parentheses as noted by Tuttle[6].

#): The Mills' data were not used for β_{eff} uncertainty evaluation in this work. Superscripts for these data mean

E): weighted mean from experiments
S): value from summation
A): average value for values of summation
M): maximum error for A)

Table 2 Recommended fractional delayed neutron family yields and the decay constants by Tuttle[12].

Fuel Element	Family No.	Fractional Group Yield α_i	Decay Constant $\lambda_i(s^{-1})$
^{232}Th	1	0.034 ± 0.003	0.0124 ± 0.0003
	2	0.150 ± 0.007	0.0334 ± 0.0016
	3	0.155 ± 0.031	0.121 ± 0.007
	4	0.446 ± 0.022	0.321 ± 0.016
	5	0.172 ± 0.019	1.21 ± 0.13
	6	0.043 ± 0.009	3.29 ± 0.44
^{233}U	1	0.086 ± 0.004	0.0126 ± 0.0006
	2	0.274 ± 0.007	0.0334 ± 0.0021
	3	0.227 ± 0.052	0.131 ± 0.007
	4	0.317 ± 0.016	0.302 ± 0.036
	5	0.073 ± 0.021	1.27 ± 0.39
	6	0.023 ± 0.010	3.13 ± 1.00
^{235}U	1	0.038 ± 0.004	0.0127 ± 0.0003
	2	0.213 ± 0.007	0.0317 ± 0.0012
	3	0.188 ± 0.024	0.115 ± 0.004
	4	0.407 ± 0.010	0.311 ± 0.012
	5	0.128 ± 0.012	1.40 ± 0.12
	6	0.026 ± 0.004	3.87 ± 0.55
^{238}U	1	0.013 ± 0.001	0.0132 ± 0.0004
	2	0.137 ± 0.003	0.0321 ± 0.0009
	3	0.162 ± 0.030	0.139 ± 0.007
	4	0.388 ± 0.018	0.358 ± 0.021
	5	0.225 ± 0.019	1.41 ± 0.10
	6	0.075 ± 0.007	4.02 ± 0.32
^{239}Pu	1	0.038 ± 0.004	0.0129 ± 0.0003
	2	0.280 ± 0.006	0.0311 ± 0.0007
	3	0.216 ± 0.027	0.134 ± 0.004
	4	0.328 ± 0.015	0.331 ± 0.018
	5	0.103 ± 0.013	1.26 ± 0.17
	6	0.035 ± 0.007	3.21 ± 0.38
^{240}Pu	1	0.028 ± 0.004	0.0129 ± 0.0006
	2	0.273 ± 0.006	0.0313 ± 0.0007
	3	0.192 ± 0.078	0.135 ± 0.016
	4	0.350 ± 0.030	0.333 ± 0.046
	5	0.128 ± 0.027	1.36 ± 0.30
	6	0.029 ± 0.009	4.04 ± 1.16
^{241}Pu	1	0.010 ± 0.003	0.0128 ± 0.0002
	2	0.229 ± 0.006	0.0299 ± 0.0006
	3	0.173 ± 0.025	0.124 ± 0.013
	4	0.390 ± 0.050	0.352 ± 0.018
	5	0.182 ± 0.019	1.61 ± 0.15
	6	0.016 ± 0.005	3.47 ± 1.7
^{242}Pu	1	0.004 ± 0.001	0.0128 ± 0.0003
	2	0.195 ± 0.032	0.0314 ± 0.0013
	3	0.161 ± 0.048	0.128 ± 0.009
	4	0.412 ± 0.153	0.325 ± 0.020
	5	0.218 ± 0.087	1.35 ± 0.09
	6	0.010 ± 0.003	3.70 ± 0.44

Note: The relative errors of the fractional yields and the decay constants are used as the error components for the uncertainty evaluations of β_{eff} and reactivity worth ρ.

Table 3 β_{eff} contributions in absolute per 10^4 fissions as functions of delayed neutron families and fuel elements for a typical proto-type sodium cooled fast reactor[20].

Fuel Element	Delayed Neutron Family						
	1	2	3	4	5	6	Total
Inner Core							
^{235}U	0.0110	0.0614	0.0542	0.1173	0.0369	0.0075	0.2883#)
^{238}U	0.1137	1.1985	1.4172	3.3943	1.9683	0.6561	8.7482
^{239}Pu	0.3149	2.3203	1.7899	2.7180	0.8535	0.2900	8.2867
^{240}Pu	0.0283	0.2759	0.1940	0.3537	0.1294	0.0293	1.0106
^{241}Pu	0.0315	0.7213	0.5449	1.2284	0.5733	0.0504	3.1497
^{242}Pu	0.0011	0.0522	0.0431	0.1103	0.0583	0.0027	0.2676
Total	0.5004$)	4.6295	4.0433	7.9220	3.6197	1.0360	21.751
Outer Core							
^{235}U	0.0042	0.0234	0.0206	0.0447	0.0140	0.0029	0.1097
^{238}U	0.0508	0.5353	0.6329	1.5159	0.8791	0.2930	3.9070
^{239}Pu	0.1804	1.3290	1.0252	1.5568	0.4889	0.1661	4.7465
^{240}Pu	0.0173	0.1690	0.1188	0.2166	0.0792	0.0179	0.6189
^{241}Pu	0.0179	0.4104	0.3100	0.6989	0.3262	0.0287	1.7921
^{242}Pu	0.0007	0.0324	0.0267	0.0684	0.0362	0.0017	0.1659
Total	0.2712	2.4993	2.1344	4.1013	1.8236	0.5103	11.340
Radial Blanket							
^{235}U	0.0025	0.0138	0.0122	0.0264	0.0083	0.0017	0.0648
^{238}U	0.0107	0.1131	0.1337	0.3202	0.1857	0.0619	0.8253
Total	0.0132	0.1269	0.1459	0.3466	0.1940	0.0636	0.8902
Axial Blanket							
^{235}U	0.0016	0.0089	0.0079	0.0170	0.0054	0.0011	0.0419
238U	0.0056	0.0592	0.0700	0.1677	0.0972	0.0324	0.4322
Total	0.0072	0.0681	0.0779	0.1847	0.1026	0.0335	0.4741
Whole Core and Blanket							
^{235}U	0.0192	0.1075	0.0949	0.2054	0.0646	0.0131	0.5048
^{238}U	0.1809	1.9060	2.2538	5.3981	3.1303	1.0435	13.913
^{239}Pu	0.4953	3.6493	2.8152	4.2749	1.3424	0.4562	13.033
^{240}Pu	0.0456	0.4449	0.3129	0.5703	0.2086	0.0473	1.6295
^{241}Pu	0.0494	1.1317	0.8549	1.9273	0.8994	0.0791	4.9418
^{242}Pu	0.0017	0.0845	0.0698	0.1786	0.0945	0.0043	0.4336
Total	0.7921	7.3239	6.4015	12.555	5.7398	1.6434	34.455
	Effective Delayed Neutron Fraction $\beta_{eff} = 0.3446$ %						

#) : Sum over all families for the isotops.
$) : Sum over all isotopic contributions to the family

Table 4 β_{eff} Sensitivity Coefficients for Fission Cross Sections

No.	Upp. En. (eV)	σ_f^{235}		σ_f^{238}		σ_f^{239}		σ_f^{240}		σ_f^{241}	
		Calculated*)	Normalized†)	Calculated	Normalized	Calculated	Normalized	Calculated	Normalized.	Calculated	Normalized
1	1.000E+7	0.002	0.002	0.078	0.052	-0.009	-0.003	0.015	0.014	0.002	0.002
2	6.065E+6	0.007	0.006	0.208	0.141	-0.032	-0.011	0.050	0.047	0.007	0.006
3	3.679E+6	0.019	0.018	0.515	0.348	-0.088	-0.032	0.138	0.130	0.018	0.018
4	2.231E+6	0.029	0.027	0.608	0.411	-0.130	-0.047	0.195	0.183	0.029	0.028
5	1.353E+6	0.034	0.032	0.063	0.043	-0.143	-0.051	0.219	0.206	0.034	0.033
6	8.209E+6	0.081	0.076	0.005	0.004	-0.318	-0.114	0.239	0.224	0.080	0.077
7	3.877E+5	0.113	0.106	0.001	0.000	-0.370	-0.132	0.058	0.054	0.114	0.110
8	1.832E+5	0.135	0.126	0.000	0.000	-0.383	-0.137	0.033	0.031	0.138	0.134
9	8.652E+4	0.129	0.121	0.000	0.000	-0.329	-0.118	0.029	0.027	0.125	0.121
10	4.087E+4	0.113	0.106	0.000	0.000	-0.255	-0.091	0.025	0.023	0.111	0.108
11	1.931E+4	0.091	0.085	0.000	0.000	-0.182	-0.065	0.015	0.014	0.088	0.086
12	9.119E+3	0.070	0.066	0.000	0.000	-0.124	-0.044	0.005	0.005	0.067	0.065
13	4.307E+3	0.038	0.036	0.000	0.000	-0.064	-0.023	0.006	0.005	0.035	0.034
14	2.035E+3	0.105	0.098	0.000	0.000	-0.179	-0.064	0.023	0.021	0.096	0.093
15	9.611E+2	0.068	0.063	0.000	0.000	-0.123	-0.044	0.014	0.013	0.054	0.052
16	4.540E+2	0.024	0.023	0.000	0.000	-0.046	-0.017	0.002	0.002	0.025	0.024
17	2.145E+2	0.007	0.007	0.000	0.000	-0.015	-0.005	0.001	0.000	0.007	0.006
18	1.013E+2	0.001	0.001	0.000	0.000	-0.005	-0.002	0.000	0.000	0.002	0.002
	Sum	1.068	1.000	1.479	1.000	-2.794	-1.000	1.065	1.000	1.032	1.000

⋆): as calculated by Eq.(**) †): Normalized so as to $\sum_g |S_{\sigma_x}^{\beta_{eff}}| = 1.0$

Table 5 Ralative $\beta_{eff}^{*)}$ Uncertainties due to Fission Cross Section Uncertaities.

Group No.	Upper Energy (eV)	Relative β_{eff} Uncertainty				
		σ_f^{235}	σ_f^{238}	σ_f^{239}	σ_f^{240}	σ_f^{241}
1	1.000E+07	0.007	3.383	-0.320	0.104	0.058
2	6.065E+06	0.015	6.045	-0.458	0.235	0.193
3	3.679E+06	0.028	14.966	-1.271	0.652	0.406
4	2.231E+06	0.042	88.344	-1.874	4.608	0.542
5	1.353E+06	0.074	11.900	-3.298	6.728	0.750
6	8.209E+06	0.298	0.847	-14.438	6.213	1.772
7	3.877E+05	0.413	0.318	-17.332	4.084	2.531
8	1.832E+05	0.591	0.299	-21.254	3.935	5.106
9	8.652E+04	0.565	0.227	-18.257	3.427	5.550
10	4.087E+04	0.413	0.166	-5.513	2.930	5.750
11	1.931E+04	0.398	0.153	-3.935	1.761	3.291
12	9.119E+03	0.462	0.074	-2.681	0.646	2.979
13	4.307E+03	0.223	0.000	-0.917	0.655	1.567
14	2.035E+03	0.307	0.155	-7.740	2.694	4.276
15	9.611E+02	0.248	0.256	-5.319	1.690	2.393
16	4.540E+02	0.089	0.000	-1.332	0.201	1.106
17	2.145E+02	0.026	0.000	-0.432	0.060	0.297
18	1.013E+02	0.002	0.000	-0.130	0.001	0.037
	Sum	1.301	99.660	-38.135	13.122	12.352

*) The tabulated isotopic(i)- and group(g)-component $\beta_{eff}(i,g)$ is normalized 100 % uncertainty as shown below,

$$R \cdot \sqrt{\sum_i \sum_g \{\beta_{eff}(i,g)\}^2} = 100.0$$

therefore, by using the normalization constant R,

$$Renormalized \quad \beta_{eff}^{Norm} = \frac{\beta_{eff}(i,g)}{R}$$

is obtained and the β_{eff}^{Norm} is shown in the table.

Table 6 Evaluated β_{eff} uncertainty and the Percentage Contribution of each Error Source.

Item	Error Sources		Method-1[i]		Method-2	
			Stat.	Syst.	Stat.	Syst.
(1)	$\nu_{d,i,m}$ Error		± 2.5		± 2.5	
(2)	$\nu_{d,m}$ Energy Dependence[ii]			+1.4		+1.7
(3)	Fission Cross Section		± 1.6		± 1.6	
(4)	Reaction Rate Ratio		± 0.1		± 0.1	
(5)	$\chi_{d,m}$ Choice		± 0.5		± 0.5	
(6)	Transport Effect[ii]	(a)		-0.3		-0.3
		(b)		0.0		0.0
(7)	Energy Group Effect	(a)	0.0[iii]		0.0	
		(b)	± 1.3		± 1.3	
(8)	Control Rod Effect	(a)	0.0		± 0.03[iv]	
		(b)	0.0		± 1.1[v]	
(9)	Cell Homogenization		0.0		± 0.3[v]	
	Statistical Treatment					
(A-1)	Simple Sum	(a)	± 4.7	+1.0	± 5.0	+1.4
		(b)	± 6.0	+1.4	± 7.4	+1.7
(A-2)	Overall Simple Sum[vi]	(a)	± 5.7		± 6.4	
		(b)	± 7.4		± 9.1	
(B)	Overall Statistical Sum	(a)	± 3.3		± 3.5	
		(b)	± 3.6		± 3.9	
(C)	Statistical Sum	(a)	± 3.0	+1.0	± 3.0	+1.4
		(b)	± 3.3	+1.4	± 3.5	+1.7
(D)	Overall Uncertainty	(a)	± 4.0[vii]		± 4.4[viii]	
		(b)	± 4.7[vii]		± 5.2[viii]	

i) Model-1 has a smaller $\nu_{d,m}$ energy dependence and no items (8) and (9) which are considered in Model-2. "Stat." and "Syst." stand for statistical(random) error and systematical error, respectively.
ii) Treated as systematical error.
iii) For number of energy groups larger than 18. The ± 1.3% of (b) is for 6 group calculation.
iv) For fully inserted central control rod.
v) From Ref. 5.
vi) Extreme case when all errors additionally contribute.
vii) (a) does not have the energy group effect (7), but (b) has the 1.3% energy group effect.
viii) (a) does not have the energy group (7) and control rod (8) effects, but (b) has both effects.

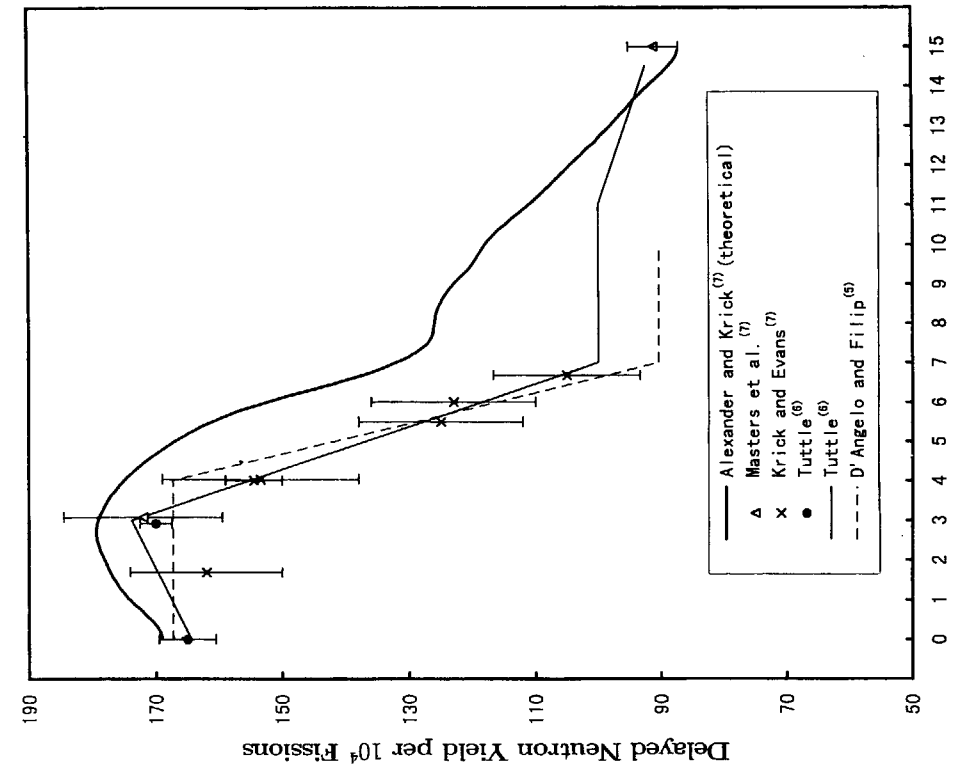

Fig. 2 Comparison of ^{235}U total delayed neutron yields as a function of incident neutron energy.

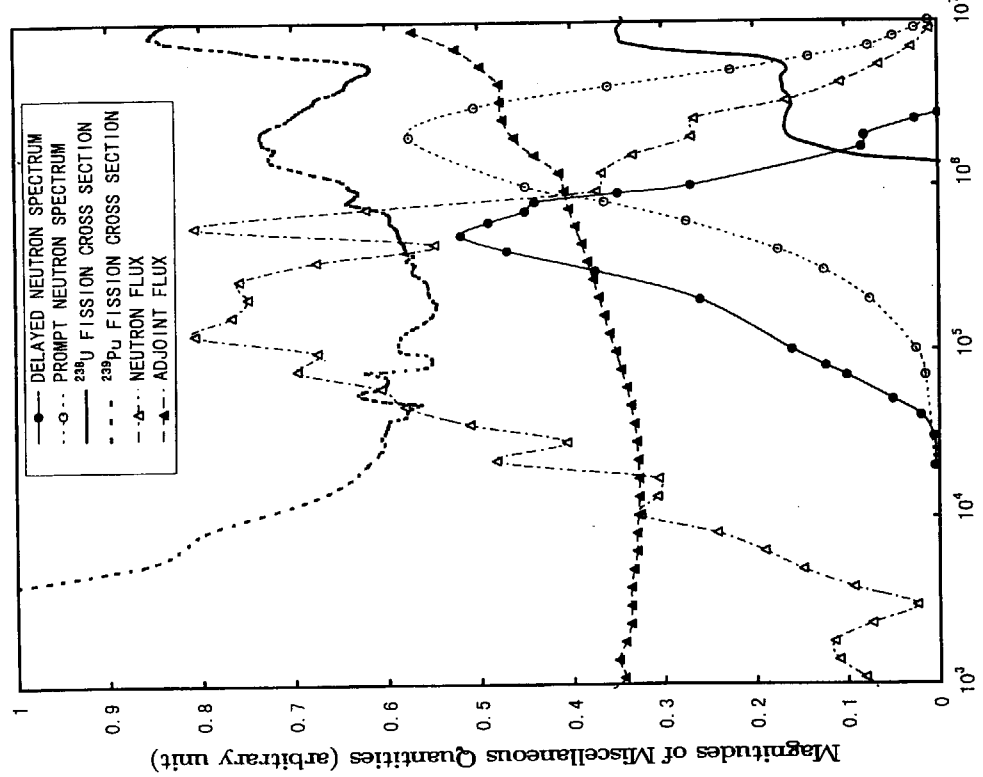

Fig. 1 Miscellaneous quantities related to effective delayed neutron fraction β_{eff} as functions of incident neutron energy. Neutron and adjoint fluxes are for a proto-type sodium cooled fast breeder reactor[20].

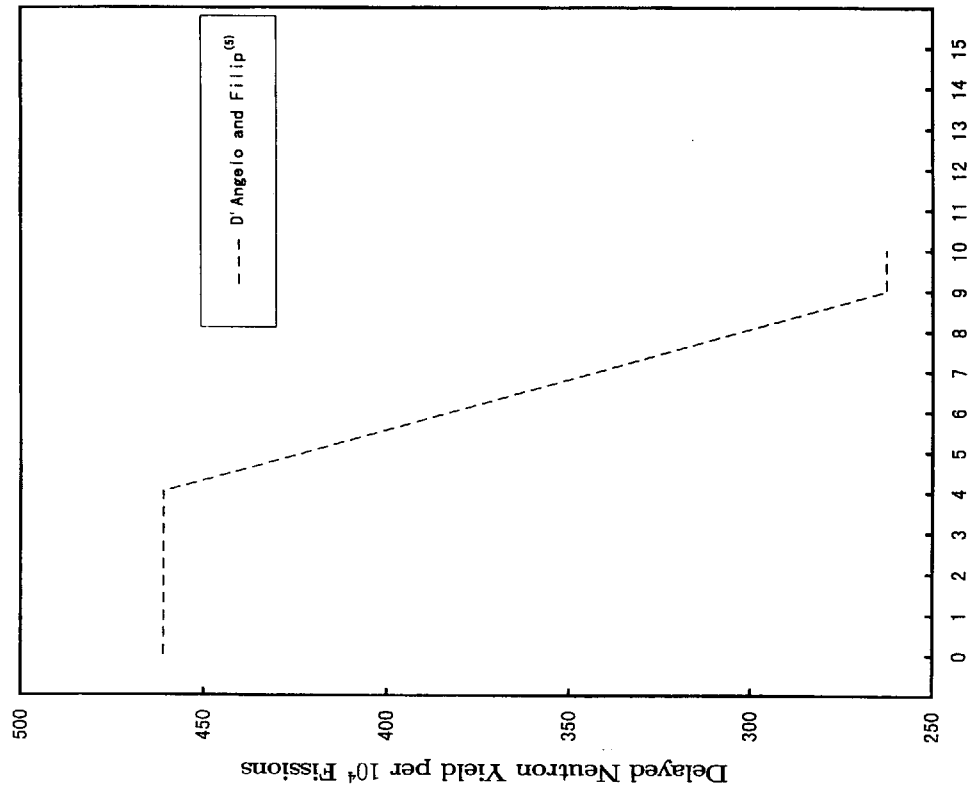

Fig. 4 Energy dependence of ^{238}U total delayed neutron yield by D'Angelo[5]. The total delayed neutron yield is reproduced from Fig. 3 of Ref. 5.

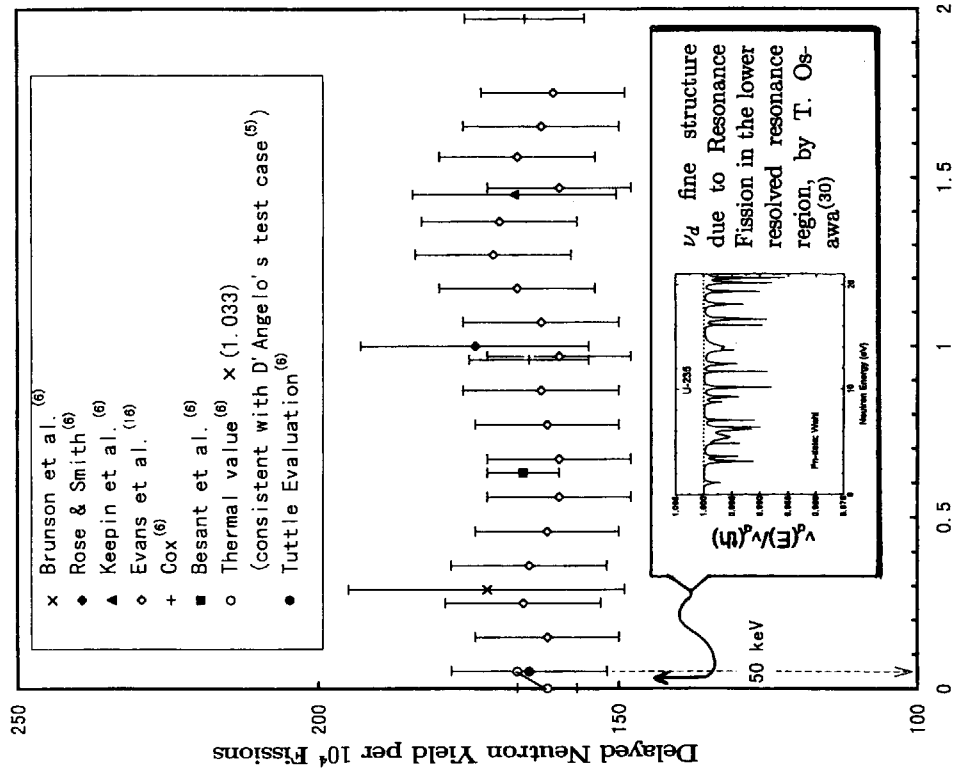

Fig. 3 Comparison of ^{235}U total delayed neutron yields in low energy region as functions of incident neutron energy. Yield at 0 MeV is the recommended value by Tuttle[6] and bold line extended to 50 keV shows the 3.3 % enhanced value of the evaluated value as proposed by D'Angelo[5].

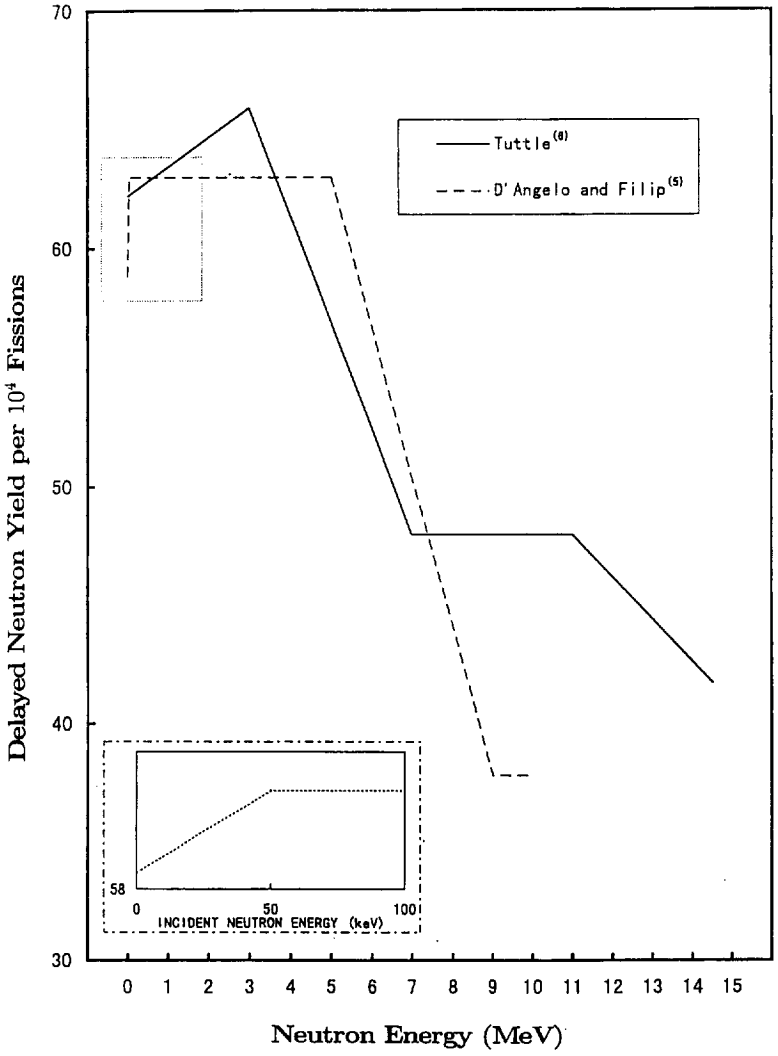

Fig. 5 Energy dependence of ^{239}Pu total delayed neutron yields as a function of incident neutron energy.

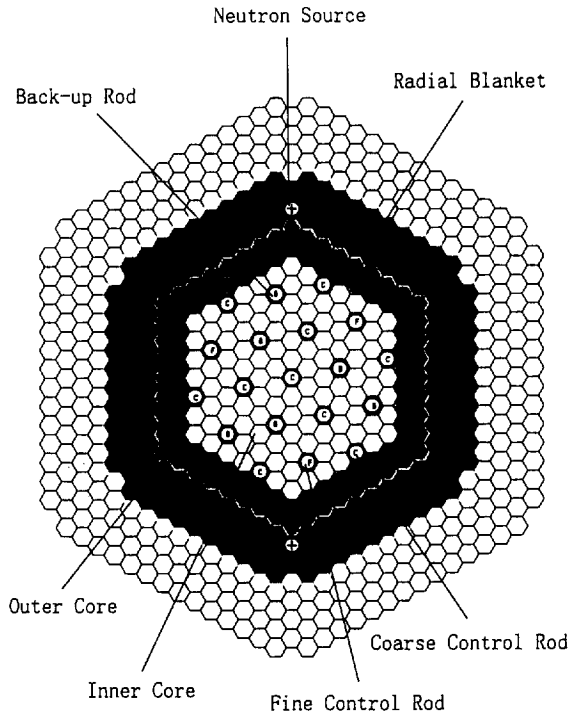

Reactor type	: Sodium cooled FBR	Breeding Ratio	: 1.2
Thermal Power (MWt)	: 714	Core Dimensions (m)	
Fuel		Equivalent Diameter	: 1.8
Core Fuel	: Mixed-oxide	Core Height	: 0.93
Blanket Fuel	: Uranium	Blanket Dimensions (m)	
Pu Enrichment (%)		Radial Blanket Thickness	: 0.3
Inner/Outer Cores	: 16/21	Upper Axial Blanket Thickness	: 0.3
Fuel Inventory (t)		Lower Axial Blanket Thickness	: 0.35
Core(U+Pu)	: 5.9		
Blanket(U)	: 17.5		

Fig. 6 Fuel loading map and core specification of a prototype sodium cooled fast breeder reactor[20].

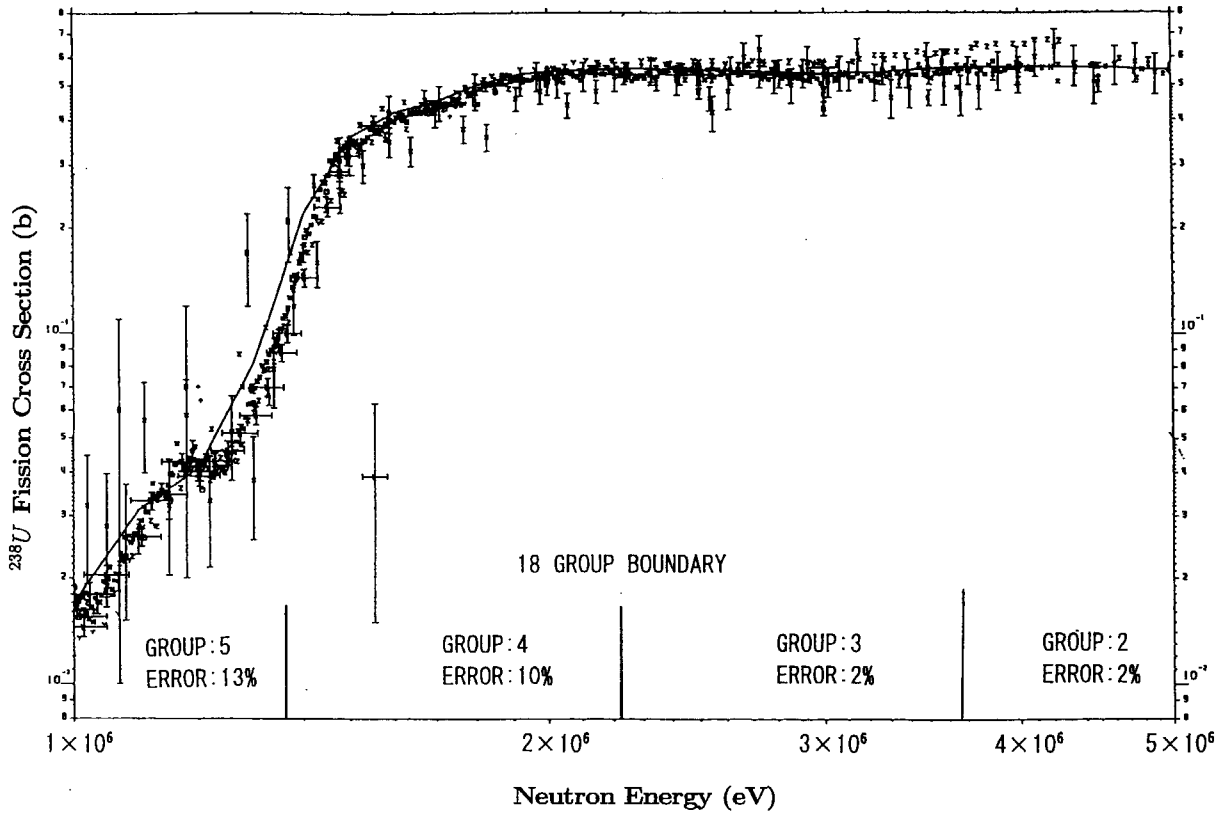

Fig. 7 ^{238}U fission cross section and its relative error as a function of incident neutron energy. This figure is shown to indicate the sharp energy dependence of ^{238}U fission cross section and the order of the relative errors. The β_{eff} value are obtained by using the 18 group cross section library prepared from the Japan Evaluated Nuclear Data Library version-2 JENDL-2[25].

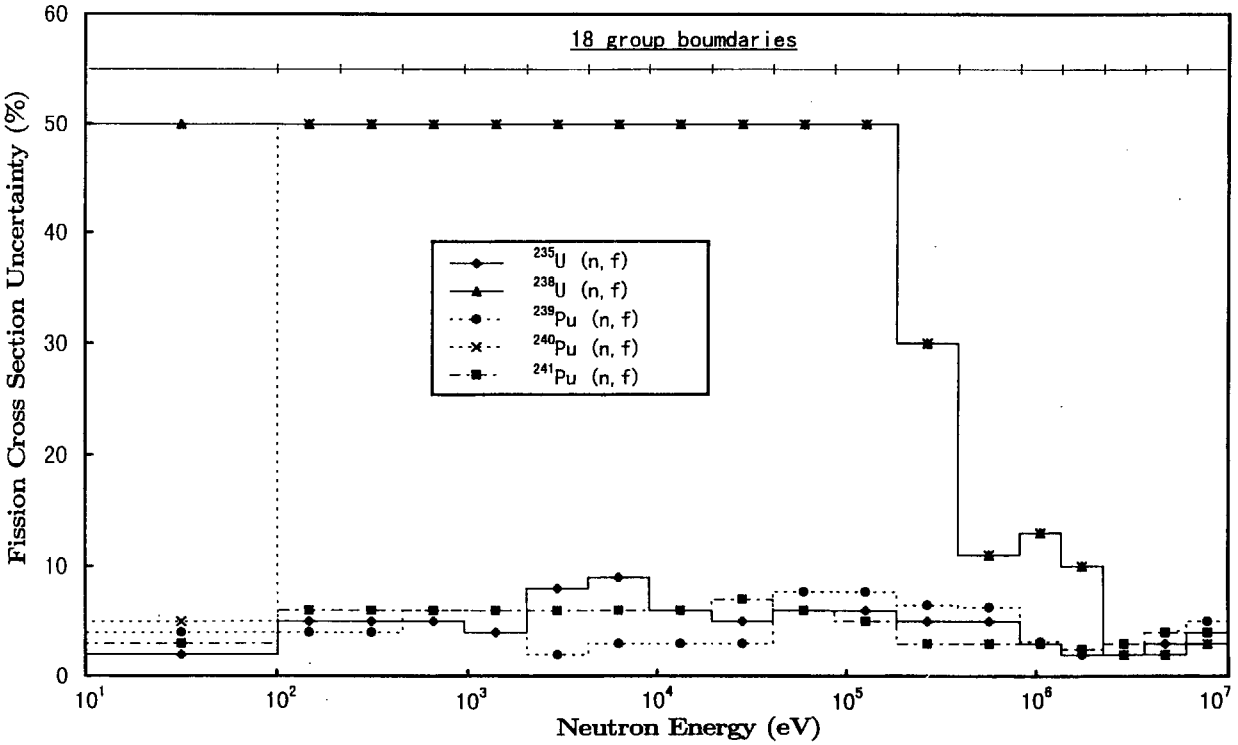

Fig. 8 Fission cross section uncertainties as functions of incident neutron energy of the 18 group structure.

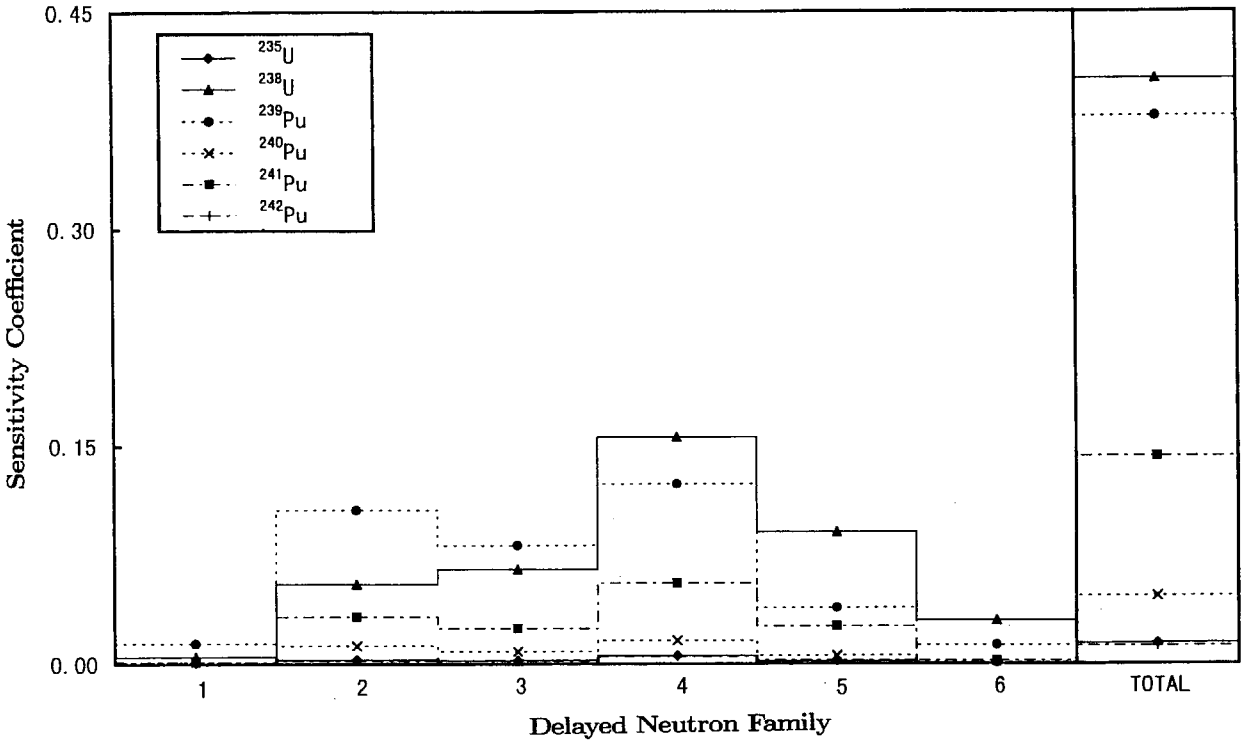

Fig. 9 Sensitivity coefficients of β_{eff} to delayed neutron family yield for a typical prototype sodium cooled fast breeder reactor[20] as functions of delayed neutron family and fuel elements.

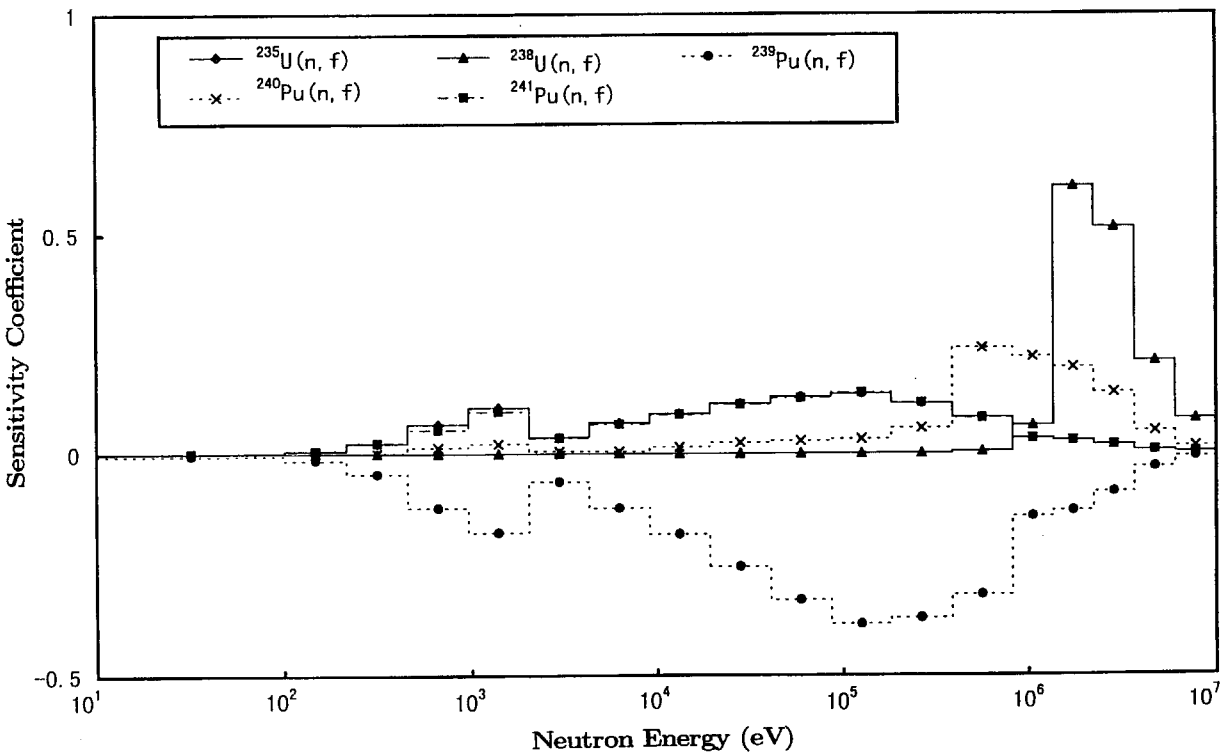

Fig. 10 Sensitivity coefficients of β_{eff} for five fission cross sections as a function of incident neutron energy in the 18 group structure.

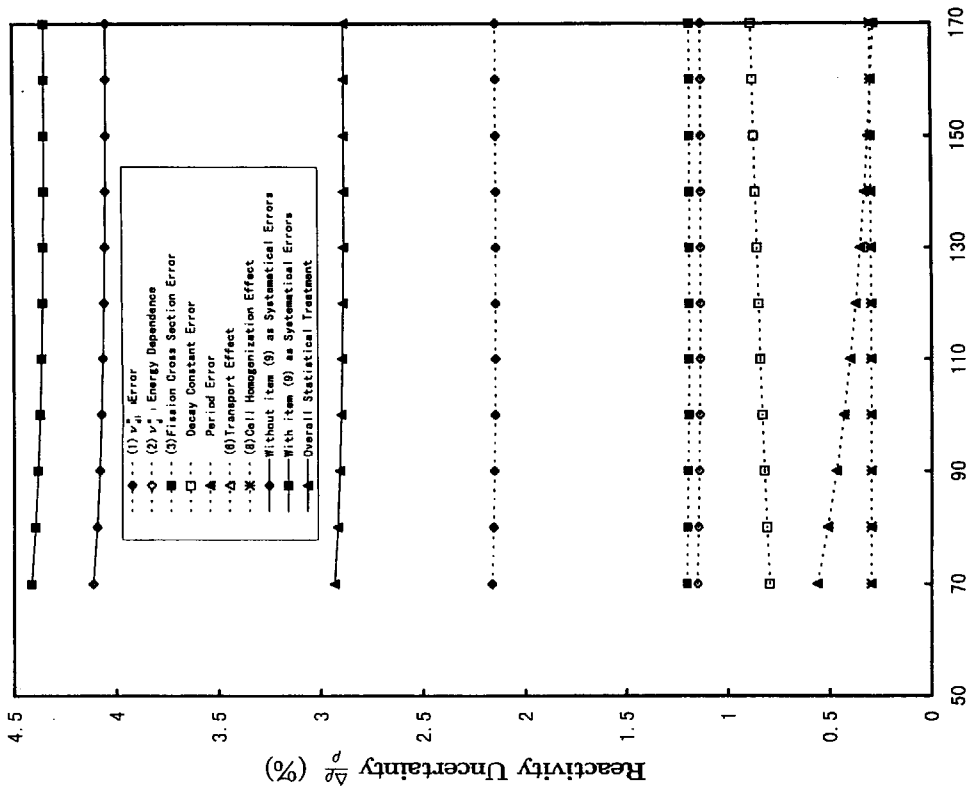

Fig. 12 Uncertainties of reactivity ρ and its components from Eq.(16) as a function of reactor period.

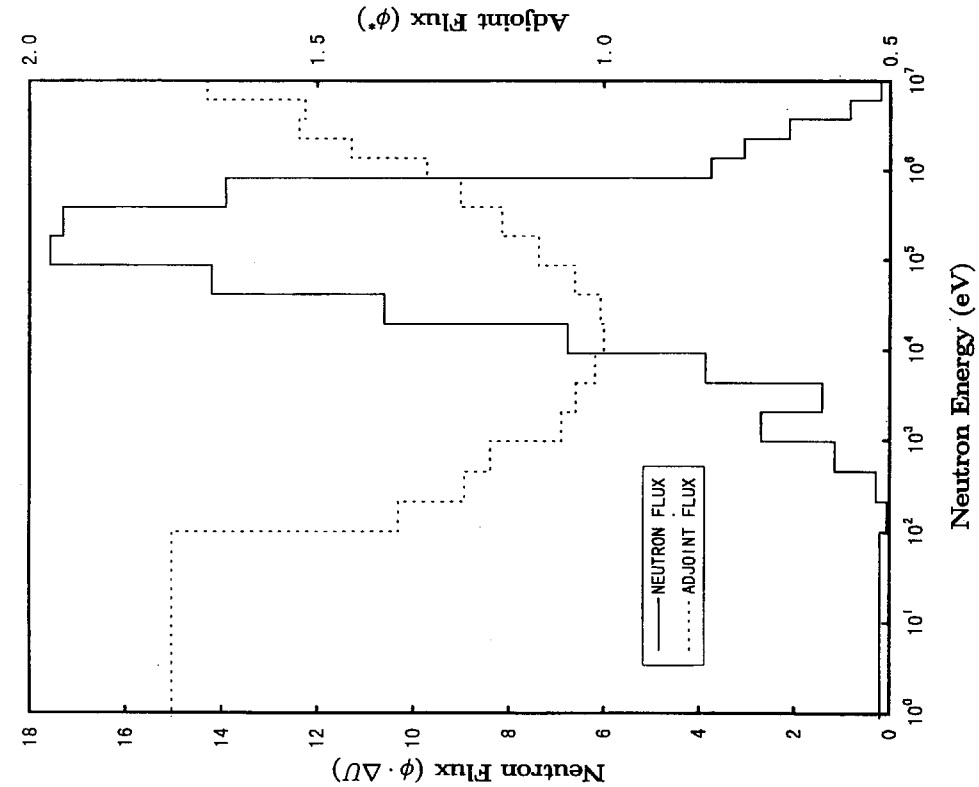

Fig. 11 Neutron and adjoint fluxes in the proto-type sodium cooled fast breeder reactor[20] as function of incident neutron energy. The fluxes are obtained by 18 group calculation using homogeneous effective cross sections.

10. Analysis of Benchmark Experiments of Effective Delayed Neutron Fraction β_{eff} at MASURCA and FCA

Takeshi Sakurai and Shigeaki Okajima
Reactor Physics Laboratory, Japan Atomic Energy Research Institute
Tokai-mura, Naka-gun, Ibaraki-ken 319-1195
e-mail: sakurai@fca001.tokai.jaeri.go.jp

An analysis was carried out for benchmark experiments of the effective delayed neutron fraction β_{eff} in two fast critical facilities: MASURCA of the Comissariat á l'Energy Atomic in France and FCA of the Japan Atomic Energy Research Institute. The β_{eff}'s were calculated by changing the delayed neutron data to test calculated prediction accuracy of the β_{eff}.

1. Introduction

The effective delayed neutron fraction β_{eff} is an important parameter as a reactivity scale of a nuclear reactor. To validate delayed neutron data of ^{235}U, ^{238}U and ^{239}Pu which have large contribution to the β_{eff} of fast critical assemblies and fast power reactors, two programs of β_{eff} benchmark experiments have been performed in two fast critical facilities: MASURCA of the Comissariat á l'Energy Atomic in France and FCA of the Japan Atomic Energy Research Institute[1,2]. These experiments have been carried out in five benchmark cores providing a systematic change in ^{235}U, ^{238}U and ^{239}Pu contribution to the β_{eff}: MASURCA R2 core fueled with enriched uranium; MASURCA ZONA2 core fueled with Mox fuel; three FCA cores which have already been described in reference[3]. Comparisons of the β_{eff}'s between wide variey of the measurement methods were carried out to improve reliability of the measurements in these benchmark experiments.

In the present work, analysis was made for the β_{eff}'s of these cores by changing the delayed neutron data. Brief descriptions are given in Chap.2 for the benchmark cores and the experimental β_{eff}.* The data and method for analysis are described in Chap.3. Results of the analysis are discussed in Chap.4.

2. Brief Descriptions of Benchmark Cores and Experimental β_{eff}

Table 1 summarizes fuel compositions of five benchmark cores and the experimental β_{eff}. The β_{eff}'s of FCA cores were taken from reference[3]. For the MASURCA croes, comparisons of the β_{eff}'s between different methods were discussed in reference[1]. Mean values of these β_{eff}'s were adopted and are shown in this table. The β_{eff} of the FCA XIX-2 core was close to that of the MASURCA Zona2 core because two cores were similar in the fuel composition. Figure 1 shows R-Z models of these cores. Each core was composed of the core-region and the

*Both of MASURCA and FCA cores are described for convenience of the reader though the FCA cores have aleady been described in reference[3].

blanket-region(s) and was simple in geometry as shown in this figure. The core-region had a contribution of more than 90% to the β_{eff} in each core.

3. Data and Method for Analysis

The β_{eff} was calculated by

$$\beta_{eff} = \frac{\sum_{m}\sum_{i=1}^{6}\int_{reactor}(\int\chi_{d:i,m}\phi^{\dagger}dE)(\int\nu_{d:i,m}N_{m}\sigma_{f\,m}\phi dE)\,dv}{\int_{reactor}(\int\chi\phi^{\dagger}dE)(\int\nu\Sigma_{f}\phi dE)\,dv}, \quad (1)$$

where

ϕ : space- and energy-dependent forward flux,
$\phi^{\dagger}$: space- and energy-dependent adjoint flux,
N_m : region-dependent atomic number density of fissionable nuclide m,
$\chi_{d:i,m}$: delayed neutron spectrum of delayed group i of nuclide m,
$\nu_{d:i,m}$: delayed neutron yield of delayed group i of nuclide m,
$\sigma_{f:m}$: region-dependent effective microscopic fission cross section of nuclide m,
χ : region-dependent fission spectrum of fuel,
ν : region- and energy-dependent number of fission neutrons per fission of fuel,
Σ_f : region- and energy-dependent macroscopic fission cross section.

3.1 Delayed Neutron Data

Delayed Neutron Spectrum

The evaluated delayed neutron spectra by Saphier[4], which have been adopted in the JENDL3.2, were used for the calculation. Furthermore, the spectra evaluated in the ENDF/B-VI[5] were used in place of those by Saphier to know the effect of changing the delayed neutron spectra on the β_{eff}. Figure 2 shows comparison of the spectra of third delayed group of ^{235}U, ^{238}U and ^{239}Pu between two evaluations. Marked difference of the spectra is found below 100 keV between two evaluations.

Delayed Neutron Yield

The β_{eff} was calculated using two delayed neutron yield sets: yields evaluated in the JENDL3.2[6] and yields evaluated by Tomlinson[7]. The former is one of the latest evaluated yield sets and the latter has been used so far for the β_{eff} calculation in critical experiments at FCA. The yields of the Tomlinson for fast fission were evaluated at the energy of fission spectrum. On the other hand, the yields of principal nuclides in the JENDL3.2 have energy dependency as shown in Fig.3. The yields at 2 MeV were obtained by an interpolation of the data in Fig.3 to make a comparison of the yields between two evaluations as shown in Table 2. A large difference of up to 9% is found for the ^{238}U yield between two evaluations. The β_{eff} was calculated by switching the delayed neutron yields as follows.

(a) yields at 2MeV of the JENDL3.2,
(b) yields for fast fission of the Tomlinson and
(c) energy dependent yields of the JENDL3.2.

3.2 Calculation of Forward and Adjoint Fluxes

The calculation of ϕ and $\phi^{\dagger}$ was made as follows by means of the group constants set JFS3-J3.2 with seventy energy group structure[8] which was generated from the JENDL3.2.

MASURCA Cores

The MASURCA fuel cells were composed of rodlet fuels, so that their heterogeneity effect on the β_{eff} was announced to be small. For this reason, the calculation was made using homogeneous atomic number densities. The ϕ and $\phi^{\dagger}$ were calculated by a SN transport theory code TWOTRAN-II[9] using the two-dimensional R-Z model.

FCA Cores

Cell averaged effective cross sections(seventy energy group) were prepared in each region in the reactor by a cell calculation in a one-dimensional infinite slab model. The SLAROM code[10] which is based on a collision probability method was used. The ϕ and $\phi^{\dagger}$ were calculated by a diffusion theory code CITATION-FBR[11] using anisotropic diffusion constants[12] in a three-dimensional X-Y-Z model. A correction for transport effect was made on the β_{eff}. This correction was estimated by comparing the results of β_{eff} between the transport code and the diffusion code with isotropic diffusion constants. These calculations were made in the two-dimensional R-Z model. The transport correction was found to be about 1%.

4. Results and Discussions

Table 3 shows comparisons of the calculated β_{eff}'s between two sets of the delayed neutron spectra: Saphier and ENDF/B-IV. The delayed neutron yields of JENDL3.2 at 2MeV were used in these calculations. The difference of calculated β_{eff} was at most 0.6% between two sets of the spectra.

Table 4 shows the ratios of calculation to experiment(C/E's) of the β_{eff}. The delayed neutron spectra of Saphier were used in these calculations. Overprediction of the β_{eff} by 3~4% was found in the case (a) in four cores of R2, ZONA2, XIX-1 and XIX-2. The C/E's decreased by 3~5% in three cores of R2, ZONA2 and XIX-2 by switching the delayed neutron yields from (a)JENDL3.2(2MeV) to (b)Tomlinson because the ^{238}U yield of Tomlinson is smaller than that of JENDL3.2(2MeV) by 9%(Table 2). On the other hand, the overprediction by 3% remained in the case (b) in the XIX-1 core where the contribution of the ^{235}U to the β_{eff} is 94%.

The agreement of the β_{eff} between calculation and experiment became good in the XIX-1 core when (c) the energy dependent yields of JENDL3.2 were used. Figure 4 shows energy breakdown of the sensitivity coefficient of the β_{eff} to the ^{235}U yield in this core and the energy dependency of the ^{235}U yield. The energy range below 100keV has large sensitivity to the β_{eff} and the yield in this energy range is smaller than that at 2MeV by 4%. Consequently, the C/E decreased by 4% in this core by switching the yields from (a) to (c).

The C/E's in the case (c) were smaller than those in the case (a) by 3~4% in all the cores. The agreement of the β_{eff} between calculation and experiment within 1% was obtained in the case (c) in four cores of R2, ZONA2, XIX-1 and XIX-2. Underprediction of the β_{eff} by 2.5% however was observed in the XIX-3 core.

Furthermore, MASURCA ZONA2 core and FCA XIX-2 core were close in the C/E of the β_{eff} in all the cases.

5. Summary

The analysis was carried out for the β_{eff} benchmark experiments at MASURCA and FCA by changing the delayed neutron yields and spectra. The difference of calculated β_{eff} up to 5% was observed between the delayed neutron yields. On the other hand, the effect of changing the delayed neutron spectrum was small and at most 0.6% in the present benchmark cores. The good agreement of the β_{eff} within 1% was obtained between calculation and experiment in four cores of R2, ZONA2, XIX-1 and XIX-2 when the energy dependent yields of JENDL3.2 were used. Underprediction of the β_{eff} by 2.5% however was observed in the XIX-3 core. Furthermore, consistent C/E's were observed between MASURCA ZONA2 core and FCA XIX-2 core which were similar in the fuel composition.

References

[1] Bertrand P., *et al.*: "BERNICE -Interlaboratory Comparison of β_{eff} Measurement Techniques at MASURCA", Proc. Int. Conf. on the Physics of Reactors, Sept. 16-20, 1998, MITO, JAPAN, E-190.

[2] Sakurai T., *et al.*: "Benchmark Experiments of Effective Delayed Neutron Fraction β_{eff} at FCA-JAERI", Proc. Int. Conf. on the Physics of Nuclear Science and Technology, Oct. 5-8, 1998, Long Island, USA, p.182 (1998, American Nuclear Society, Inc.).

[3] Sakurai T. and Okajima S.: "Benchmark Experiments of Effective Delayed Neutron Fraction β_{eff} at FCA", in this specialist's meeting.

[4] Saphier D., *et al.*: "Evaluated Delayed Neutron Spectra and Their Importance in Reactor Calculations", Nucl. Sci. Eng. 62, 660 (1977).

[5] Rose P. F. and Dunford C. L.: "Data Formats and Procedures for the Evaluated Nuclear Data File ENDF-6", BNL-NCS- 44945 (1990).

[6] Nakagawa T., *et al.*: "Japanese Evaluated Nuclear Data Library Version 3 Revision-2 JENDL-3.2.", Journal of Nucl. Sci. Technol, 32, 1259, (1995).

[7] Tomlinson L.: "Delayed Neutrons from Fission, A Compilation and Evaluation of Experimental Data", AERE-R- 6993 (1972).

[8] Takano H., *et al.*: "Benchmark Tests of JENDL-3.2 for Thermal and Fast Reactors", Proc. Int. Conf. Nuclear Data for Science and Technology, Gatlinburg, USA, 809 (1994).

[9] Lathrop K. D. and Brinkley F. W.: "TWOTRAN-II: An Interfaced Exportable Version of the TWOTRAN Code for Two-Dimensional Transport", LA- 4848-MS (1973).

[10] Nakagawa M. and Tsuchihashi K.: "SLAROM : A Code for Cell Homogenization of Fast Reactor", JAERI 1294 (1984).

[11] Iijima S.: Private communication, Japan Atomic Energy Research Institute.

[12] Benoist P.: "Streaming Effects and Collision Probabilities in Lattices", Nucl. Sci. Eng., 34, 285 (1968).

Table 1 Main characteristics of β_{eff} benchmark cores

Facility and Core	MASURCA R2	MASURCA Zona2	FCA XIX-1	FCA XIX-2	FCA XIX-3
Fuel	Enriched Uranium	Mox	Enriched uranium	Plutonium, Natural uranium	Plutonium
Fuel enrichment	30%	25%	93%	23%	(92% fissile Pu)
Moderator	Sodium	Sodium	Graphite	Sodium	Stainless steel
Core dimensions(cm) Radius(R_C) x Height(H_C)	48 x 60	50 x 60	33 x 51	36 x 61	35 x 61
Experimental β_{eff}(pcm)	720 ±2.6%	346 ±2.7%	742 ±3.0%	364 ±2.8%	250 ±1.6%
Contribution of principal nuclides to β_{eff}*					
^{235}U	76%	2%	94%	11%	9%
^{238}U	24%	49%	6%	47%	11%
^{239}Pu	—	41%	—	41%	76%

*Calculation

Table 2 Comparison of delayed neutron yields of principal nuclides between evaluations

Nuclide	^{235}U	^{239}Pu	^{238}U
JENDL3.2(2MeV)	1.67*	0.647	4.8
Tomlinson(fast fission)	1.65	0.639	4.4

* Delayed neutrons per 100 fissions

Table 3 Comparison of β_{eff}* between evaluated delayed neutron spectra of Saphier and ENDF/B-VI

Core	MASURCA R2	MASURCA Zona2	FCA XIX-1	FCA XIX-2	FCA XIX-3
Saphier	752pcm	357pcm	775pcm	376pcm	251pcm
ENDF/B-VI	756pcm	359pcm	774pcm	377pcm	253pcm
Relative difference	0.56%	0.59%	-0.13%	0.42%	0.59%

* Delayed neutron yields of JENDL3.2 were used.

Table 4 Comparison of C/E of β_{eff} between delayed neutron yields

Facility and core	MASURCA R2	MASURCA ZONA2	FCA XIX-1	FCA XIX-2	FCA XIX-3
(a) JENDL3.2 (yields at 2MeV)	1.044	1.031	1.044	1.033	1.004
(b) Tomlinson (yields for fast fission)	1.013	0.980	1.027	0.984	0.984
(c) JENDL3.2 (energy dependent yields)	1.010	1.004	1.006	1.005	0.975

* Delayed neutron spectra of Saphier were used.

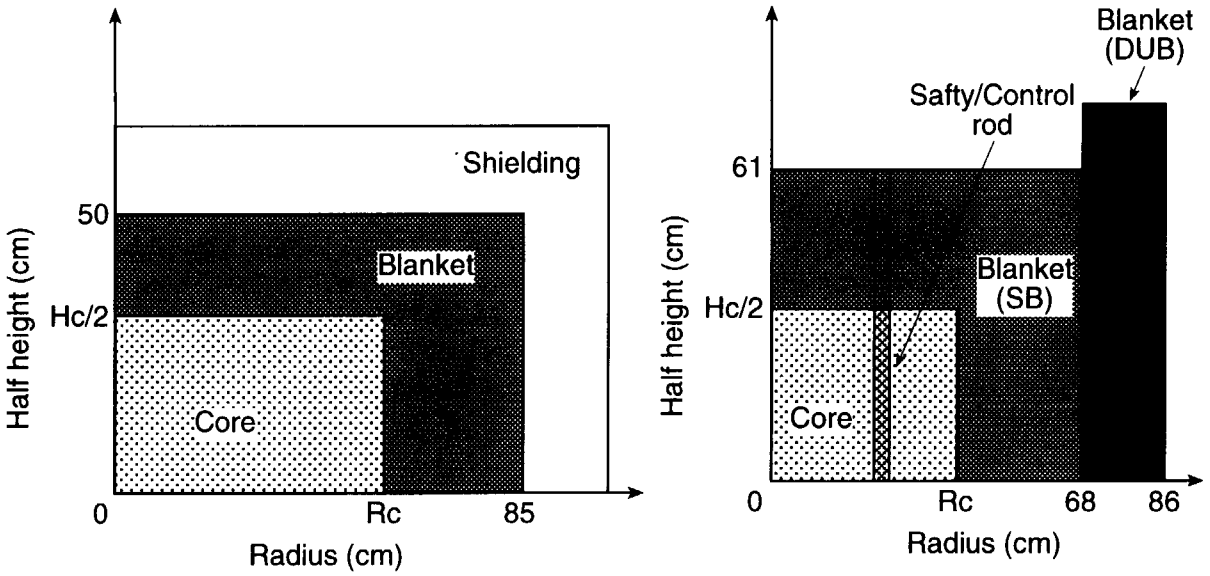

(a) MASURCA cores

(b) FCA cores

Fig.1 Cylindrical model of β_{eff} benchmark experiment cores. Core dimensions (R_c and H_c) are given in Table 1.

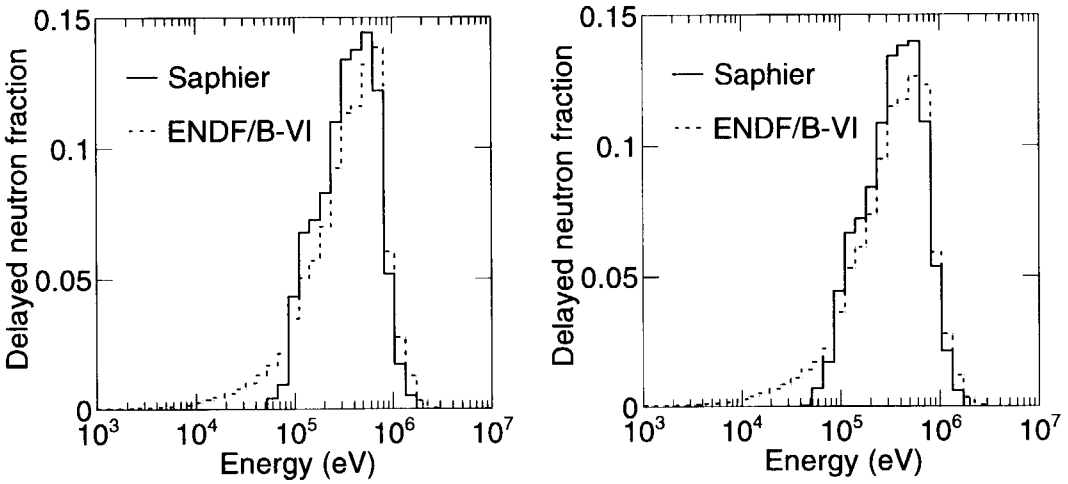

(a) ^{235}U fission.　　(b) ^{238}U fission.

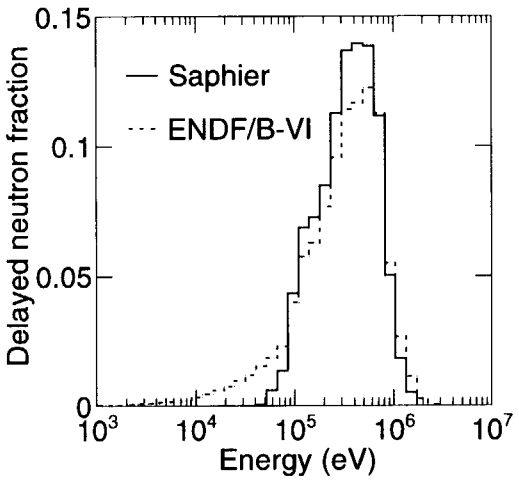

(c) ^{239}Pu fission.

Fig.2 Comparisons of delayed neutron spectra of third delayed group between Saphier and ENDF/B-VI

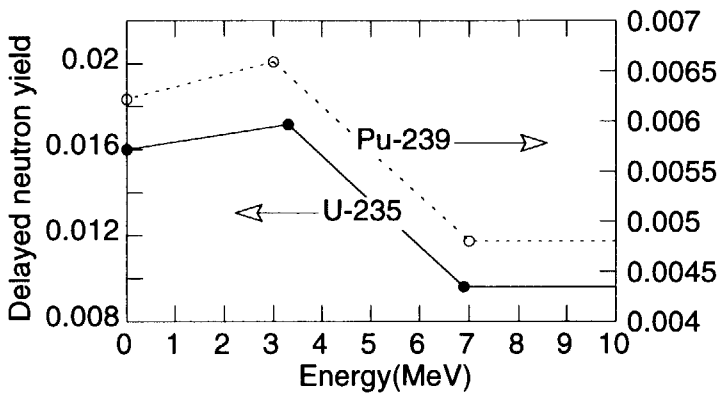

(a) ^{235}U and ^{239}Pu

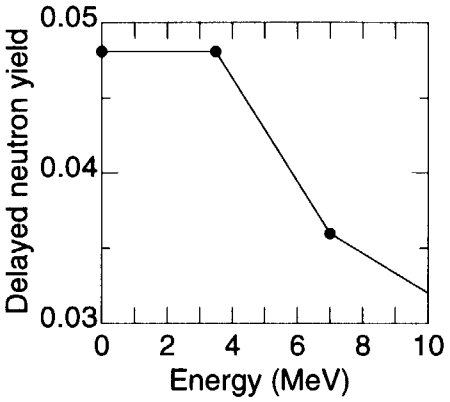

(b) ^{238}U

Fig.3 Energy dependency of delayed neutron yields of principal nuclides in JENDL3.2. The yield values are given at three energy points(thermal, ~3MeV and ~7 MeV) for each nuclide below 10MeV. Between these energy points, the yields are given by linear interpolation in both energy and yield.

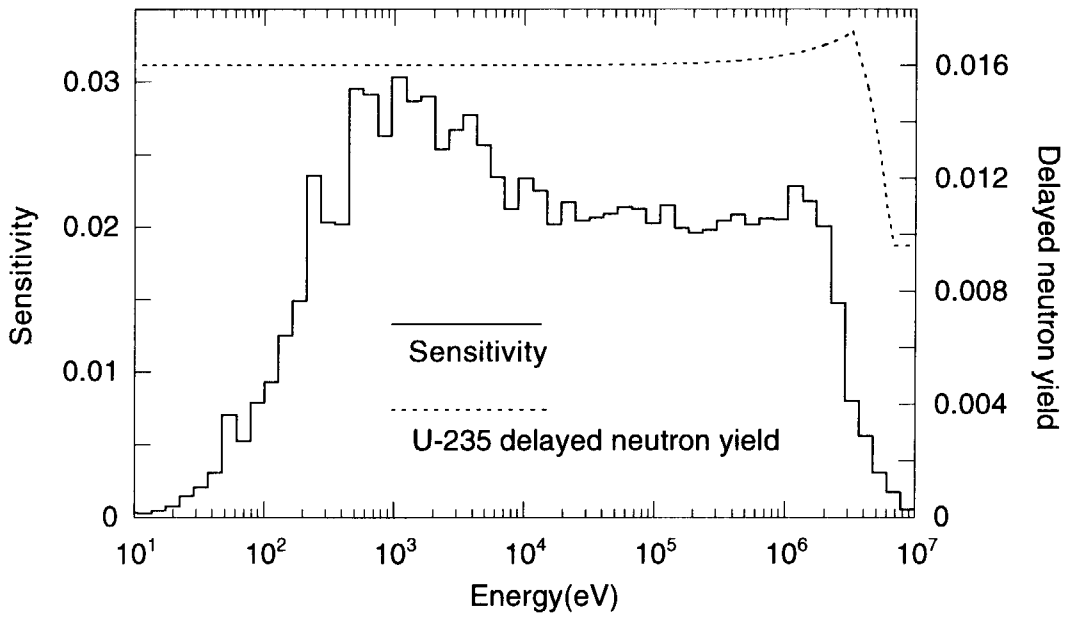

Fig.4 Energy breakdown of sensitivity coefficient of β_{eff} to ^{235}U delayed neutron yield in XIX-1 core and energy dependency of ^{235}U delayed neutron yield.

JAERI－Conf 99－007

11. Importance of Delayed Neutron Data in Transmutation System

Kazufumi TSUJIMOTO
Neutron Science Center, Japan Atomic Energy Research Institute
Tokai-mura, Naka-gun, Ibaraki-ken, Japan 319-1195
E-mail:ktsuji@omega.tokai.jaeri.go.jp

The accelerator-driven transmutation system has been studied at the Japan Atomic Energy Research Institute. This system is a hybrid system which consists of a high intensity accelerator, a spallation target and a subcritical core region. The subcritical core is driven by neutrons generated by spallation reaction in the target region. There is no control rod in this system, so the power is controlled only by proton beam current. The beam current to keep constant power change with effective multiplication factor of subcritical core. So, the evaluation of delayed neutron fraction which is strongly connected to the measurement of subcritical level is important factor in operation of accelerator-driven system. In this paper, important nuclides for the delayed neutron fraction of ADS will be discussed, moreover, present state of delayed neutron data in evaluated nuclear data library is presented.

1. Introduction

The Japanese long-term program called OMEGA has started in 1988 for research and development of new technologies for partitioning and transmutation of minor actinides and fission products. The main aims of this program are exploring the possibility to utilize high-level waste as useful resources and widening options of future waste management. Further improvements of long-term safety assurance in the waste management can be expected through establishing the partitioning and transmutation technology. Nuclides in high-level waste to be transmuted are minor actinides (MA) and long-lived fission products (LLFP). MA should be transmuted mainly through fission reactions because the transmutation of MA by neutron capture reactions has the possibility of increasing higher actinides, while the thermal capture is main transmutation reaction for LLFP. The main nuclides of MA from power reactor, such as Np, Am and Cm, have threshold fission reaction. So, hard neutron spectrum is desirable for the transmutation of MA.

Under the OMEGA Program, the Japan Atomic Energy Research Institute (JAERI) is proceeding with the research and development on proton accelerator-driven system (ADS).[1] The ADS is a hybrid system which consists of a high intensity proton accelerator, a spallation target and a subcritical fuel region. The concept of ADS is shown in Fig. 1. MA from power reactors are used for a fuel of the ADS. The spallation target is made by

heavy metal nuclides. Many spallation neutrons are generated by spallation reaction of protons from a high intensity linear accelerator in the spallation target. The subcritical fuel region surrounding the spallation target is driven by the spallation neutrons.

There is no control rod in JAERI proposed ADS, so the power will be controlled only by the accelerator beam current. The proton beam current necessary to constant power of ADS is related to the multiplication factor (k-eff) of the system. The delayed neutron fraction which connects to the monitoring of subcritical level in ADS is one of important factor. In this paper, important nuclides for the the delayed neutron fraction of ADS will be discussed after basic characteristics of ADS are mentioned. Moreover, present state of delayed neutron data in evaluated nuclear data library will be mentioned.

2. Proposed Accelerator-Driven Transmutation System

Design of the current reference ADS follows that of liquid sodium cooled fast reactors.[2] This is the ADS consisting of a tungsten target and a nitride fuel subcritical core cooled by liquid sodium. Nitride is adopted as the fuel material because of a high thermal conductivity and a high melting point. The main reason to chose sodium as coolant is good thermal properties. In the ADS, heat removal from not only the fuel but also the target becomes important. The thermal properties of liquid sodium are good, so liquid sodium is suitable for this purpose. Moreover, there are established technology and rich experience on the handling of sodium. So, it is possible to decrease research and development for ADS .

On the other hand, a fast reactor design using heavy liquid metal coolant (lead or lead-bismuth) in place of sodium has been proposed in Russia.[3] JAERI showed also a compact integrated reactor system with an safety core concept.[4] There are some advantages in system with heavy liquid metal coolants in comparison with the sodium cooled system, though the thermal property is inferior to that of sodium. The neutron slowing down power of lead or lead-bismuth is smaller than that of sodium, and hence neutron spectrum becomes harder in the heavy liquid metal cooled core. In the ADS, heavy liquid metals are simultaneously able to be used as the coolant and the spallation target. From these reasons, recently, a preliminary design study was started for lead-bismuth cooled option of ADS at JAERI .[5] The major reason to choose lead-bismuth is that the melting point of lead-bismuth is almost the same as that of sodium while that of lead is considerably higher. The corrosion which is one of the most important problems in the heavy liquid metal cooled system is significant at high temperatures. The concepts for both sodium cooled and lead-bismuth cooled ADS are shown in Fig. 2. The major specifications of proposed ADSs are summarized in Table 1. For neutronic calculations, the ATRAS code system[1] and the ABC-SC code system[6] were used with the JENDL-3.2 library for neutronic calculations.

In present design, proposed ADS is operated by 1.5 GeV proton beam. The spallation neutron spectrum from Pb-Bi target with 1.5 GeV incident proton compared with Pu-239 fission spectrum in Fig. 3. Though the energy of incident proton is so high, spallation neutron spectrum is not so hard spectrum. The peak energy is lower than one of fission spectrum. The delayed neutron fraction, ν_d, decrease at higher energies, while the lack of the energy dependence of ν_d below ~4 MeV. The neutron spectrum of ADS is not so different from one of conventional design FBR since the relatively soft spectrum of spallation neutron. The energy break down of fission reaction of Am-241 which is main component of MA from LWR is shown in Fig. 4. Fig. 4 shows the result in ADS and MOX fuel FBR. The peak energy of fission reaction of Am-241 is about 1 Mev in both core. The reaction rate above 10 MeV in ADS is only 0.2 %. Therefore, for the evaluation of the delayed neutron fraction of ADS, it is possible to use the data used by the calculation of conventional fast reactor.

The transmutation of MA and the burnup reactivity swing are especially important to estimate the performance of ADS. The system is designed to transmute MA from 10 units of the existing LWR with reactor power of 1 GWe. The proton beam power needed to operate ADS is related to the multiplication factor (k-eff) of the system. Therefore, the minimization of the burnup swing is an important factor in operation of ADS. As a result of the parametric survey, it was found that the burnup swing depends on the initial Pu content. The burnup reactivity swing is minimized in the core with the initial Pu loading of 40%.[5] The changes of the multiplication factor and the proton beam power for the optimized lead-bismuth cooled ADS are shown in Fig. 5. The figure indicates that the change of proton beam power is about 30%, though the burnup swing in 10 years operation is only 1.8%. The maximum beam power is needed at the maximum system subcritical level and corresponds to about 60 MW.

3. Delayed neutron fraction for ADS

The present state of delayed neutron data in evaluated nuclear data file is mentioned before discussion of delayed neutron fraction of ADS. Table 2 shows the present state of delayed neutron data for major Pu and MA nuclides in JENDL-3.2, ENDF-B/VI and JEF-2.2 libraries. ENDF-B/VI contains data for all nuclides except for Cm-244. On the other hand, JENDL-3.2 and JEF-2.2 include only major Pu isotope. Though JENDL-3.2 has part of delayed neutron data for all nuclides, complete set is necessary for evaluation of delayed neutron fraction.

As a matter of fact, contribution of these nuclides for delayed neutron fraction in ADS is discussed. The effective delayed neutron fraction and contribution of main nuclides evaluated using ENDF-B/VI library are shown in Table 3. In Table 3, effective delayed neutron fraction at BOC of first and fifth cycle for cores using MA from UO2 and MOX

fueled LWR. This is because the isotope composition of MA is different between UO2 and MOX fueled LWR, and relative ratio of higher actinide increase with burnup. In case of MA from UO2, the contribution of Np-237 is so high, and that of Pu-238 quite increase with burnup. Np-237 is main composition in MA from UO2, so production of Pu-238 by capture reaction of Np-237 is significant. The contributions of each nuclide to total fission are shown in Table 4. The increase of fission rate of Pu-238 is remarkable from Table 4. On the other hand, in case of MA from MOX, the contribution of Am-241 and Am-242m is so high. This is because AM-241 is main composition in MA from MOX, and Am-242m produced from Am-241 has relatively high fission cross section. While the contribution of Cm-244 can not be evaluated because of the lack of primary data, it can be estimated same level as Cm-245 from Table 4. From these results, important nuclides for the evaluation of delayed neutron fraction in ADS are Np-237, Pu-238, Am-241, Am-242m, Am-243, Cm-244 and Cm-245. The complete set of these nuclides are desirable in future nuclear library from view point of MA transmutation system.

4. Concluding remarks

The conceptual design study of ADS are in progress at JAERI under the OMEGA program. Basic characteristics of JAERI proposed ADS are shown in this paper. In operation of ADS, it is important to survey subcriticality of system because there is no control rod in ADS. So, the delayed neutron data is important about MA which is used as fuel in ADS. The present state of delayed neutron data about MA in evaluated nuclear data library is not sufficient. For the future version of nuclear library, important nuclides to evaluate the delayed neutron fraction in ADS are proposed.

References

[1] Takizuka, T., et al. : "Accelerator-Driven Transmutation System Demonstration Experiment at JAERI", Proc. Global '97, vol.1 p.422 (1997).

[2] T. Sasa, T., et al. : "Conceptual Design Study and Code Development for Accelerator-Driven Transmutation System", Proc. Global '97, vol.1 p.435 (1997).

[3] E. P. Velikhov et.al , "The High Safety and Economy NPP with Liquid Lead Cooled Reactor", Nuclear Power and Industry Ministry, USSR, Moscow (1990).

[4] Takano, H., et al. : "A Design Study for Inherent Safety Core, Aseismicity and Heat Transport System in Lead-Cooled Nitride-Fuel Fast Reactor", Proc. ARAA'94, vol.1 p.549 (1994).

[5] Tsujimoto, K., et al. : "Conceptual Study of the Lead-bismuth Cooled Accelerator-driven Transmutation System", Proc. AccApp'98 (1998).

[6] Gunji, Y., et al. : "A Computer Code System for Actinide Transmutation Calculation in Fast Reactors - ABC-SC -", JAERI-M 92-032 (1992) (in Japanese).

Table 1 Specific parameters for both sodium cooled and lead-bismuth cooled ADS

Item	sodium cooled ADS	lead-bismuth cooled ADS
Thermal output	800 MWt	
Accelerator type	proton linac	
Beam energy	1.5 GeV	
Target	Solid Tungsten	Liquid lead-bismuth
Initial k-eff	0.95	
Core height	850 mm	1000 mm
Diameter	1440 mm	2440 mm
Fuel	TRU-nitride (^{15}N enriched)	
(Pu/MA)	40%Pu+60%MA	
inert matrix	ZrN	
Initial MA loading	2000 kg	2500 kg
Burnup swing	4.0 %dk/k	1.8 %dk/k
MA transmutation rate	7.4%/year	10 %/year

Table 2 Present state of delayed neutron data for major minor actinides in evaluated nuclear library

	JENDL-3.2	ENDF-B/VI	JEF-2.2
Np-237	△	○	×
Pu-238	△	○	×
Pu-239	○	○	○
Pu-240	○	○	○
Pu-241	○	○	○
Pu-242	△	○	×
Am-241	△	○	×
Am-242m	△	○	×
Am-243	△	○	×
Cm-244	△	×	×
Cm-245	△	○	×

○: all data exit,△: only ν_{di} and λ_i,×: no data

Table 3 The effective delayed neutron fraction of ADS evaluated by ENDF-B/VI library and contribution of main nuclides

	MA from UO2		MA from MOX	
	1 cycle BOC	5 cycle BOC	1 cycle BOC	5 cycle BOC
β_{eff}	1.98×10^{-3}	1.60×10^{-3}	1.72×10^{-3}	1.40×10^{-3}
Np-237	24.3%	23.8%	2.2%	2.5%
Pu-238	0.5%	18.4%	1.0%	14.4%
Pu-239	36.3%	16.0%	37.2%	14.2%
Pu-240	9.6%	9.9%	9.5%	11.7%
Pu-241	20.7%	11.6%	29.6%	13.4%
Pu-242	2.0%	3.9%	4.6%	9.0%
Am-241	3.7%	3.8%	10.3%	9.6%
Am-242m		4.8%		12.3%
Am-243	2.5%	2.8%	5.7%	6.2%
Cm-245		2.6%		5.1%

Table 4 Contribution of main nuclides to total fission in ADS

	MA from UO2		MA from MOX	
	1 cycle BOC	5 cycle BOC	1 cycle BOC	5 cycle BOC
Np-237	16.9%	13.9%	1.4%	1.3%
Pu-238	1.1%	31.3%	1.8%	21.9%
Pu-239	48.2%	18.1%	44.5%	14.5%
Pu-240	8.4%	7.3%	7.4%	7.7%
Pu-241	11.0%	5.2%	14.3%	5.5%
Pu-242	0.8%	1.4%	1.7%	2.8%
Am-241	7.9%	6.9%	19.4%	15.4%
Am-242m		4.4%		10.3%
Am-243	2.6%	2.5%	5.4%	4.9%
Cm-244	2.4%	3.9%	4.1%	7.5%
Cm-245		3.9%		6.7%

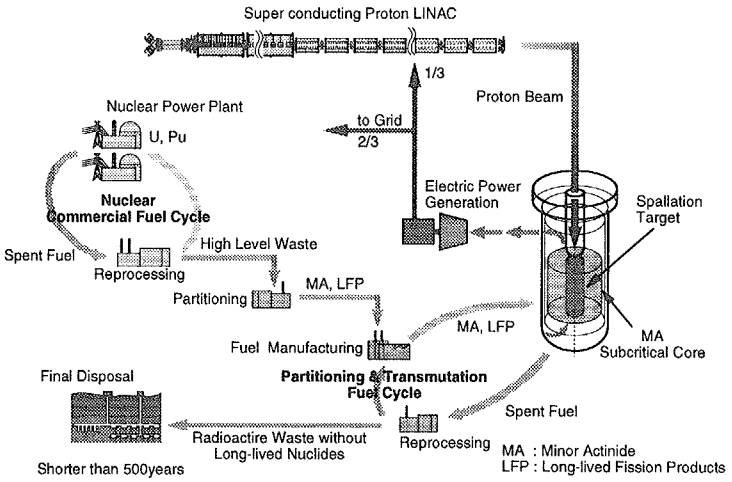

Fig. 1 Concept of the accelerator-driven transmutation system

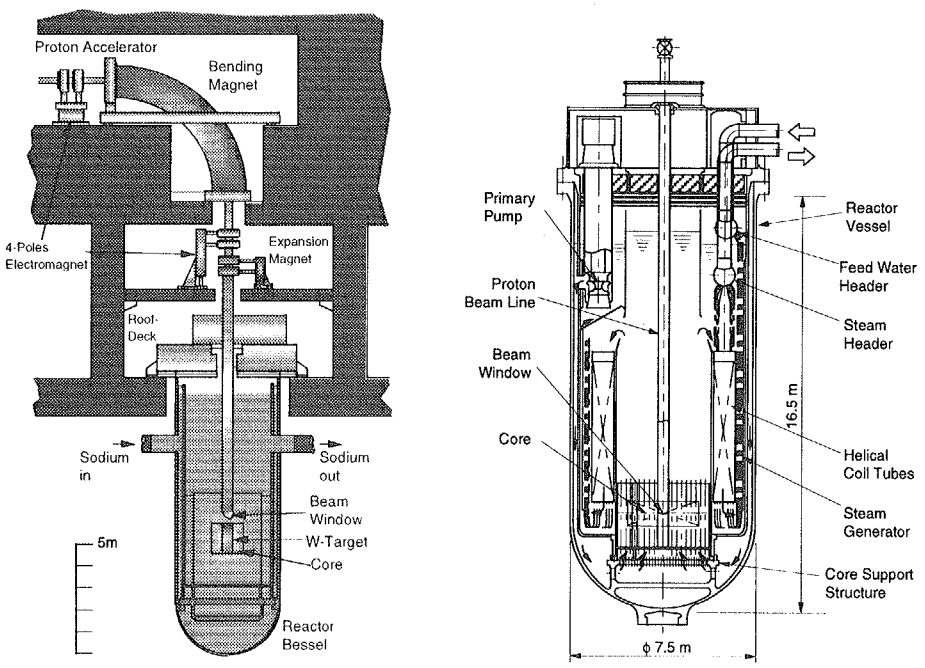

(a) sodium cooled ADS (b) lead-bismuth cooled ADS

Fig. 2 Preliminary design of ADS plant

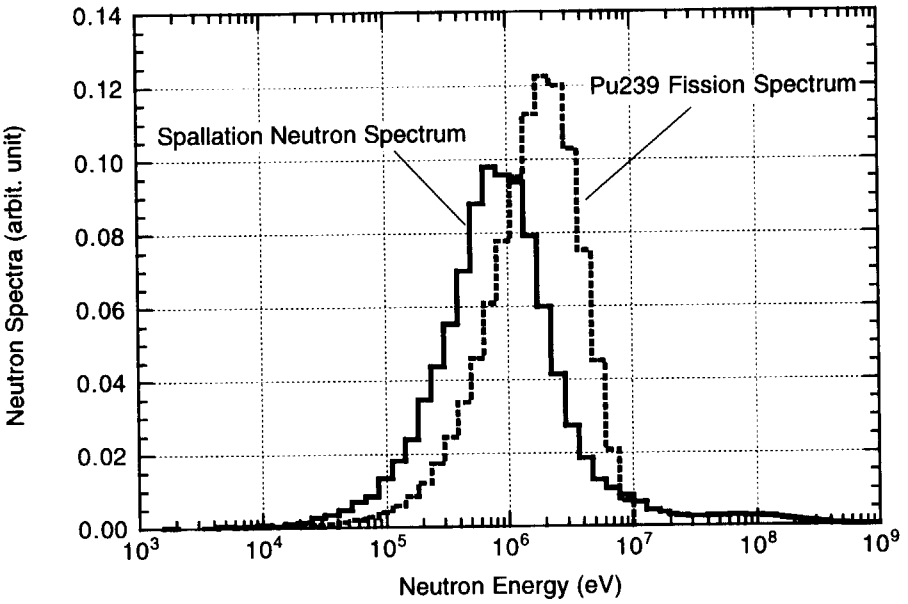

Fig. 3 Comparison between neutron spectra from spallation target (Pb-Bi) with 1.5 GeV proton injection and Pu-239 fission spectra

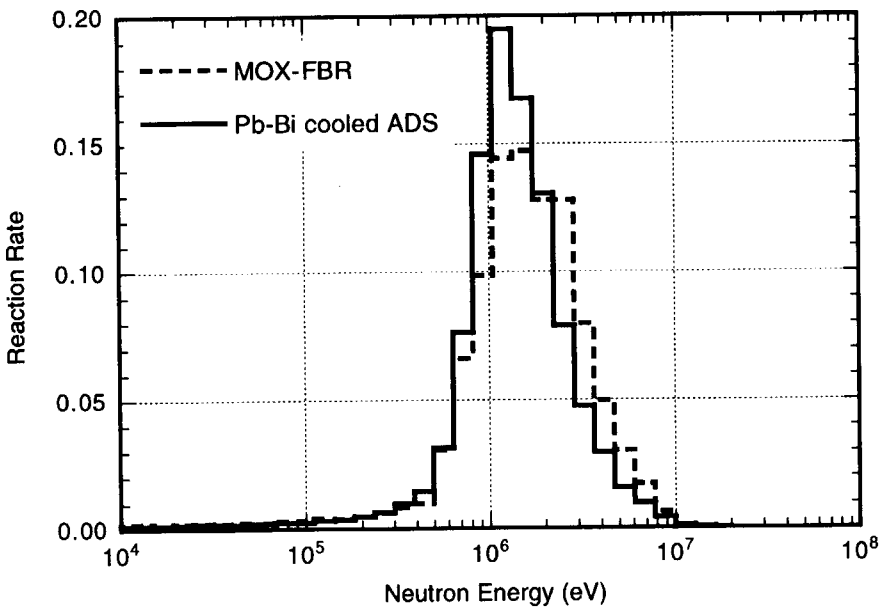

Fig. 4 Energy breakdown of Am-241 fission reaction in ADS and MOX-FBR

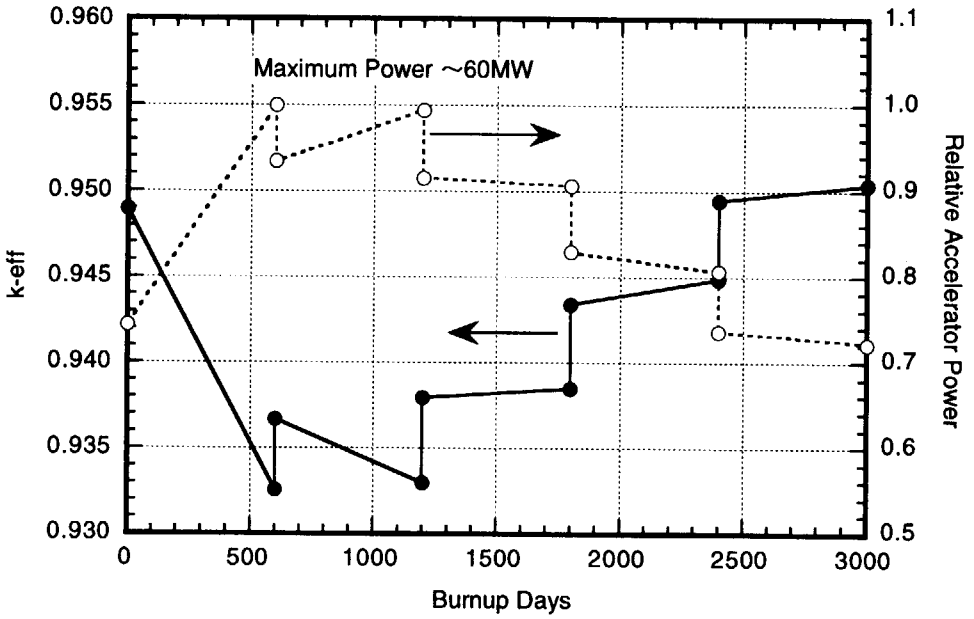

Fig. 5 Changes of k-eff and proton beam power for supposed ADS

12. Study of mass yield and neutron emission for thermal neutron fission

Katsuhisa NISHIO

Advanced Science Research Center, Japan Atomic Energy Research Institute

Tokai-mura, Naka-gun, Ibaraki-ken 319-11

e-mail: nishio@tdmalph1.tokai.jaeri.go.jp

Abstract

Correlation between fission yield and neutron multiplicity was discussed for thermal neutron induced fission of ^{233}U. The slope of neutron multiplicity with total kinetic energy depends on the fragment mass and showed the minimum at about 130 u. The total excitation energy determined from the neutron data was 22 ~ 25 MeV and agreed with that estimated by subtracting the total kinetic energy from the Q-value within 1 MeV, thus satisfied the energy conservation. In the symmetric fission, where the mass yield was drastically suppressed, the total excitation energy was significantly large and reached about 40 MeV. It suggested that the fragment pairs were preferentially formed in a compact configuration at the scission point.

1. Introduction

It is considered that mass yield of fission fragments reflects the shell-effects of nucleus. When the liquid-drop model is adopted to calculate the potential energy with respect to deformation parameters describing the nuclear shape, one obtains the symmetric mass division and cannot explain the asymmetric mass yield curve observed in the low energy fissions such as $^{235}U(n_{th},f)$ and $^{252}Cf(s.f)$. The asymmetric mass division is successfully explained when the shell-effects of the nucleus are included in the potential energy calculation [1]. In this Strutinsky method [2], the nuclear potential energy is calculated by the sum of the liquid-drop energy (E_{LD}) and the shell- and paring- energy correction (δU). Brosa *et al.* [3] have adopted this method in their potential energy calculation and found several fission paths (fission channels). The multi-channel fission model is widely used at present to interpret the experimental data.

As the fission fragments are neutron-rich nuclei, the fragment having mass number of ~ 130 is very close to the double-magic nucleus ^{132}Sn. The pronounced stability of the fragment near 130 u can be understood from the large negative shell-energy correction of δU = ~ – 7 MeV (determined by referring the data in [4]). Wilkins *et al.* made discussions of mass yield curve in their scission point model [5], where the

mass yield is enhanced when the total energy of the system at the scission point is lowered. In this calculation, they explained the asymmetric mass yields by taking into account the shell-energy correction of the deformed fragments (especially, the neutron-shell is important). This model shows the important role of the shell-effects of the fragment on the scission configuration.

The deformation energies of the fragments at the scission point are transformed to the excitation energies when the fragments are fully accelerated. As the excitation energy is dissipated largely by prompt neutrons, the measurement of the neutron multiplicity for the specified fragment allows us to determine the scission configuration. Recently, simultaneous measurement of fission fragments and neutrons was made with improved accuracy for the thermal neutron fissions of ^{235}U and ^{233}U [6]-[8]. In this paper, discussions for the correlation between the mass division and the neutron multiplicity for ^{233}U(n_{th},f) will be given.

2. Fragment mass and total kinetic energy

The fission yield as functions of the fragment mass (m^*) and total kinetic energy (TKE) for ^{233}U(n_{th},f) is shown in Fig.1 (a). In this figure, the larger points indicate the higher yield (note that the very low yield is omitted to avoid confusion). The average value of the total kinetic energy $\overline{TKE}(m^*)$ is shown by the dashed curve. In this figure, the Q-value for the ^{233}U(n_{th},f) system, $Q_{max}(m^*)$, is shown by the solid curve. The $Q_{max}(m^*)$ has the maximum values at $m^* \approx 132$ u, and the localized minimum at the symmetric fission. The liquid-drop model predicts the largest Q-value at the equal mass division in accordance with the highest surface energy of both fragments. In the real nuclei, the maximum appears around 102/132 u because of the largest negative shell-energy correction to the fragment of $m^* \approx 132$ u. Most of the fission events appeared only in the region of $TKE < Q_{max}(m^*)$. The shape of $\overline{TKE}(m^*)$ is similar to that of $Q_{max}(m^*)$ in the point that the maximum value is observed around $m^* = 128 \sim 132$ u and the pronounced minimum at the symmetric fission. One can find an anomalous behaviour of the $\overline{TKE}$ in the symmetric fission when the average total excitation energy of the system, $\overline{TXE}$ ($= Q_{max} - \overline{TKE}$), is calculated. This value in the symmetric fission reaches about 40 MeV and is about 1.7 times as large as that in the typical asymmetric fission.

The $\overline{TKE}$ for specified mass division is considered to be equal to the Coulomb potential energy at the scission point, determined by the charge-center distance (CCD). If the average CCD at the scission point is constant in every mass division, the maximum $\overline{TKE}$ would appear at the symmetric fission, as far as the initial kinetic energy in $\overline{TKE}$ is not predominant. The measured $\overline{TKE}$ indicated the significant change of the CCD against the mass division and that the CCD near the symmetric fission is long compared to that for the fission of around 120/132 u.

3. Correlation between fragment yield and neutron multiplicity

The average total neutron multiplicity $\overline{\nu^{tot}}(m^*)$, which is the sum of neutrons form both fragments, is plotted in Fig.1 (b). The $\overline{\nu^{tot}}$ in $125<m_H^*<150$ u lies between 2.3 and 2.6. However, in the symmetric fission, the neutron multiplicity amounts to 4.0. The data indicates the larger total deformation energy at the scission point for the symmetric fission compared to the typical asymmetric fission. It is correlated with the large CCD for the symmetric fission predicted from the $\overline{TKE}(m^*)$.

The neutron multiplicity is plotted in Fig.1 (c) as a function of the total kinetic energy for the fragment of 85 u (solid triangle), 102 u (solid circle) and 132 u (open circle). For every fragment, the linear relation is observed between the neutron multiplicity and the TKE. The data points for each mass are fitted to a linear function, and the results are displayed in the figure. The fitted line intersects the maximum value of the total kinetic energy $TKE_{\max}$, at which the neutron emission ceases. It is evident from Fig.1 (a) and (c) that (1) the complementary fragments of 132 and 102 u have nearly equal $TKE_{\max}$ and (2) the $TKE_{\max}$ is approximately equal to the $Q_{\max}$. The slope, $-d\nu/dTKE$, is determined by the fitting process and the results are shown in Fig.2. The slope is approximately constant in the light fragment group except the region of $m^*<90$ u, where the slight increase is with mass is observed. In the heavy fragment group of $m^*<145$ u, the slope increases with mass and seems to have the minimum around 130 u. This data reflects the scission configuration as follows: If two deformed fission fragments are nearly touching at the scission point, the total kinetic energy can be calculated from the charge-center distance (CCD) between the two defromed fragment. The deformation energy of the fragment, which is the energy difference against ground state shape, is transformed into excitation energy when the fragment is fully accelerated. Hence, the deformation energy is directly coupled into the neutron multiplicity. For a given mass division, the change of TKE is brought by the shift of the CCD, and the shift caused by elongation or shrinkage of both fragments on their center axis. Paying attention to the nearly symmetric fission region ($m_L^*/m_H^* \approx 104/130$ u), the data in Fig.2 suggest that the large part of the change of the CCD is caused by the light fragment deformation. The $-d\nu/dTKE(m^*)$ seems to reflect the seems to reflects the shell-effects shell-effects of fragments at the instance of nuclear rupture.

Figure 3 shows the total neutron multiplicity as a function of heavy fragment mass, $\nu_{TKE}^{tot}(m^*)$, for a TKE-window of 5 MeV width. The average neutron multiplicity $\overline{\nu^{tot}}(m^*)$ given in Fig.1 (b). is also shown in this figure. The $\overline{\nu^{tot}}$ varies rather slowly with mass in $130<m^*<150$ u, while the ν_{TKE}^{tot} determined for the narrow energy window change quite rapidly and decreases with mass. The results strongly reflects the mass dependence of the Q-value shown in Fig.1 (a). Limiting the total kinetic energy of the system to a narrow window, the total excitation energy (TXE) which is calculated by subtracting TKE from $Q_{\max}$ shows a mass dependence similar to that of $Q_{\max}(m^*)$. Therefore, the ν_{TKE}^{tot} decreases with increasing heavy fragment mass for $m_H^*>130$ u. On the other hand, the average total excitation energy $\overline{TXE}$ is nearly constant with mass for $m_H^*>130$ u, and hence the $\overline{\nu^{tot}}$ is not mass dependent so strongly for $130<m_H^*<150$ u. The experimental mass yield determined for a given TKE-window,

$y_{TKE}(m^*)$, is also shown in Fig.3. The yield is normalized so that the sum of the yield in $m^* > 170$ u is 100%. The comparison between $y_{TKE}(m^*)$ and $\nu_{TKE}^{tot}(m^*)$ suggests that the fission events close to the symmetric region, where the total excitation energy is high, are almost forbidden and consequently the asymmetric mass distribution is mainly formed. The Q-value of the system also sets limitation to the mass formation. The $Q_{\max}$ corresponding to the TKE-window, determined from Fig.1 (a), is marked by an arrow in each section of the figure. As seen in the figures of the *TKE*-windows greater than 180 MeV, the mass yield terminates at the corresponding $Q_{\max}$ position, and the maximum value in $y_{TKE}(m^*)$ increases quite rapidly with TKE.

4. System excitation energy

The average excitation energy of fragment can be estimated from the average neutron multiplicity $\bar{\nu}(m^*)$ and average neutron emission energy $\bar{\eta}(m^*)$ [8] as

$$\overline{E}_{ex} = \bar{\nu}(m^*)\left\{\bar{\eta}(m^*) + \overline{B_n}(m^*)\right\} + \overline{E_\gamma}(m^*) \quad . \tag{1}$$

where $\overline{B_n}(m^*)$ is the effective neutron binding energy, and $\overline{E_\gamma}(m^*)$ the energy dissipated by γ-rays. In the present analysis the 60% value of the $\overline{B_n}(m^*)$ is used for $\overline{E_\gamma}(m^*)$. The effective neutron binding energy is calculated by using the mass table in ref.[4]. Then, the total excitation energy for a mass division becomes

$$\overline{TXE}(m^*) = \overline{E}_{ex}(m^*) + \overline{E}_{ex}(A_c - m^*) \ , \tag{2}$$

where A_c is the mass of the compound nucleus. In Fig.4, the calculated $\overline{TXE}(m^*)$ is shown by solid circles with statistical error bars. It is evident that the total excitation energy in $128 < m_H^* < 152$ u is between 22 and 25 MeV. On the contrary, in the symmetric fission, the system holds remarkably high excitation energy of about 40 MeV.

In Fig.4, the difference, $Q_{\max}(m^*) - \overline{TKE}(m^*)$, is plotted. The errors in these values are shown only in the heavy fragment side. The solid curve with the statistical error bars shows the results determined by using the present $\overline{TKE}(m^*)$ and the dotted curve by using the data in ref.[9]. In this process, a properly broadened $Q_{\max}(m^*)$ is applied in order to wash out the odd-even effects. In the region of typical asymmetric fission, $130 < m_H^* < 150$ u, the $\overline{TXE}$ from the neutron data agrees with that determined by the kinetic energy data within about 1 MeV. In the symmetric fission, although statistical error is large, the $\overline{TXE}$ determined from the two methods agree with each other and shows quite high values. The high value should be due to the substantial total deformation energy of the fragments at the scission points and also causes the marked dip in $\overline{TKE}(m^*)$ as shown in Fig.1 (a).

In Fig.4, the mass yield obtained in the present measurement is indicated and compared with $\overline{TXE}(m^*)$. It is clear that the mass yield is enhanced in the region with low $\overline{TXE}$. In other words, the

symmetric fission having high $\overline{TXE}$ value is forbidden. Figure 4 suggests that, at the exit of the potential surface of the fissioning nucleus, the nascent fragments are preferentially formed so as to have a compact configuration at the scission point. The correlation between $y_{TKE}(m^*)$ and $v_{TKE}^{tot}(m^*)$ shown in Fig.3 also supports this idea.

5. Summary

The average excitation energy of fragment is estimated from the experimental data for $^{233}U(n_{th},f)$. The total excitation energy of the system estimated from the neutron data lies between 22 and 25 MeV and agreed well with that determined by subtracting the total kinetic energy from the Q-value within 1 MeV. In the symmetric fission, where the mass yield is drastically suppressed, the total excitation energy is significantly large and reaches about 40 MeV. It suggests that fragment pairs are preferentially formed in a compact configuration at the scission point.

References

[1] P. Moller and J.R. Nix, in Proceedings of the conference in physics and chemistry, Rochester, Vol.1 IAEA (1974) p.103.

[2] V.M. Strutinsky, Nucl. Phys. A95 (1967) 420; V.M. Strutinsky, Nucl. Phys. A122 (1968) 1.

[3] U. Brosa, S. Grossmann and A. Muller, Phys. Rep. 197 (1990) 167.

[4] P. Moller and J.R. Nix, At. Data and Nucl. Data Tables, 26 (1981) 165.

[5] B.D. Wilkins *et al.*, Phys. Rev. C, 25 (1976) 1832.

[6] K. Nishio *et al.*, Nucl. Instr. Meth., A385 (1997) 171.

[7] K. Nishio *et al.*, Nucl. Phys., A632 (1998) 601.

[8] K. Nishio *et al.*, J. Nucl. Sci. Technol., 35 (1998) 631.

[9] F. Pleasonton, Phys. Rev., 174 (1968) 1500.

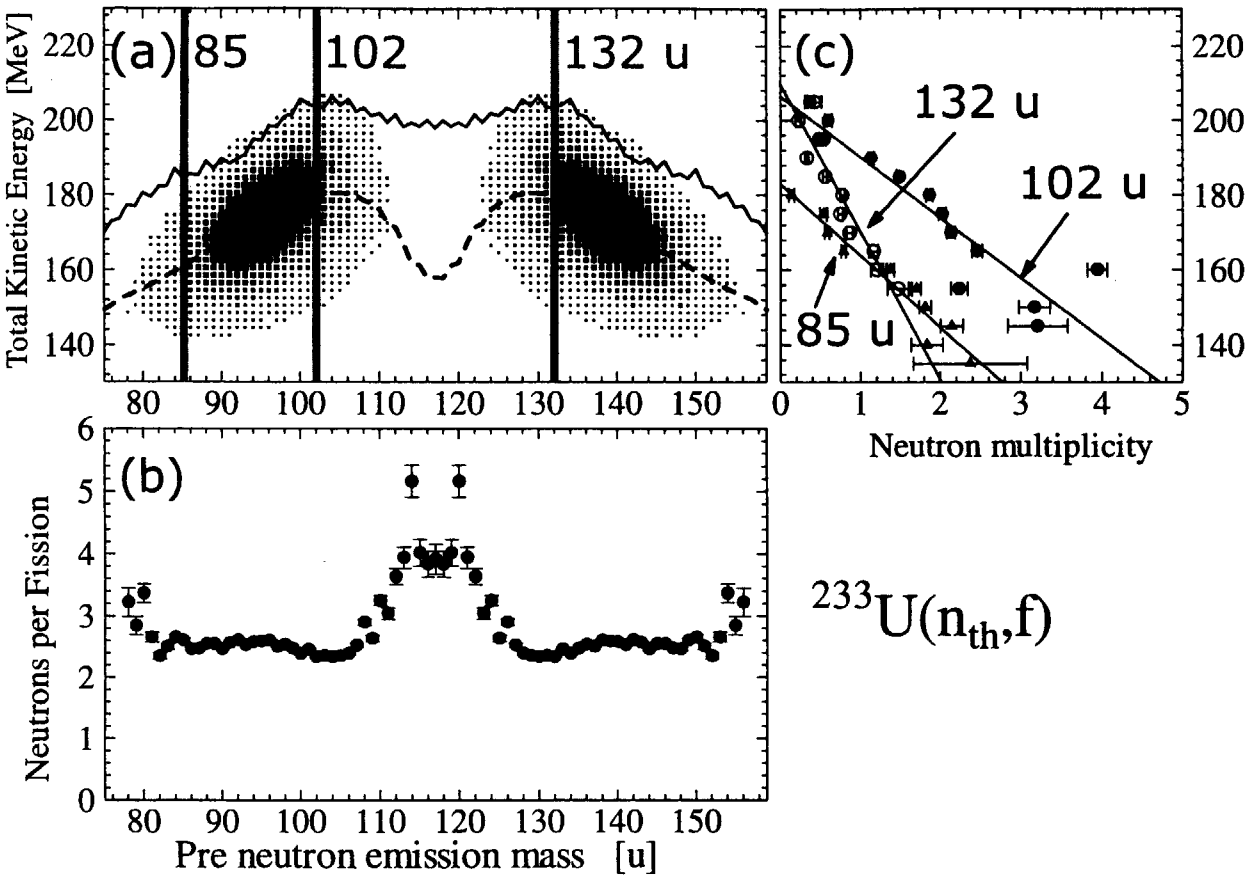

Fig.1 (a) Two dimensional yield of fission events plotted as functions of fragment mass and total kinetic energy for $^{233}U(n_{th},f)$. Points with larger area show higher fission probability. The dashed curve is the average total kinetic energy plotted as a function of fragment mass. Maximum Q-value, $Q_{max}(m^*)$, is also shown by the solid curve. (b) Average total neutron multiplicity, $\nu^{tot}(m^*)$, as a function of fragment mass. (c) Neutron multiplicity for fragments of mass 85, 102 and 132 u plotted as a function of total kinetic energy.

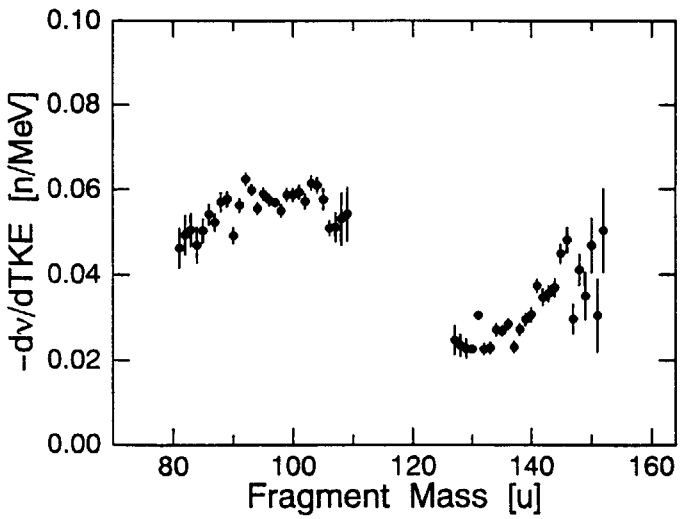

Fig.2 Slope of neutron multiplicity with mass plotted as a function of fragment mass.

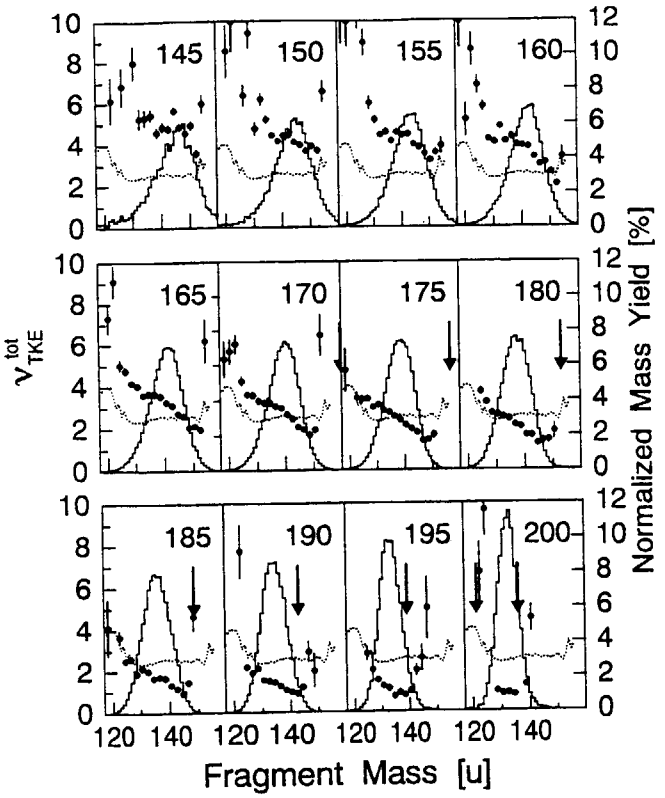

Fig.3 Total neutron multiplicity plotted as a function of heavy fragment mass (solid circles with statistical error bars). The numerical value in each section of the figure represents the center of TKE -window having 5 MeV width. The average total neutron multiplicity in Fig.1 (b) is shown by the dotted curve in every section. For these two plots, see the ordinate on left side. The stepwise distribution is the normalized mass yield formed in each window, $y_{TKE}(m)$. For this, see the ordinate on right side.

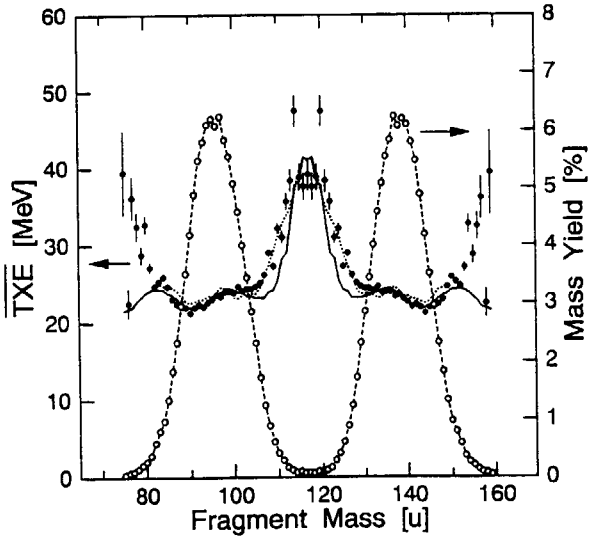

Fig.4 Total excitation energy determined from the neutron data (solid circles with statistical error bars). The solid curve with statistical error bars (thin bars indicated only in the heavy fragment region) is the $Q_{max}(m) - TKE(m)$ calculated by using the present total kinetic energy. The corresponding value determined by using the total kinetic energy in ref.[9] is shown by the dotted curve. Open circles connected with the dashed curve represent the mass yield (see ordinate on right hand side).

13. Systematic Features of Mass Yield Curves in Low-energy Fission of Actinides

Yuichiro NAGAME
Advanced Science Research Center, Japan Atomic Energy Research Institute
Tokai-mura, Ibaraki 319-1195, Japan
e-mail: nagame@popsvr.tokai.jaeri.go.jp

Abstract

Characteristics of mass yield curves in fission of wide range of nuclides from pre-actinides through transactinides are reviewed and the following points are discussed. (1) Systematic trends of the mass yield distributions in low-energy proton-induced fission of actinides and in spontaneous fission of actinides are discussed in terms of weighted mean mass numbers of the light and heavy asymmetric mass yield peaks and widths of the heavy asymmetric mass yields. (2) Gross features of the two kinds of mass yield curves, symmetric and asymmetric ones, as a function of a fissioning nucleus. (3) Competition between the symmetric and asymmetric fission as a function of not only Z (proton number) but also N (neutron number) of a fissioning nucleus. (4) Experimental verification of the existence of two kinds of deformation paths in low energy fission of actinides; the first path is initiated at higher threshold energy and ends with elongated scission configuration, giving a final mass yield distribution centered around the symmetric mass division, "symmetric fission path". In the second path, a fissioning nucleus experiences lower threshold energy and results in more compact scission configuration, which gives a double humped mass distribution always centered around A=140 for the heavier fragment, "asymmetric fission path". (5) Interpretation of the "bimodal fission" observed in the spontaneous fission of heavy actinides as the presence of the two fission paths of the ordinary asymmetric one and a strongly shell-affected symmetric path from the systematic analysis of scission configurations. (6) A dynamical fission process deduced from the analysis of the experimental mass yield curves and the correlation data of neutron multiplicity and fragment mass and total kinetic energy. (7) Prediction of the characteristics of gross properties of fission in superheavy nuclei around $^{280}114$. (8) Characteristics of highly asymmetric fission: formation cross section as a function of excitation energy and angular distribution. (9) Based on the systematic analysis of the heavy asymmetric mass yield curves in thermal neutron- and proton-induced fission of actinides, and spontaneous fission of medium and heavy actinides, the relation between the fragment shell structure and the shape of the mass yield curves which reflect the final mass division process is discussed.

D.C. Hoffman & M.M. Hoffman, Ann. Rev. Nucl. Sci. 24, 151(1974)

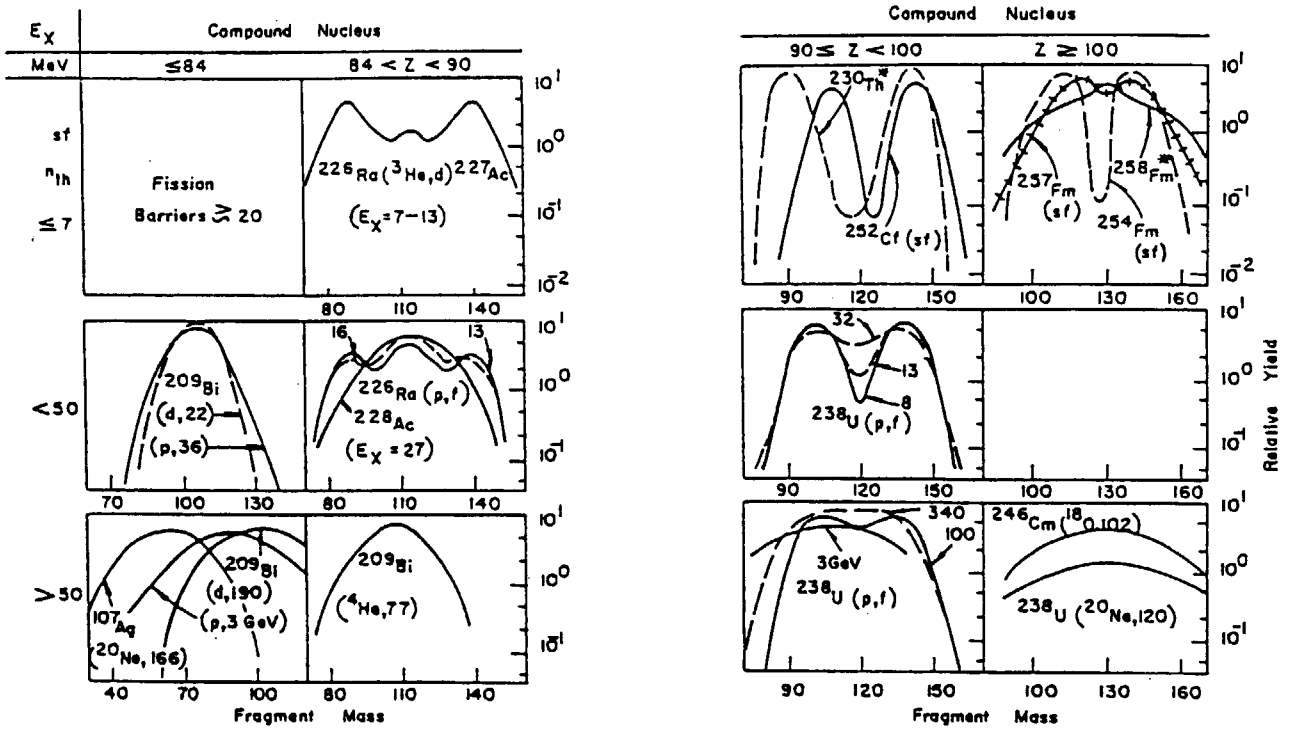

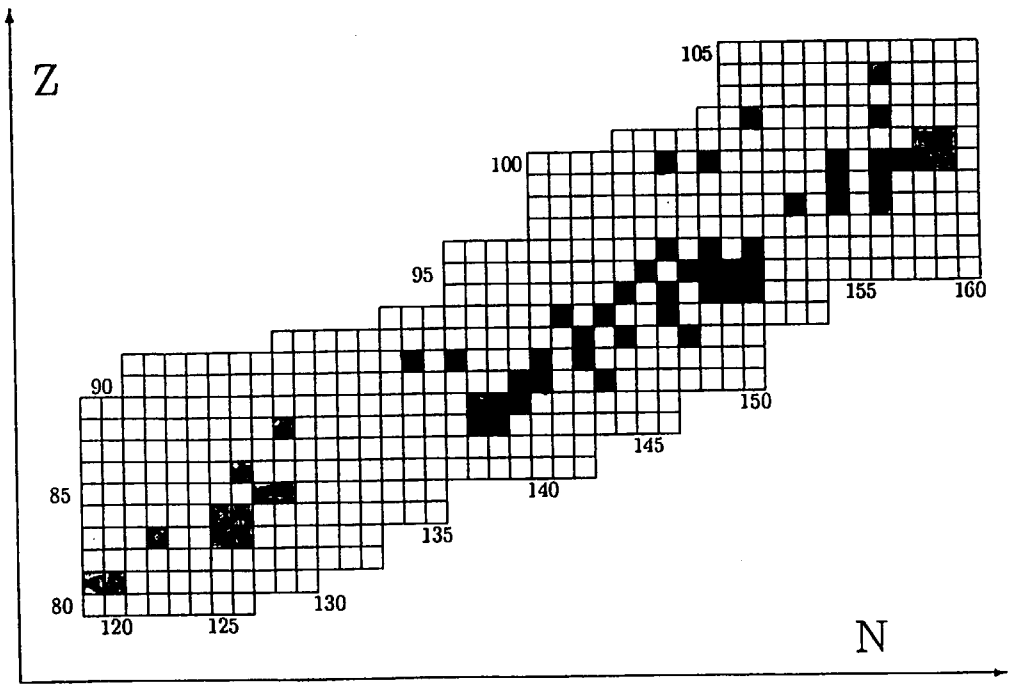

●: symmetric
●: symmetric & asymmetric
●: asymmetric

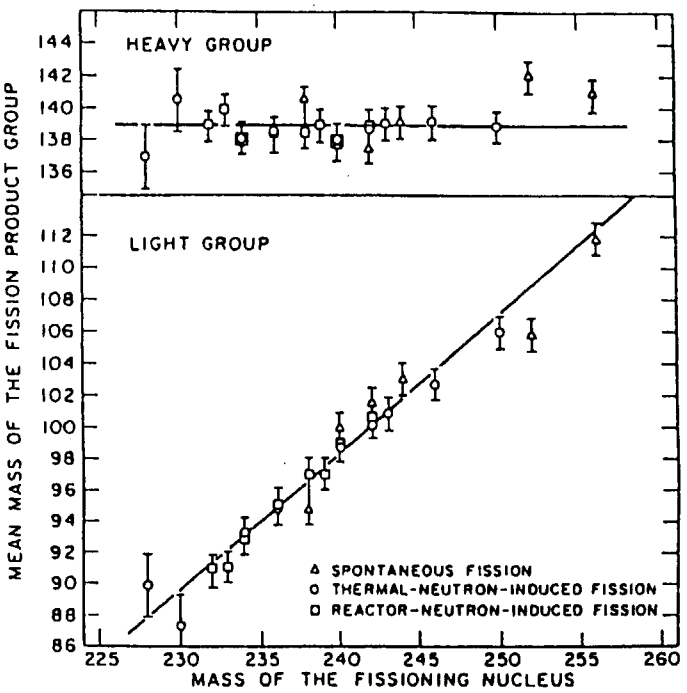

Figure 4 Average masses of light and heavy groups as a function of the mass of the fissioning nucleus (26).

K.F. Flyn et al. P.R.C 5. 1725(1972).

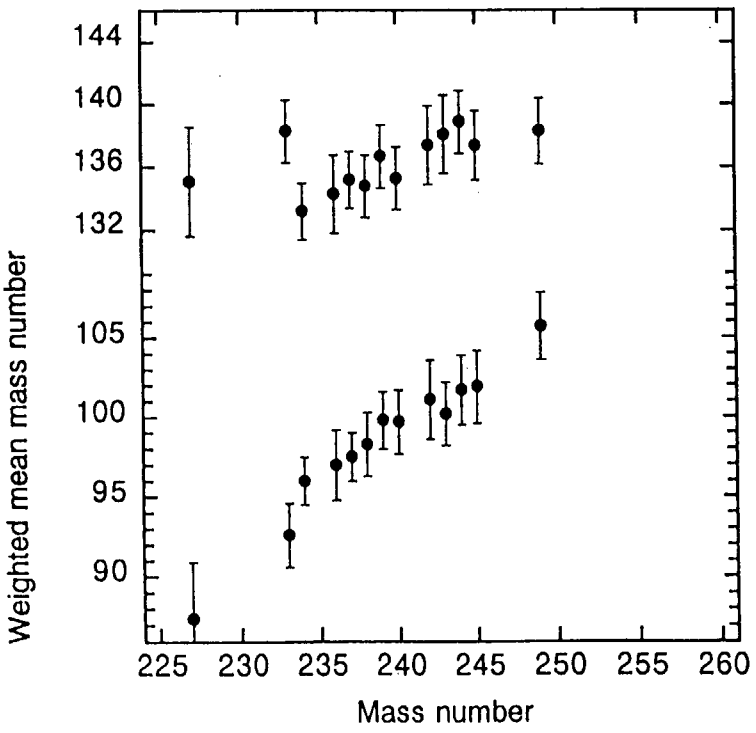

Z. Qin et al. Radiochim. Acta(in press).

$p + {}^{248}Cm$

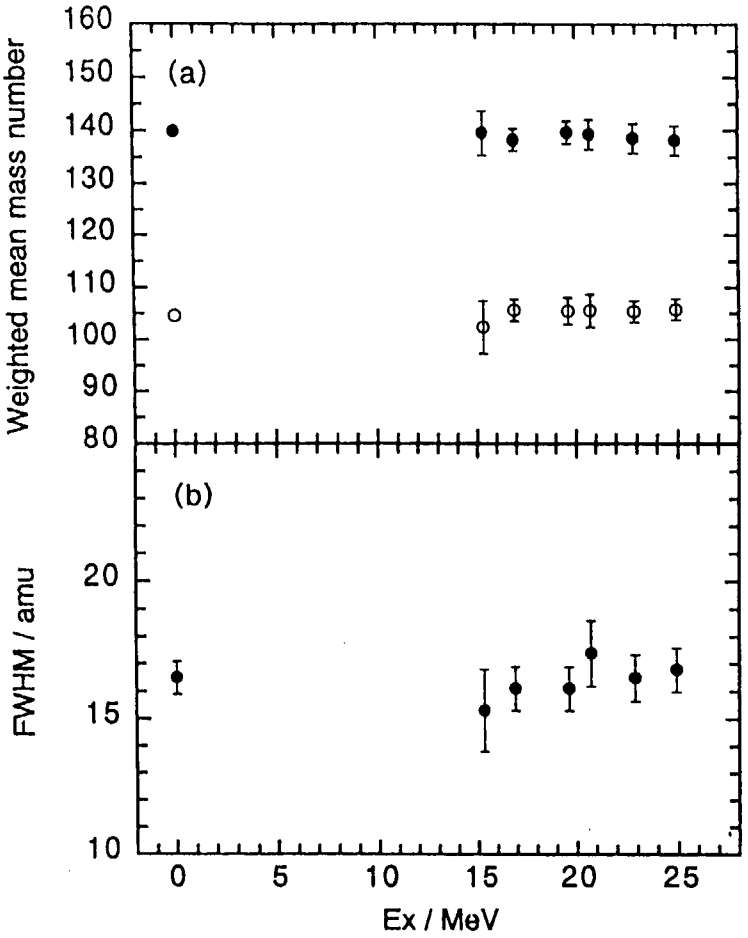

$^{248}Cm(SF)$

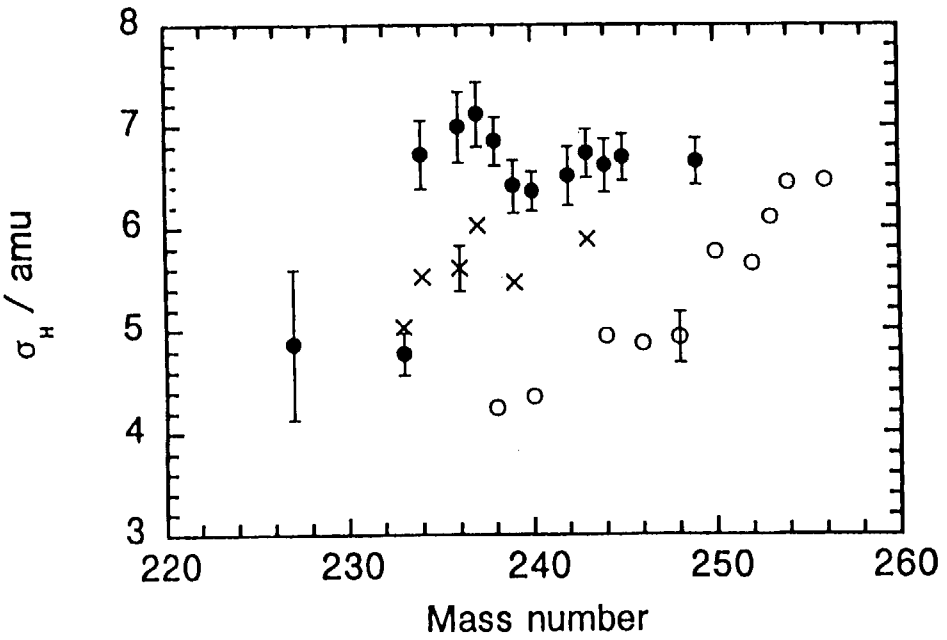

M.R. Lane, P.R.C 53, 2893(1996)

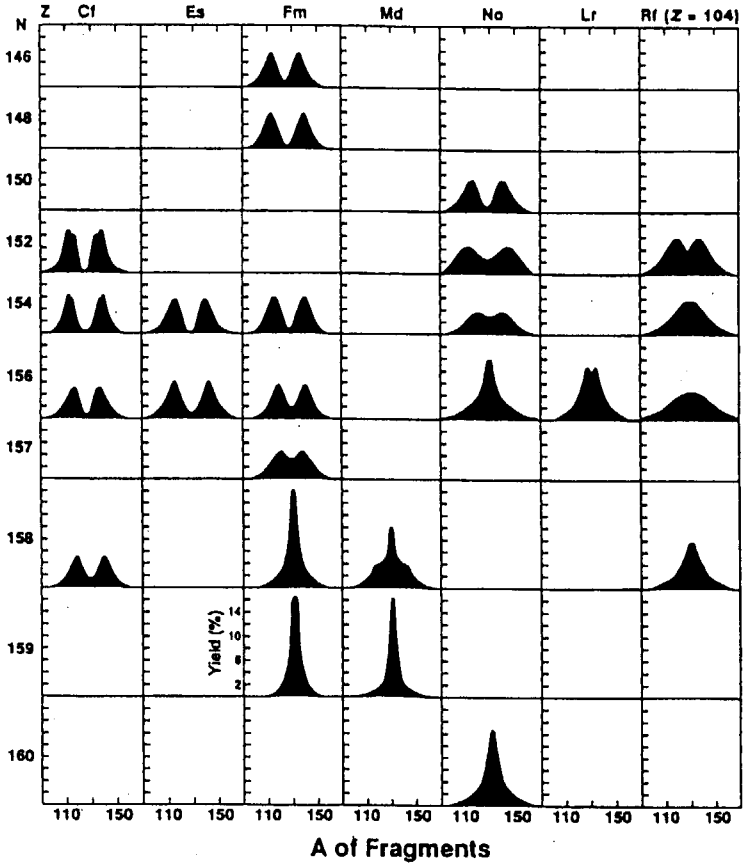

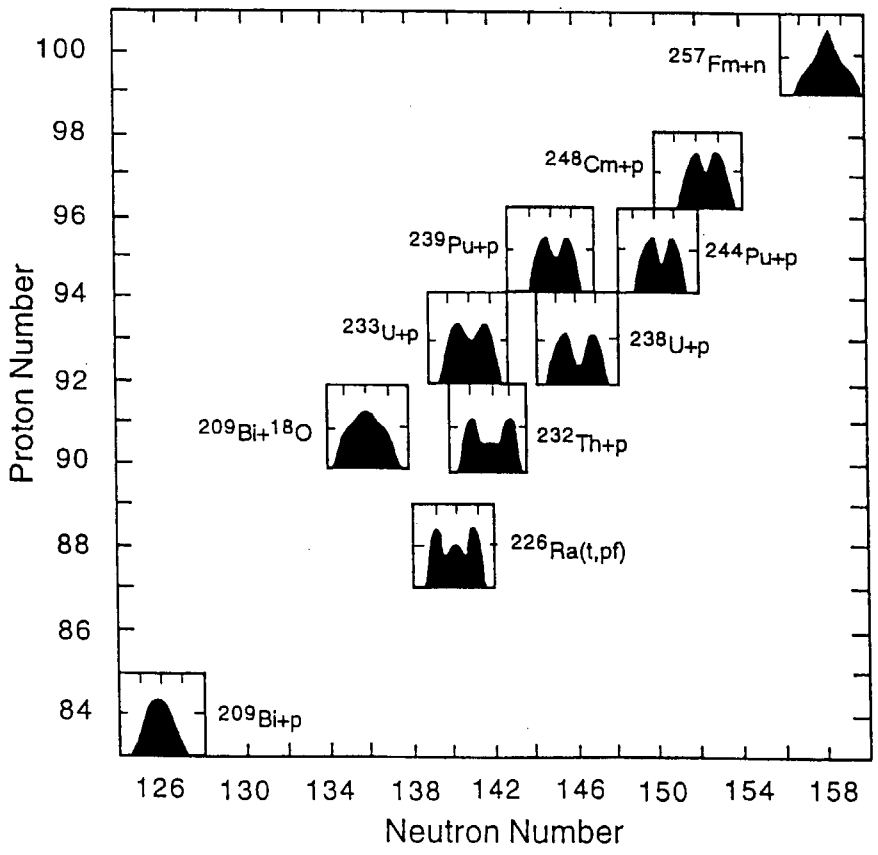

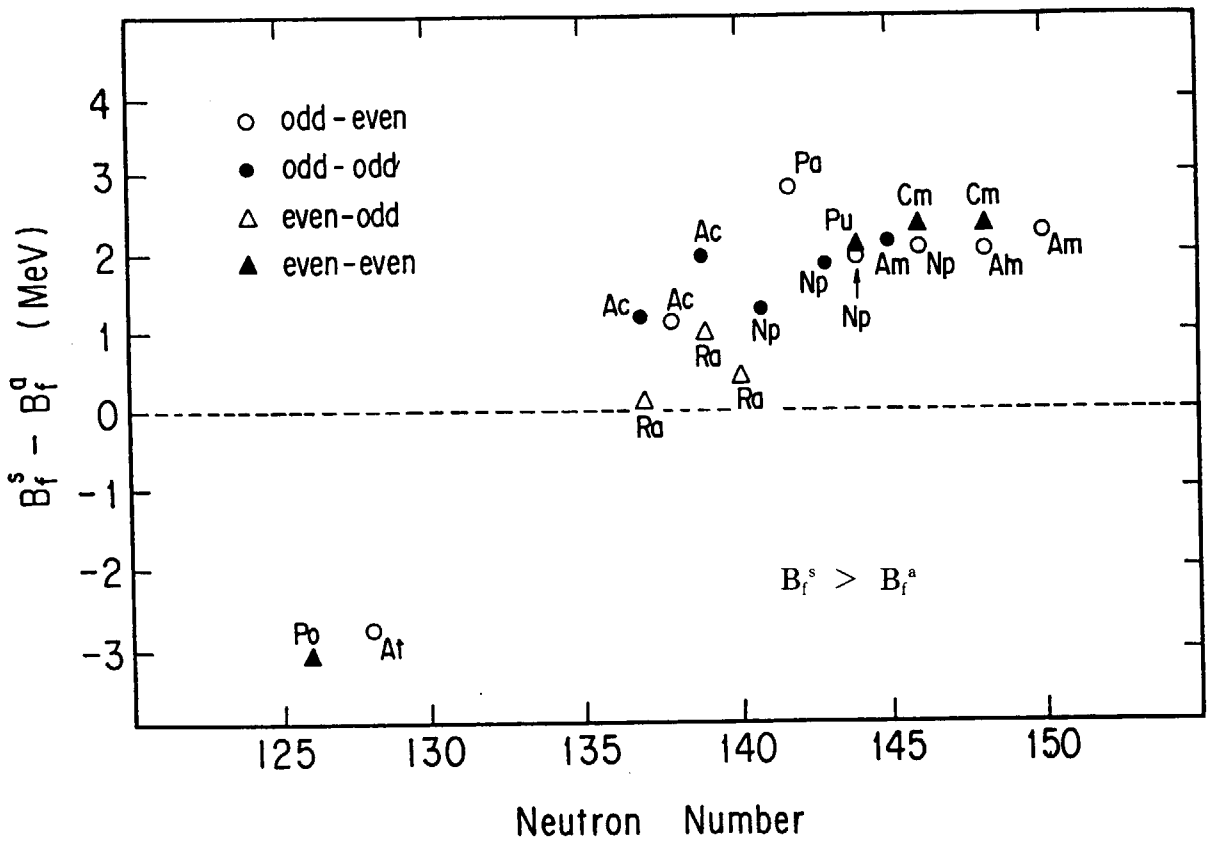

K.-H. Schmidt et al. / Nuclear Physics A630 (1998) 208c–214c

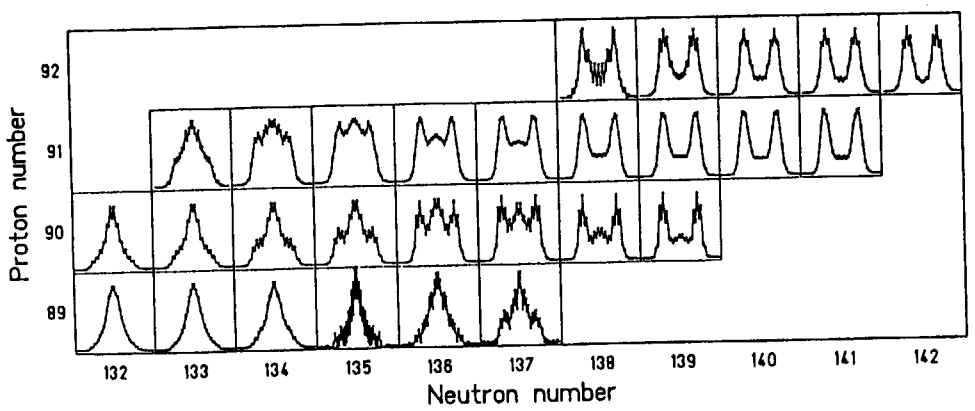

15 MeV p + ^{232}Th, ^{238}U, ^{244}Pu, ^{248}Cm

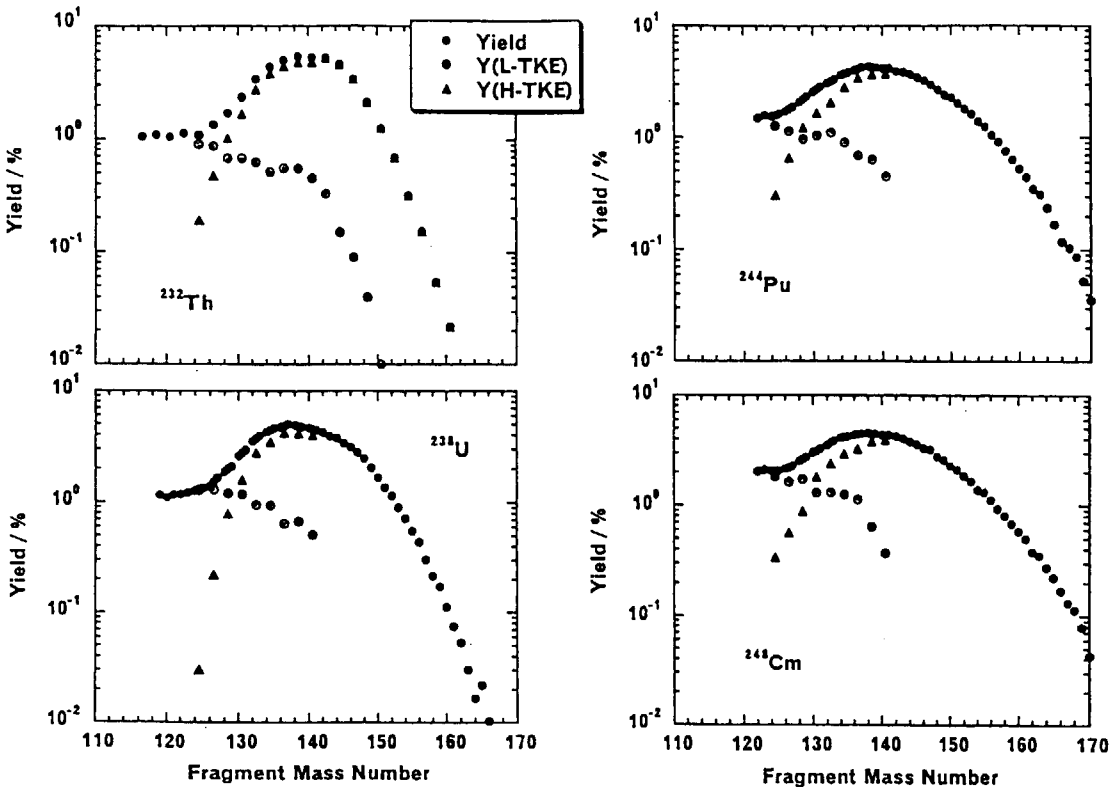

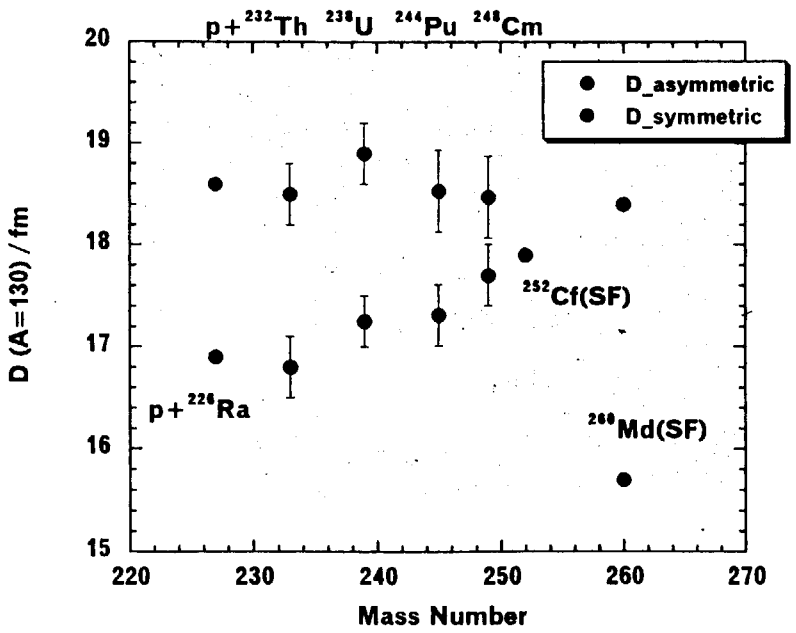

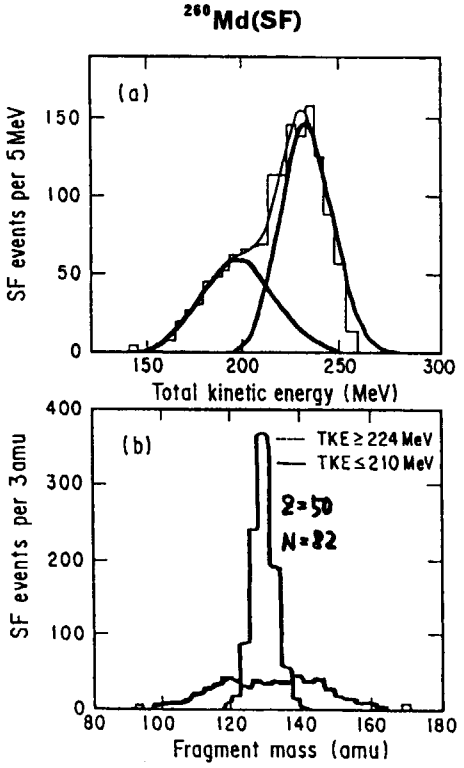

p + ^{226}Ra : E. Konechny and H.W. Schmitt, Phys. Rev. 172, 1213 (1968).
^{252}Cf(SF) : Yu.A. Barashkov et al., Sov. J. Nucl. Phys. 13, 668 (1971).
^{260}Md(SF) : J.F. Wild et al., Phys. Rev. C 41, 640 (1990).

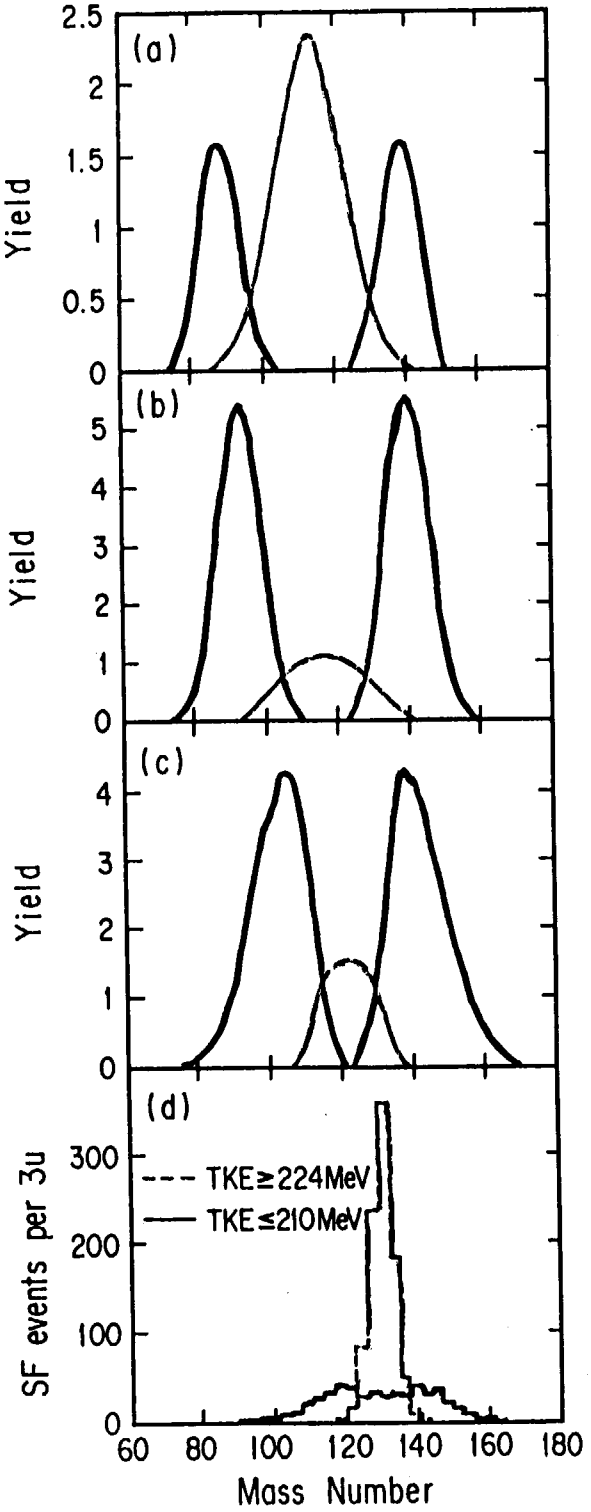

13 MeV p + ^{226}Ra

15 MeV p + ^{232}Th

15 MeV p + ^{244}Pu

^{260}Md(SF)

Correlation between final mass division and fragment shell structure

The heavier wing of the heavy asymmetric yield curve becomes broad with A_l, while the lighter wing of that constitutes the steep cliff around the mass region A=130.

CN	^{233}Pa	^{239}Np	^{245}Am	^{249}Bk
N/Z	1.56	1.57	1.58	1.57
A_L(N=50)	82	82	82	82
A_H	151	157	163	167

Heavy fragment shell structure with A=132 (Z=50, N=82)

Effect of the complementary light fragment with N=50

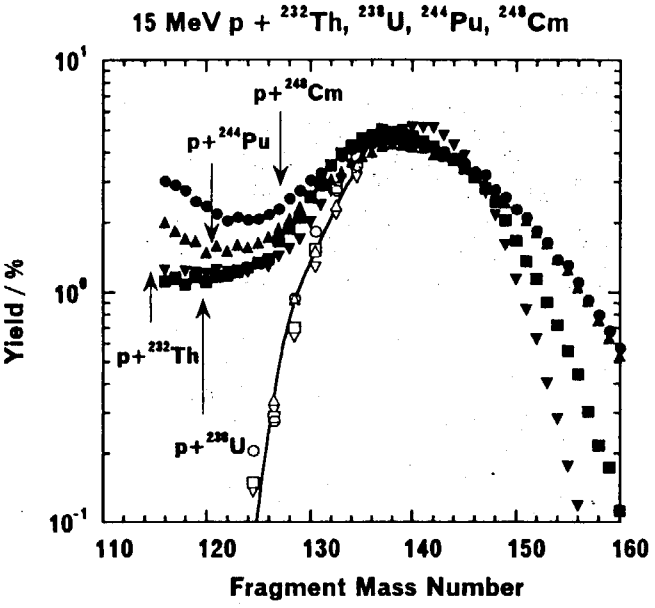

Radiochim. Acta 76. 173(1997).

K. Tsukada *et al.*

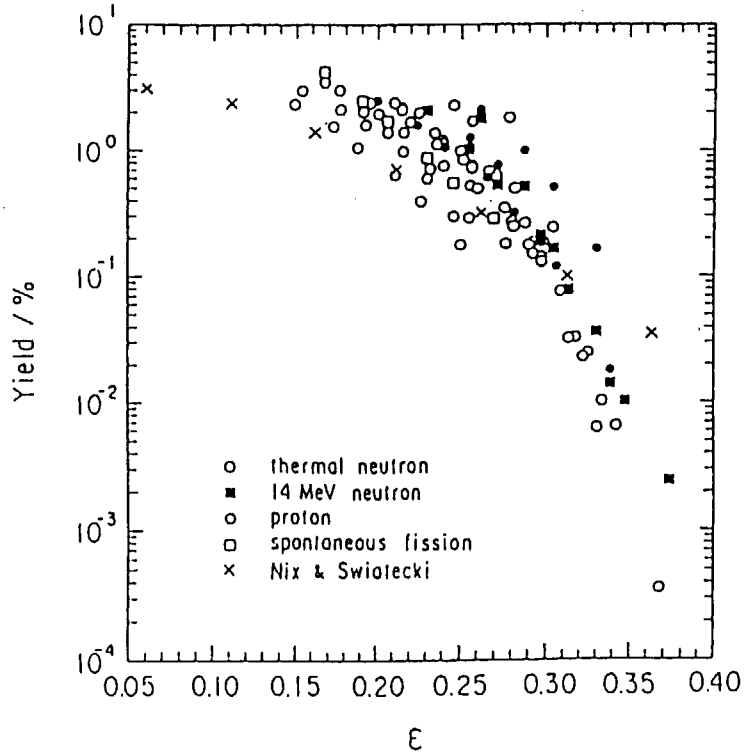

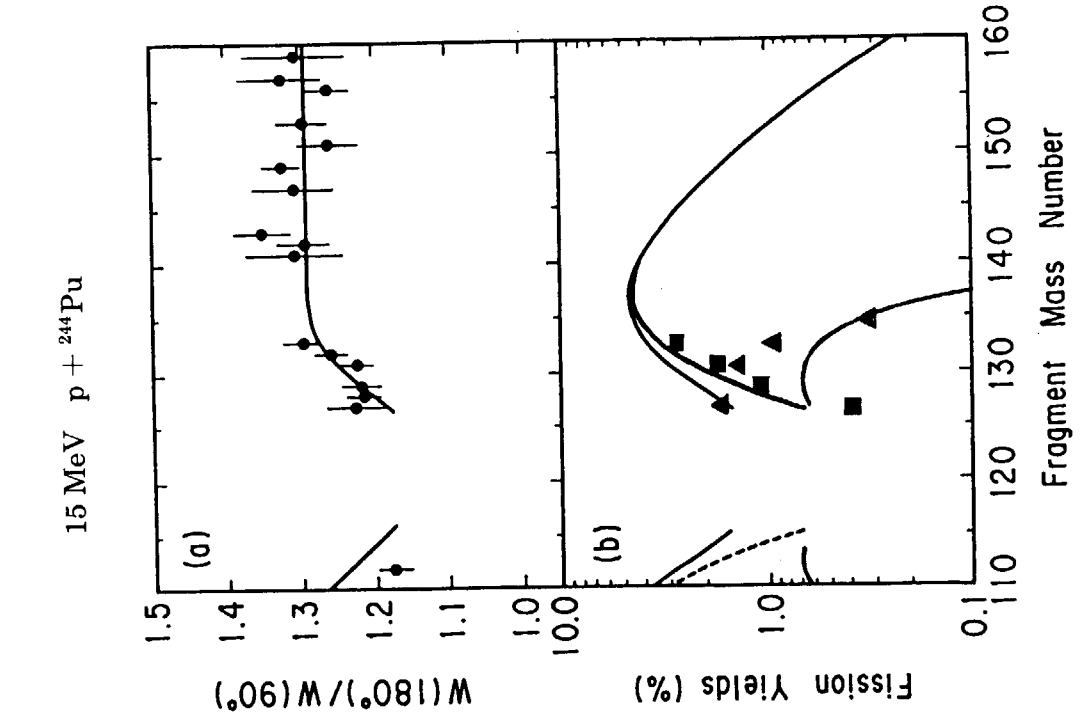

$$\frac{W(180^\circ)}{W(90^\circ)} = 1 + \frac{\langle I^2 \rangle}{4K_e^2} \qquad \kappa_e^2 = \frac{\beta_{eff} \cdot T_{saddle}}{\hbar^2}$$

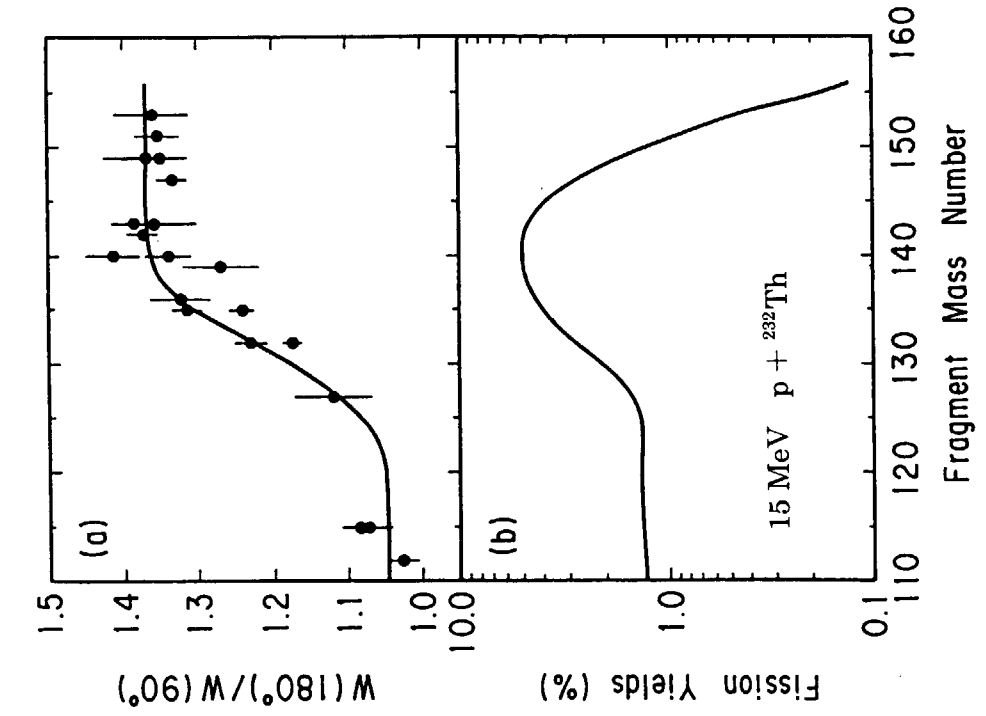

References

[1] Hoffman D.C. and Hoffman M.M.: Ann. Rev. Nucl. Sci. **24**, 151 (1974).

[2] Flyn K.F. *et al.*: Phys. Rev. C **5**, 1725 (1972).

[3] Qin Z. *et al.*: Radiochim. Acta (in press).

[4] Lane M.R. *et al.*: Phys. Rev. C **53**, 2893 (1996).

[5] Ohtsuki T. *et al.*: Phys. Rev. C **48**, 1667 (1993).

[6] Nishinaka I. *et al.*: Phys. Rev. C **56**, 891 (1997).

[7] Schmidt K.-H. *et al.*: Nucl. Phys. **A630**, 208c (1998).

[8] Nagame Y. *et al.*: Phys. Lett. B **387**, 26 (1996), J. Radioanal. Nucl. Chem. **239**, 97 (1999).

[9] Zhao Y.L. *et al.*: J. Radioanal. Nucl. Chem. **239**, 113 (1999), Phys. Rev. Lett. (in press).

[10] Zhao Y.L.: Ph. D. Thesis, Tokyo Metropolitan University (1999).

[11] Tsukada K. *et al.*: Radiochim. Acta **76**, 173 (1997).

[12] Tsukada K. *et al.*: Eur. Phys. J. A **2**, 153 (1998).

14. IAEA CRP on Fission Yield Data and Activity of WG in Japanese Nuclear Data Committee

J. Katakura and T. Fukahori

Nuclear Data Center
Japan Atomic Energy Research Institute
Tokai-mura, Naka-gun, Ibaraki-ken, 319-1195, Japan
e-mail: katakura@ndc.tokai.jaeri.go.jp

Abstract

The outline of the coordinate research program on fission yield data organized by International Atomic Energy Agency and the working group on the subject newly organized in Japanese Nuclear Data Committee are presented.

1 Introduction

Fission Products Yield Data are essential for the evaluation of the delayed neutron yields, which is the subject of this Specialists' meeting, from the microscopic data through summation calculation. In the summation calculation, the fission product yield and probability of delayed neutron emission of fission product nuclides are required. In the community of Japanese nuclear data field, the activity of the fission product yields evaluation had not been energetic. The JENDL [1] and JNDC libraries [2] adopt the evaluated fission product yield data from the foreign libraries with needed modification. For example the JNDC library has fission product yield data for 1227 fission product nuclides. The primary data of the file are, however, those from the compilation by Rider and Meek. As this situation is not desirable for the project producing Japanese evaluated libraries, it has been looked for to start the activity of evaluating the fission yield data. Under the situation, IAEA started a coordinate research program for fission product yield data for transmutation of minor actinide nuclear waste. This is a good opportunity to activate the Japanese evaluation work. For these reasons, a working group was organized under the Japanese Nuclear Data Committee (JNDC). In this report the brief description of the research program and the working group are described.

2 Outline of IAEA CRP on Fission Yield Data

The research program entitled "Fission Product Yield Data Required for Transmutation of Minor Actinide Nuclear Waste" was organized in the year of 1997. The first research coordinate meeting was held on November 5 - 7, 1997 at the IAEA headquarter, Vienna. At the time Japanese group had not joined the program yet. Fukahori, however, attended the meeting as an observer to obtain the information about the meeting. After the meeting, a discussion was held on the tasks expected in the program. The Japanese group finally joined the program in July, 1998. The term of the program is for four years. In this section the outline of the program and the first meeting is described.

2.1 Scope of the program

As a concept of the transmutation of minor actinide nuclides, it is proposed to use the accelerator driven systems to incinerate the minor actinide waste which would need the high energy fission yields data. The energy region would be extended up to 150 MeV, although the conventional reactor covers the energy region up to 20 MeV. For such high energy region, there is no available experimental data, evaluated data file and calculational tools. The scope of the program is, then, to develop fission yield systematics and nuclear models as a tool for an evaluation of energy dependent fission yields up to 150 MeV. In order to achieve the scope a computer code will be developed/adopted that will allow the calculation of fission yields for any given actinide nuclides at any desired neutron energies, although with varying accuracy.

2.2 Outline of the first meeting

The first meeting was held on November 5 - 7, 1997 at the IAEA headquarter, Vienna, Austria. Fukahori attended the meeting. He made a report of the meeting on Journal of Atomic Energy Society of Japan [3]. The outline of the meeting is presented here in accordance with the report.

In the meeting, the confirmation of the goal of the program, the status of both of experiment and theory/model and the tasks to be performed were discussed. As a goal of the program, the energy region up to 150 MeV were confirmed. The energy region is below the threshold of pion production and covers the region where cascade model calculation guarantees the accuracy to a certain extend. Target nuclides are Th, Pa, U, Np, Pu, Am, Cm and Cf. Ternary fission emitting such nuclides as p, t, α, etc. is also considered. As for the review of experimental data, the status of experimental data by neutron, photon and charged particle induced fission were reviewed. The data base of fission yields by neutron (thermal to 14 MeV), photon (7 to 50 MeV) and charged particle (mainly proton) has been compiled by BNFL group. Five-Gaussian model and Z_p & A_p model have been used to analyze the mass distribution and dependence on excitation energy. New experiment on ^{237}Np were reported. The distributions of mass, charge and kinetic energy and mean neutron number emitted were measured for 1, 5 and 8 MeV neutrons at IPPE, Russia. The measurements of proton induced fissions on ^{141}Pr, ^{159}Tb, ^{169}Tm, ^{nat}W, ^{208,nat}Pb and ^{232}Th at ECN/Petten were also reported. In the review of the theory and model, Wahl model [4] on mass and charge distribution was presented. The model is now applicable to the $Z_f = 90-98$, $A_f = 230-252$ and $E_x < 20$ MeV. It is going to be extend up to 150 MeV. Basically it is based on Gaussian fit of 2 to 5 sets. The input data are Z_f, A_f and E_n or $E_c (c = p, d, t, {}^3\mathrm{He}, {}^4\mathrm{He})$. The mean neutron number emitted, mass distribution, independent yields and cumulative yields can be calculated by the model. The floppy diskettes containing the code were distributed at the meeting. The systematics of energy dependent fission product yields taking multi-chance fission and angular momentum into consideration was reviewed. In this systematics, total cross section and fission probability after prompt neutron emission are needed to be separately calculated. Brosa model [5] was also reviewed in the meeting. After these reviews, the tasks to be performed in the CRP were discussed and set as follows:(1) Multi-chance fission study to find out the systematics, (2) Differences among neutron, charged particle and photon induced fission, (3) Cascade model for high energy region, (4) Examination of several models, (5) Survey and analysis of experimental data, (6) Measurement if needed, (7) Development of systematics up to 150 MeV, (8) Recommendation of program and parameter database for fission product yields evaluation.

In these tasks, the Japanese contribution to the CRP program is possibly expected to carry out the following tasks: (1) Collection of experimental data, (2) Study of multi-Gaussian fit model, (3) Analysis using cascade model and quantum molecular dynamics (QMD) [6] method.

3 Outline of WG on fission yields data in JNDC

The working group on fission product yields data was organized in JNDC for the evaluation of fission yields data. The activity of the group is primarily aimed to start up the evaluation of fission yields for future JENDL library. The high energy library of JENDL is one of the important motivation of the future compilation for the application to the incineration of the nuclear waste using an accelerator driven reactor. As there is no available experimental data of fission products yields for the high energy region, such evaluation tools as systematics or a kind of model calculation are indispensable for obtaining the evaluated fission yields data. Even in the low energy region, reliable uncertainties of fission products yields are required for use of MOX fuel in a fission reactor, incineration of nuclear waste using a fast reactor and so on. In the JNDC library the data of uncertainties are not included and the users needing them require the reliable uncertainty data. Therefore, the evaluation of the uncertainties of fission yields is included in the activity of the working group. Then the working group will reevaluate the fission yields data in the JNDC library including the uncertainty evaluation and will provide the fission yields for minor actinide nuclides needed for the incineration of nuclear waste. In the course of the process, the tools for the evaluation will be developed. The working group of the fission yields evaluation in the JNDC has just started the activity. The persons who are interested in the fission product yields data are invited to join the working group.

4 Summary

The outlines of the IAEA CRP program on fission product yields and the activity of working group in JNDC are briefly described. The IAEA program is scheduled to perform the tasks in four years. The working group of JNDC, however, will continue the evaluation work in order to provide the reliable yield data for the JENDL project. We will appreciate any suggestions from the members of JNDC for the activity.

References

[1] Nakagawa T., et al.: J. Nucl. Sci. Technol., 32, 1259 (1995)

[2] Tasaka K., et al.: "JNDC Nuclear Data Library of Fission Products - Second Version -", JAERI 1320, Japan Atomic Energy Research Institute (1990)

[3] Fukahori T. and Katakura J.: J. At. Energy Soc. Japan, 40, 363 (1998) [in Japanese]

[4] Wahl A.C.: At. Data and Nucl. Data Tables, 39, 1 (1988)

[5] Brosa, U., et al.: Phys. Rep., 197[4], 167 (1990)

[6] Niita, k., et al.: Phys. Rev., C52, 2620 (1995)

15. Action for Delayed Neutron Data Evaluation

Shigeaki OKAJIMA
Reactor Physics Group, Department of Nuclear Energy System
Japan Atomic Energy Research Institute
Tokai-mura, Naka-gun, Ibaraki-ken 319-1195
e-mail: okajima@fca001.tokai.jaeri.go.jp

Status of NEA/NSC/WPEC/SG6 activities on delayed neutron data evaluation is shortly reviewed. From this review the actions in evaluating the delayed neutron data are proposed to contribute the revise work for the JENDL-3.3 library.

1. Introduction

The delayed emission of neutrons in fission was observed by R. Roberts, R. Meyer and P. Wang in 1939[1]. N. Bohr and J. A. Wheeler were interpreted this phenomenon as the result of nuclear excitation following the β-decay of fission fragments[2]. Ya. B. Zeldovich and Yu. B. Khariton first noted the importance of delayed neutrons in controlling the rate of a fission chain reaction in 1940[3] - more than two years before the first controlled nuclear chain reaction, CP-1, was achieved.

Since then numerous investigations have been performed on the characteristics of delayed fission neutrons, half-lives, yields and energies. In 1950-1970, the delayed neutron data initially produced were principally the aggregate precursor data (macroscopic data) such as fission product yields. These data are directly measurable and can be used in reactor applications. The basic work in this period was performed by Keepin[4], which resulted in the now familiar six-group modeling of delayed neutron parameters. The next two decades (1970-1990) have focused on the measurement, modeling and evaluation for the individual precursor data (microscopic data), primarily fission yields, the delayed neutron emission probabilities (P_n) and spectra (χ_d). These advances in these data have been based upon work in nuclear physics investigating the detailed structure of nuclei. Some the integral data have also been developed in this period, and small advances in the macroscopic data such as ν_d and χ_d have also been made.

In reactor technology, recent trends include the increased use of mix-oxide fuels and the move to increased enrichment and burn-up in current light water reactor designs as well

as the development of fast reactor designs such as the actinide burning reactor. Accurate predictions of the kinetic response of these new reactor fuels require reliable data concerning delayed neutron production. These trends illustrate the necessity for improving the delayed neutron data available for transuranic nuclides and resolving the discrepancies existing in the current data. The current delayed neutron data have been shown to contribute significantly to the large uncertainties in the reactivity scale for fast reactors. To reflect these trends and to reduce these uncertainties, the improvements in the basic delayed neutron data and integral benchmark are necessary.

In this paper, status of activities on delayed neutron data evaluation is reviewed and the actions to the delayed neutron data evaluation are proposed to revise for JENDL-3.3.

2. Importance of Delayed Neutron in Reactor Control

There are two different critical states in a nuclear reactor; the prompt critical and the delayed critical. In the former state the time scale of the chain reaction is determined by the prompt neutron generation time, which, roughly speaking, is the average time between birth and death of a neutron. On the other hand, in the latter one the time scale is determined mainly by the mean life of the delayed neutrons, in other words, the delayed neutrons act as pacemakers' for the chain reaction in the reactor. If a step of reactivity will be inserted into the reactor and consequently the effective multiplication factor of the reactor will become beyond the prompt critical, the asymptotically exponential increase of the neutron flux will be much rapid. To avoid such a situation, the delayed neutrons slow down the system behavior, making reactor control simpler, and the fraction of them gives a criteria in reactivity insertion to shift from the delayed critical to the prompt critical. The delayed neutrons are therefore vital for the reactor control although they are a very small fraction (less than 1%) of fission neutrons. Since the energy spectrum for delayed neutrons is considerably softer than that for prompt fission neutrons, the effect of the delayed neutrons will be different from the prompt neutrons. Therefore, the effective delayed neutron fraction, β_{eff}, should be used in the application of the reactor control.

In the practical application in the reactor analysis, the β_{eff} allows the conversion between calculated and measured reactivity values and plays an important role in the theoretical interpretation of reactivity measurement.

3. Recent Activities on Delayed Neutron Data Evaluation

In 1990, to improve the delayed neutron data available for transuranic nuclides and to resolve the discrepancies existing in the current data, the NEA Nuclear Science Committee (NSC) Working Party on International Nuclear Data Evaluation and Cooperation (WPEC) was set up the technical subgroup (SG6). The activities in SG6 were divided in three

different levels:

Level 1 : The measurement, evaluation and summation of microscopic delayed neutron data which are related to the fission process (i.e. yields of different fission chain, delayed neutrons emission probabilities, decay constants etc.).

Level 2 : The measurement and evaluation of macroscopic delayed neutron data which related to the total delayed neutron yield per fission, delayed neutron spectra, relative abundances (i.e. data at least partially integrated on different fission chains and decay time). These data contain global parameters which are directly measurable and these can be used in reactor applications.

Level 3 : The measurement and analysis of β_{eff} as the integral test of delayed neutron data. This provides important and stringent tests related to applications such as reactor kinetics calculations.

At the time, there was a strong need to bring together the different on-going activities in the fields of measurement, evaluation and theory since those were nearly independently developed. The experimental efforts comprised both differential and integral measurements.

In 1990, the first specialist meeting[5] in SG6 was held to review the status of delayed neutron data, to identify prominent discrepancies, and to prioritize areas for improvement in the data. Both experimental and theoretical activities directly related to the delayed neutron data have been in progress around the world; the FP yields measurements in level 1, the total delayed neutron yields measurements and the delayed neutron group parameters measurements in level 2 and the international benchmark experiments for β_{eff} in level 3.

The second meeting[6] was held to get a clear picture of the state-of-the-art concerning the activities in three levels. The meeting also devoted to discuss about the short-term strategy to meet the main SG6 targets. The meeting also allowed a picture of the present mean and long-term delayed neutron data targets, to be met in the frame of a possible new subgroup in WPEC. The meeting drew a conclusion that the SG6 will issue the state-of-the-art report with recommending best delayed neutron data for the major actinides and then will be closed in 1999.

SIGMA committee in Japan decided to establish a working group on delayed neutrons to support the SG6 activities in 1996. This working group have been mainly covered the level 1 and level 3 activities of SG6 as follows:

Summation calculations of FP nuclides,

Theoretical interpretation of FP yields through the fission process

Integral experiments of β_{eff} for not only fast but also thermal systems.

4. Actions to revision work for JENDL-3.3 delayed neutron data

In short time range, the integral data of β_{eff} in fast and thermal systems should be

collected and can be used for the evaluation of delayed neutron data ν_d for the major actinides. If the measured data related to the time behavior of the neutron flux, such as the stable period data, the rod drop experimental data, are available, the group parameters of delayed neutrons can be evaluated. From these evaluation, the best delayed neutron data for the major actinides can be recommended to the adoption in JENDL-3.3.

The considerable experience of the summation calculation have been accumulated in the decay heat evaluation with reasonably small uncertainties. This experience will successfully produce the delayed neutron data evaluation with the microscopic data. For the time being the summation method seems to be less reliable than the integral-type measurements in the delayed neutron data evaluation since the fission yields and the decay data for the delayed neutron precursors are not known sufficiently well either experimentally or theoretically. In middle and long time range, therefore, the accumulation of the microscopic data are necessary to get the reliable evaluation of the delayed neutron data. A new experimental plan to obtain the reliable data for delayed neutron precursors, if necessary, will be proposed to modern facility of radioactive nuclear beam as the advanced experimental studies of the nucleosyntheses of heavy elements or the so-called *r-process* as well as of the nuclear structures and reaction. This plan will be expected to stimulate the research activities in not only reactor physicists but also nuclear physicists and astrophysicists.

References

[1] Roberts, R., Meyer, R. C., Wang, P.: *Phys. Rev.*, **55**, 510 (1939).

[2] Bohr, N., Wheeler, J. A.: *Phys. Rev.*, **56**, 426 (1939).

[3] Zeldovich, Ya. B., Khariton, Yu. B.: Zh. eksp. teor. Fiz., **10**, 477 (1940).

[4] Keepin, G. R.:"*Physics of Nuclear Kinetics*," Addison-Wesley Publishing Co. Inc., Reading, Massachusetts (1965).

[5] Blanchot, J. *et al.*: "*Satus of Delayed Neutron Data - 1990*," NEACRP-L-323, NEANDC-299"U", (1990).

[6] D'Angelo, A.: "*Status Report of the WPEC Subgroup 6 activities*," (prepared for the 9th WPEC meeting in Cadarache, France) (1997).

Resume of the Free Discussion

At the end of the meeting the free discussion was held on the future activity of the delayed neutron working group of JNDC for the next JENDL, JENDL-3.3. The resume is attached here as original form in Japanese because we are afraid that the translation to English may lose the nuance of the discussion.

遅発中性子専門家会合
フリーディスカッション「遅発中性子 WG の今後に向けて」

まず、岡嶋氏より原子炉における遅発中性子の重要性に関する明快な説明があり、引き続き以下のような基調報告がなされた。

○ 遅発中性子データは、(1) 放出数 -ν_d-、(2) 各群の時定数 -λ_i-、(3) 各群への配分 -α_i- からなる。FCA や MASURCA の測定で評価できるのは ν_d であり、一方、λ_i と α_i は反応度が入った瞬間からの中性子検出率の時間変化率と密接に関連している。実際、このような時間変化率の実験データを用いて、Spriggs は λ_i と α_i の値の妥当性をチェックしている。

○ 1) マクロの実験データ（臨界実験や中性子 activity の時間変化）の収集、2) Pn 値の測定やこれに基づく総和計算、3) 応用のためのデータベースの作成等は今後も継続的にやってゆく必要がある。

○ 岡嶋講演に関する Q & A

Q：時間変化率データとして使える実験データはあるのか？（瑞慶覧）

A：臨界実験での反応度特性試験に際して、制御棒校正データ（例えば、ペリオドデータ）が取られているはずで、この種のデータが利用できるはずである。（岡嶋）

引き続きディスカッションに入り、以下のような意見が出された。

○ 遅発中性子 WG では U-235、-238、Pu-239 の ν_d を FCA、TCA、VHTRC 等のデータで検証し、必要なら動かすことを考えている。但し、λ_i と α_i は既存のデータセットからそのまま採用したい。遅発中性子を直接測った日本独自の測定デー

タがない点が苦しい。（吉田）

○ 国産のデータがなくても評価はできる。主要3核種に限定せず、評価済みデータの推薦というかたちでもよいから、他の重要なfissileのデータはWG作業の対象範囲に入れて頂きたい。また、Minor Actinideについても、評価担当者はデータニーズを把握しておくべきだ。（中川）

○ 主要3核種以外にもPu-240、Pu-241などのデータは不可欠だ。
（瑞慶覧，辻本ほか）

○ 臨界実験での反応度特性試験データについて、軽水炉系のTCAやVHTRCでも利用可能なデータがあると考えて良いか？（吉田）

○ 与えられたλ_iとα_iのセットが時間変化率を正しく再現するか否かをチェックすることはできる。TCAやVHTRCにもこの目的に利用できるデータはある。
（山根(剛)，中島）

○ 逆に、時間変化率のデータからλ_iとα_iをフィッティングして得ることは非常に難しい。（山根(剛)）

○ 総和計算から遅発中性子データを作成したBradyとEnglandの試みは、遅発中性子データの歴史に於いて画期的な試みであった。しかし、ENDF/B-6では、ν_dは従来の評価値を、λ_iとα_iは総和計算結果を採用したため、遅発中性子データの統一性がなく、その結果、時間変化率から得る反応度に対して必ずしも良好な結果を与えないのが現状である。この点で、総和計算の扱いは難しい。（岡嶋）

○ BradyとEnglandの試みは、原子炉での実用上の必要を上回る51の核分裂システムに対して、遅発中性子総和計算を可能にしたという意味で画期的であった。問題は、総和計算の入力となるprecursorごとの核分裂収率と崩壊データの質である。（親松）

○ 大局的理論のパラメータを最適化するなどして、総和計算の精度向上に努めるべきだ。（瑞慶覧）

○ 大局的理論だけでなく、一般的に言って、現在理論でPnを推定できる精度は、先ほど私が発表した程度（ファクター以内で合えば良い方で、オーダーで違うものも多い。）である。また、ガンマ線との競合係数をどう取り入れるかという不定性も残っている。しかし、パラメータの最適化も含めていろいろ工夫し、総和計算に応用する価値はある。（橘）

○ 総和計算の位置づけをもっとよく考える必要がある。第6群のような短寿命のグループでの計算の信頼性は低くても、炉特性の観点から重要でかつ寄与するPrecursor数が限られている第2～4群には適用できるといった可能性もある。Precursor　毎の遅発中性子放出率Pnの測定を提案することは極めて重要で、それには相応の説得力をもった説明が必要である。他の分野（原子核実験や天体核合成）と協力して行く余地があると思われる（親松）

○ ENDF/Bフォーマットの性質上、エネルギースペクトルが欠けていると、α_i（各群への配分）のデータをファイル化できないことに留意してほしい。また、JENDL-3.2で採用しているSaphierのスペクトルは低エネルギー側が欠落しているのという問題がある。（中川）

Appendix A Program of the Specialists' Meeting on Delayed Neutron Nuclear Data

Program of the Specialists' Meeting on Delayed Neutron Nuclear Data
- To the Evaluation for JENDL 3.3 -

Jan. 28 (Thur.)

13:30 - 13:45

1. Opening Address — A. Hasegawa (JAERI)

13:45 - 15:15

2. Status of Basic Data and Evaluated Data — Chairman: A. Hasegawa (JAERI)

2.1

K. Oyamatsu (Nagoya Univ.)

2.2 Present Status of Delayed Neutron Data in the Major Evaluated Nuclear Data File

T. Nakagawa (JAERI)

15:15 - 15:30 Coffee Break

3. Measurement of Delayed Neutron Emission and Effective Delayed Neutron Fraction

Chairman: Y. Yamane (Nagoya Univ.)

3.1 The Recent Measurements of Delayed Neutron Emission from Minor Actinide Isotopes Conducted at Texxas A&M University

M. Andoh (JAERI)

3.2 Benchmark Experiments of Effective Delayed Neutron Fraction beff at FCA

T. Sakurai (JAERI)

3.3 Measurement of the Effective Delayed Neutron Fraction for the TCA Cores

K. Nakajima (JAERI)

18:00 - 20:00 Reception (Akogi-ga-ura Club)

Jan. 29 (Fri.)

9:00 - 10:30

4. Evaluation of Delayed Neutron Data — Chairman: J. Katakura (JAERI)

4.1 Possible Fractuations in Delayed Neutron Yields in the Resonance Region of U-235

T. Ohsawa (Kinki Univ.)

4.2 Estimmmation of Delayed Neutron Emission Probability by Using the Gross Theory of Nuclear b-decay

T. Tachibana (Waseda Univ.)

4.3 Activity of the Delayed Neutron Working Group of JNDC and the International Evaluation Cooperation - WPEC/SG6

T. Yoshida (Musasi Inst.Tech.)

10:30 - 10:45 Coffee Break

10:45 - 12:00

5. Effective Delayed Neutron Fraction In Fast Reactor System

Chairman: T. Yamane (JAERI)

5.1 Evaluation Method for Uncertainty of Effective Delayed Neutron Fraction beff

A. Zukeran (Hitach. Co.)

5.2 Analysis of Benchmark Experiments of Effective Delayed Neutron Fraction beff at MASURCA andf FCA

T. Sakurai (JAERI)

12:00 - 13:00 Lunch

13:00 - 15:00

6. Chairman: A. Zukeran (Hitachi Co.)

6.1 Improtance of Delayed Neutron Data in Transmutation System

K, Tsujimoto (JAERI)

6.2 Study of Mass Yield and Neutron Emission for Thermal Neutron Fission

K. Nishio (JAERI)

6.3 Systematic Feasures of Mass Yield Curves in Low-energy Fission of Actinides

Y. Nagame (JAERI)

6.4 IAEA CRP on Fission Yield Data and Activity of WG in Japanese Nuclear Data Committee

J. Katakura (JAERI)

15:00 - 15:15 Coffee Break

15:15 - 16:00

7. Free Discussion on the future activity of the Delayed Neutron WG

Chairman: T. Yoshida (Musashi Inst. Tech.)

7.1 Keynote talk: Action for Delayed Neutron Data Evaluation

S. Okajima (JAERI)

16:00 - 16:10

8. Closing Remarks T. Yoshida (Musashi Inst. Tech.)

This is a blank page.

国際単位系 (SI) と換算表

表1　SI基本単位および補助単位

量	名称	記号
長さ	メートル	m
質量	キログラム	kg
時間	秒	s
電流	アンペア	A
熱力学温度	ケルビン	K
物質量	モル	mol
光度	カンデラ	cd
平面角	ラジアン	rad
立体角	ステラジアン	sr

表2　SIと併用される単位

名称	記号
分，時，日	min，h，d
度，分，秒	°，′，″
リットル	l，L
トン	t
電子ボルト	eV
原子質量単位	u

1 eV = 1.60218 × 10^{-19} J

1 u = 1.66054 × 10^{-27} kg

表5　SI接頭語

倍数	接頭語	記号
10^{18}	エクサ	E
10^{15}	ペタ	P
10^{12}	テラ	T
10^{9}	ギガ	G
10^{6}	メガ	M
10^{3}	キロ	k
10^{2}	ヘクト	h
10^{1}	デカ	da
10^{-1}	デシ	d
10^{-2}	センチ	c
10^{-3}	ミリ	m
10^{-6}	マイクロ	μ
10^{-9}	ナノ	n
10^{-12}	ピコ	p
10^{-15}	フェムト	f
10^{-18}	アト	a

表3　固有の名称をもつSI組立単位

量	名称	記号	他のSI単位による表現
周波数	ヘルツ	Hz	s^{-1}
力	ニュートン	N	$m \cdot kg/s^2$
圧力，応力	パスカル	Pa	N/m^2
エネルギー，仕事，熱量	ジュール	J	N·m
工率，放射束	ワット	W	J/s
電気量，電荷	クーロン	C	A·s
電位，電圧，起電力	ボルト	V	W/A
静電容量	ファラド	F	C/V
電気抵抗	オーム	Ω	V/A
コンダクタンス	ジーメンス	S	A/V
磁束	ウェーバ	Wb	V·s
磁束密度	テスラ	T	Wb/m^2
インダクタンス	ヘンリー	H	Wb/A
セルシウス温度	セルシウス度	℃	
光束	ルーメン	lm	cd·sr
照度	ルクス	lx	lm/m^2
放射能	ベクレル	Bq	s^{-1}
吸収線量	グレイ	Gy	J/kg
線量当量	シーベルト	Sv	J/kg

表4　SIと共に暫定的に維持される単位

名称	記号
オングストローム	Å
バーン	b
バール	bar
ガル	Gal
キュリー	Ci
レントゲン	R
ラド	rad
レム	rem

1 Å = 0.1 nm = 10^{-10} m

1 b = 100 fm^2 = 10^{-28} m^2

1 bar = 0.1 MPa = 10^5 Pa

1 Gal = 1 cm/s^2 = 10^{-2} m/s^2

1 Ci = 3.7 × 10^{10} Bq

1 R = 2.58 × 10^{-4} C/kg

1 rad = 1 cGy = 10^{-2} Gy

1 rem = 1 cSv = 10^{-2} Sv

（注）

1. 表1～5は「国際単位系」第5版，国際度量衡局 1985年刊行による。ただし，1 eVおよび1 uの値はCODATAの1986年推奨値によった。
2. 表4には海里，ノット，アール，ヘクタールも含まれているが日常の単位なのでここでは省略した。
3. barは，JISでは流体の圧力を表わす場合に限り表2のカテゴリーに分類されている。
4. EC閣僚理事会指令ではbar，barnおよび「血圧の単位」mmHgを表2のカテゴリーに入れている。

換算表

力

N(=10^5 dyn)	kgf	lbf
1	0.101972	0.224809
9.80665	1	2.20462
4.44822	0.453592	1

粘度　1 Pa·s(N·s/m^2) = 10 P(ポアズ)(g/(cm·s))

動粘度　1 m^2/s = 10^4 St(ストークス)(cm^2/s)

圧力

MPa(=10 bar)	kgf/cm^2	atm	mmHg(Torr)	lbf/in^2(psi)
1	10.1972	9.86923	7.50062 × 10^3	145.038
0.0980665	1	0.967841	735.559	14.2233
0.101325	1.03323	1	760	14.6959
1.33322 × 10^{-4}	1.35951 × 10^{-3}	1.31579 × 10^{-3}	1	1.93368 × 10^{-2}
6.89476 × 10^{-3}	7.03070 × 10^{-2}	6.80460 × 10^{-2}	51.7149	1

エネルギー・仕事・熱量

J(=10^7 erg)	kgf·m	kW·h	cal(計量法)	Btu	ft·lbf	eV
1	0.101972	2.77778 × 10^{-7}	0.238889	9.47813 × 10^{-4}	0.737562	6.24150 × 10^{18}
9.80665	1	2.72407 × 10^{-6}	2.34270	9.29487 × 10^{-3}	7.23301	6.12082 × 10^{19}
3.6 × 10^6	3.67098 × 10^5	1	8.59999 × 10^5	3412.13	2.65522 × 10^6	2.24694 × 10^{25}
4.18605	0.426858	1.16279 × 10^{-6}	1	3.96759 × 10^{-3}	3.08747	2.61272 × 10^{19}
1055.06	107.586	2.93072 × 10^{-4}	252.042	1	778.172	6.58515 × 10^{21}
1.35582	0.138255	3.76616 × 10^{-7}	0.323890	1.28506 × 10^{-3}	1	8.46233 × 10^{18}
1.60218 × 10^{-19}	1.63377 × 10^{-20}	4.45050 × 10^{-26}	3.82743 × 10^{-20}	1.51857 × 10^{-22}	1.18171 × 10^{-19}	1

1 cal = 4.18605 J（計量法）

= 4.184 J　（熱化学）

= 4.1855 J　（15 °C）

= 4.1868 J（国際蒸気表）

仕事率　1 PS（仏馬力）

= 75 kgf·m/s

= 735.499 W

放射能

Bq	Ci
1	2.70270 × 10^{-11}
3.7 × 10^{10}	1

吸収線量

Gy	rad
1	100
0.01	1

照射線量

C/kg	R
1	3876
2.58 × 10^{-4}	1

線量当量

Sv	rem
1	100
0.01	1

（86年12月26日現在）